USGS
science for a changing world

Catalog of Earthquake Parameters and Description of Seismograph and Infrasound Stations at Alaskan Volcanoes—January 1, 2013, through December 31, 2017

Data Series 1115

U.S. Department of the Interior
U.S. Geological Survey

Cover. Photograph showing seismic station CLCO, at Concord Point, Chuginadak Island, Islands of Four Mountains, Aleutian Islands, Alaska. The south flank of little-studied Tana Volcano rises in the background. This remote, solar-powered seismic station also hosts the Cleveland Volcano web camera and an array of infrasound sensors. (Photograph by Max Kaufman, University of Alaska Fairbanks Geophysical Institute, used with permission.)

Catalog of Earthquake Parameters and Description of Seismograph and Infrasound Stations at Alaskan Volcanoes—January 1, 2013, through December 31, 2017

By James P. Dixon, Scott D. Stihler, Matthew M. Haney, John J. Lyons, Dane M. Ketner, Katherine M. Mulliken, Thomas Parker, John A. Power

Data Series 1115

U.S. Department of the Interior
U.S. Geological Survey

U.S. Department of the Interior
DAVID BERNHARDT, Secretary

U.S. Geological Survey
James F. Reilly II, Director

U.S. Geological Survey, Reston, Virginia: 2019

For more information on the USGS—the Federal source for science about the Earth, its natural and living resources, natural hazards, and the environment—visit https://www.usgs.gov or call 1–888–ASK–USGS.

For an overview of USGS information products, including maps, imagery, and publications, visit https://store.usgs.gov.

Suggested citation:
Dixon, J.P., Stihler S.D., Haney, M.M., Lyons, J.J., Ketner, D.M., Mulliken, K.M., Parker, T., and Power, J.A., 2019, Catalog of earthquake parameters and description of seismograph and infrasound stations at Alaskan volcanoes—January 1, 2013, through December 31, 2017: U.S. Geological Survey Data Series 1115, 92 p., https://doi.org/10.3133/ds1115.

ISSN 2327-638X (online)

Acknowledgments

The contents of this report reflect a great deal of hard work by a large number of people, including Alaska Volcano Observatory, Alaska Earthquake Center (AEC), and U.S. Geological Survey (USGS) personnel and various students, interns, and volunteers. We thank the AEC, Global Seismograph Network, National Tsunami Warning Center, and Transportable Array for the use of their data. We thank Brian Shiro (USGS) and Gabrielle Tepp (USGS) for formal reviews of the text and figures.

Contents

Figures

Tables

Conversion Factors

International System of Units to U.S. customary units

Multiply	By	To obtain
	Length	
kilometer (km)	0.6214	mile (mi)
	Pressure	
pascal (Pa)	0.2088	pound per square foot (lb/ft^2)

Abbreviations

A1VCO	A1 voltage control oscillator
AEC	Alaska Earthquake Center
ANSS	Advanced National Seismic System
AQMS	ANSS Quake Monitoring System
AVO	Alaska Volcano Observatory
ERH	horizontal error
ERZ	vertical error
GOAT	IRIS Gap/Overlap Analysis Tool
GSN	Global Seismograph Network
Hz	hertz
IRIS	Incorporated Research Institutions for Seismology
M_c	magnitude of completeness
M_d	duration magnitude
M_h	human set magnitude
M_L	local magnitude
NTWC	National Tsunami Warning Center
Pa	Pascals
RMS	root mean square
SEED	Standard for the Exchange of Earthquake Data
sps	samples per second
TA	Transportable Array
UHF	ultrahigh frequency
USGS	U.S. Geological Survey
VCO	voltage-controlled oscillator
VHF	very high frequency
V_P	P-wave or compressional-wave velocity
V_S	S-wave or shear-wave velocity
WSG	World Geodetic System

Datum

Horizontal coordinate information is referenced to the World Geodetic System 1984 (WGS 84).

“This page intentionally left blank”

Catalog of Earthquake Parameters and Description of Seismograph and Infrasound Stations at Alaskan Volcanoes—January 1, 2013, through December 31, 2017

By James P. Dixon,[1] Scott D. Stihler,[2] Matthew M. Haney,[1] John J. Lyons,[1] Dane M. Ketner,[1] Katherine M. Mulliken,[3] Thomas Parker,[1] and John A. Power[1]

Abstract

Between January 1, 2013, and December 31, 2017, the Alaska Volcano Observatory (AVO) located a total of 28,172 earthquakes at volcanoes in Alaska. The annual totals are 3,840, 5,819, 5,297, 6,151, and 7,065 earthquakes for the years 2013 through 2017, respectively. This represents an average of 5,634 earthquakes per year, which is comparable to the yearly number of earthquakes AVO located in the previous decade when AVO monitored a similar number of volcanoes. During the reporting period, there was significant seismic activity at 20 of the 34 volcanoes monitored by a seismograph network (Akutan Peak, Aniakchak Crater, Augustine, Mount Cerberus, Mount Cleveland, Fourpeaked Mountain, Mount Gareloi, Great Sitkin, Ilimana, Kanaga, Korovin, Makushin, Mount Martin, Okmok Caldera, Pavlof, Shishaldin, Mount Spurr, Tanaga, Ugashik-Peulik, and Mount Veniaminof) and two volcanoes without a monitoring network (Mount Recheshnoi and Bogoslof Island). Instrumentation highlights for this period include the establishment of a new subnetwork on Mount Cleveland, an accelerated transition from analog to digital telemetry at most subnetworks, and an increased number of broadband and infrasound sensors throughout the AVO network. The operational highlight was the return of seismic monitoring at Korovin and Ugashik-Peulik Volcanoes following network repairs. This catalog includes hypocenters, magnitudes, and statistics of the earthquakes located in 2013–17, along with the associated station parameters, and velocity models.

Introduction

In 1988, the Alaska Volcano Observatory (AVO) was established as a cooperative program of the U.S. Geological Survey (USGS), the Geophysical Institute at the University of Alaska Fairbanks, and the Alaska Division of Geological & Geophysical Surveys. AVO initially monitored four volcanoes in the Cook Inlet region (Mount Spurr, Redoubt Volcano, Iliamna Volcano, and Augustine Volcano) and in the following three decades, established seismograph networks on 34 of the 54 historically active volcanoes in Alaska (Cameron and Schaefer, 2016) (fig.1). The primary objectives of the AVO seismic program are the real-time seismic monitoring of active and potentially hazardous Alaskan volcanoes and the investigation of seismic processes associated with active volcanism.

Between January 1, 2013, and December 31, 2017, the AVO located a total of 28,172 earthquakes at volcanoes in Alaska. The annual totals are 3,840, 5,819, 5,297, 6,151, and 7,065 earthquakes, respectively, for the years 2013 through 2017, respectively. This represents an average of 5,634 earthquakes per year, which is comparable to the yearly number of earthquakes AVO located in the previous decade when AVO monitored a similar number of volcanoes. During the reporting period, there was significant seismic activity at 20 of the 34 volcanoes monitored by a seismograph network.

The seismically monitored volcano list includes volcanoes with a local seismograph network designed for the location of earthquakes in the vicinity of the volcano and a period of recording exceeding 6 months without prolonged station outages. The 29 monitored volcanoes are shown in figure 1. Five of the 34 historically active volcanic centers with seismograph networks were not on the formal list of permanently monitored volcanoes in the AVO weekly update at the end of 2017. Fourpeaked Mountain was delisted on February 8, 2014, due to the failure of all seismograph stations.

Little Sitkin, Mount Cerberus (the active vent on Semisopochnoi Island), and Mount Wrangell (unlisted in 2012) volcanoes remained off the official monitored list. The Little Sitkin and Cerberus subnetworks do not have stable telemetry and the Wrangell subnetwork was too recently reestablished to be listed. Mount Cleveland, with two seismograph stations, does not have a sufficient number of stations to locate most earthquakes that occur in the Islands of the Four Mountains (fig. 1). Korovin and Ugashik-Peulik Volcanoes were reinstated on the formal list of permanently monitored volcanoes on February 21, 2013, and May 22, 2013, respectively. Between 2013 and 2017, Aniakchak Crater was removed on January 24, 2014,

[1]U.S. Geological Survey.

[2]University of Alaska Fairbanks Geophysical Institute.

[3]Alaska Division of Geological & Geophysical Surveys.

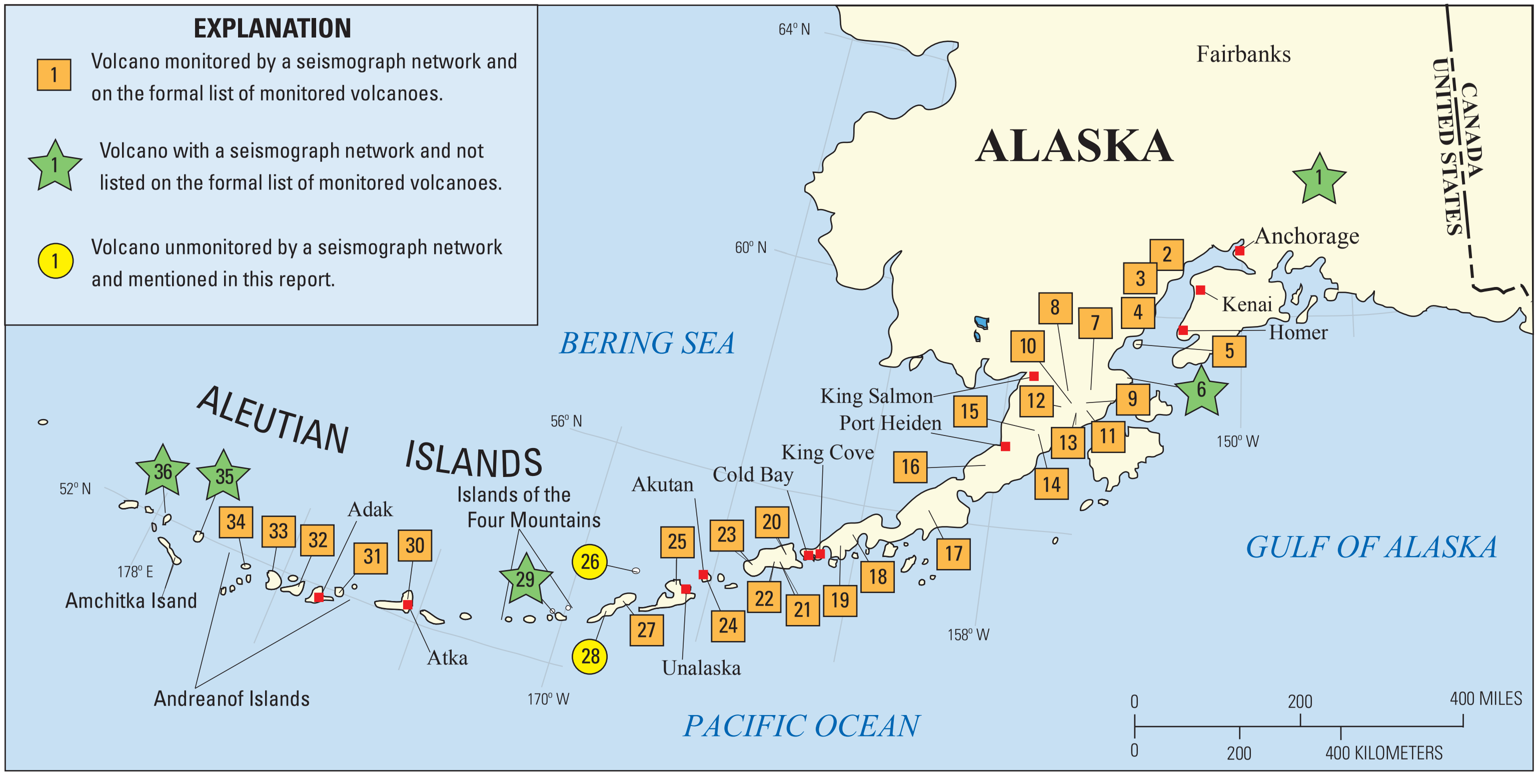

Map modified from Brantley and others (2004), USGS Fact Sheet 2004–3084

Volcanoes

1. Mount Wrangell
2. Mount Spurr
3. Redoubt
4. Iliamna
5. Augustine
6. Fourpeaked Mountain
7. Snowy Mountain
8. Mount Griggs
9. Mount Katmai
10. Novarupta
11. Trident
12. Mount Mageik
13. Mount Martin
14. Ugashik-Peulik
15. Ukinrek Maars
16. Aniakchak Crater
17. Mount Veniaminof
18. Pavlof
19. Mount Dutton
20. Isanostski
21. Shishaldin
22. Fisher Caldera
23. Westdahl Peak
24. Akutan Peak
25. Makushin
26. Bogoslof Island
27. Okmok Caldera
28. Mount Recheshnoi
29. Mount Cleveland
30. Korovin
31. Great Sitkin
32. Kanaga
33. Tanaga
34. Mount Gareloi
35. Mount Cerberus
36. Little Sitkin Island

Figure 1. Map showing location of volcanoes monitored by the Alaskan Volcano Observatory mentioned in this report. Red squares show locations of towns and other sites mentioned in this report.

and added back on October 23, 2015. All three of the subnetworks added back to the formal monitored list had significant maintenance performed to upgrade network infrastructure.

This report describes the type and location of (1) seismograph and infrasound instrumentation deployed in the field; (2) earthquake detection, recording, analysis, and data archival systems; (3) seismic-velocity models used for earthquake locations; and (4) a summary of earthquakes located in 2013–17. A summary of earthquake origin times, hypocenters, magnitudes, and location quality statistics (headers described in appendix 7), and a metadata file for the AVO seismograph network (including but not limited to station location, station type, and system-response information) in the format of a dataless Standard for the Exchange of Earthquake Data (SEED) volume (International Federation of Digital Seismograph Networks, 2012) are included in a data supplement to this report (available only online at https://doi.org/10.3133/ds1115).

Instrumentation

The permanent AVO seismograph network is composed of 25 subnetworks with an average of 8 seismograph stations each and 10 regional seismograph stations for a total of 212 stations at the end of 2017 (table 1, fig. 2). In the past 5 years, ten new seismograph stations were established. Six broadband stations were added to the Augustine subnetwork over a 3-year period (two in 2013, one in 2014, and three in 2015). Two short-period seismograph stations were installed on Cleveland Volcano in 2014. The final new installations were within the Iliamna subnetwork—a broadband station in 2015 and a three-component short-period station in 2016. Additionally, two station installations were direct replacements for older stations. On Pavlof Volcano, PV6A was established in 2016 north of where PV6 had been located before its destruction in a previous Pavlof eruption, giving it a greater chance of surviving a future eruption. On Mount Wrangell, WAZA was removed in 2016 and reoccupied in 2017.

The composition of the AVO network is slowly transitioning from a short-period network to a broadband network (fig. 2, table 2). As new seismograph stations are installed, broadband sensors are the preferred instrument choice for these new sites. As opportunities present themselves, short-period sensors are being replaced with broadband sensors with a dozen short-period stations converted in the past 5 years. As a result, the number of broadband seismograph stations nearly doubled over the past 5 years and the proportion of broadband sites moved from 16 percent in 2012 to 29 percent in 2017. At the end of 2017, the AVO seismograph network consisted of 172 short-period and 62 broadband stations.

AVO is increasingly using infrasound sensors to detect eruptive activity. Stand-alone microphones and infrasound arrays are used in the monitoring of volcanoes with and without local seismograph instrumentation. Infrasound sensors have been co-located with seismograph sensors for decades with increasing numbers installed in the last 8 years in the AVO network. Where infrasound sensors are co-located, typically the sensor was a single-channel infrasound station. However, three infrasound arrays are co-located with seismograph stations. The four-element Akutan array is collocated with AKS; the five-element Cleveland array is collocated with CLCO; and the six-element Sand Point array (SDPI) is co-located with the National Tsunami Warning Center seismograph station SDPT. Stand-alone infrasound arrays are located on Umnak Island (OKIF) and in Adak, Alaska (ADKI). OKIF is a four-element array outside the Okmok Caldera, whereas ADKI is a six-element array between Kanaga and Great Sitkin Volcanoes. The use of infrasound arrays as opposed to single stations, allows AVO to use the relative arrival times of acoustic waves on each sensor to determine the source of the infrasound signal.

The single-component short-period seismograph stations were equipped with either Sercel L-4 or Teledyne-Geotech S-13 seismometers with a natural period of 1 hertz (Hz). AVO also operated three-component, short-period instruments during 2013–17. Such sites used L-4, Sercel L-22, or S-13 seismometers. The L-22 seismometer has a natural period of 2 Hz. Broadband stations were operated with either a Güralp CMG-40T seismometer (frequency range: 0.033–50 Hz), Güralp CMG-6TD seismometer (frequency range: 0.033–50 Hz), Nanometrics Trillium Compact (frequency range: 0.008-100 Hz), or Nanometrics Trillium 40 seismometer (frequency range: 0.025–50 Hz). The Augustine Volcano subnetwork has the only strong-motion station (AU22) in the AVO seismograph network used a Kinemetrics Episensor EST strong-motion sensor (frequency range is 0–500 Hz) and was collocated with a broadband sensor.

The majority of short-period stations (88 percent) were digitized at 100 samples per second (sps). The Mount Cerberus and Little Sitkin Island subnetworks were recorded at 50 sps due to limitations in data rates using very small aperture terminal telemetry between the recording hubs located on Amchitka Island and Anchorage. Broadband stations were digitized at 50 sps with the exception of IVE in the Iliamna Volcano subnetwork, which was recorded at 20 sps due to poor telemetry.

Infrasound sensors in the AVO network come primarily from the Chaparral Physics brand. Models in use are series M2, M21/25 and M60/64 infrasound sensors. The series M21/25 sensors are used at three of the five infrasound arrays operated by AVO (OKIF, AKS, ADKI). The other two infrasound arrays (CLCO and SDPI) use sensors developed by the USGS Cascades Volcano Observatory. As short-period stations are upgraded to digital broadbands, hut-mounted single station infrasound sensors (Chaparral model M64) are being added at some sites. These are ultra-high-pressure variations of the M64 and can record as much as +/-1,000 pascal (Pa) on scale, which is useful for recording strong explosions close to the source. Chaparrel M2 series microphones are used in

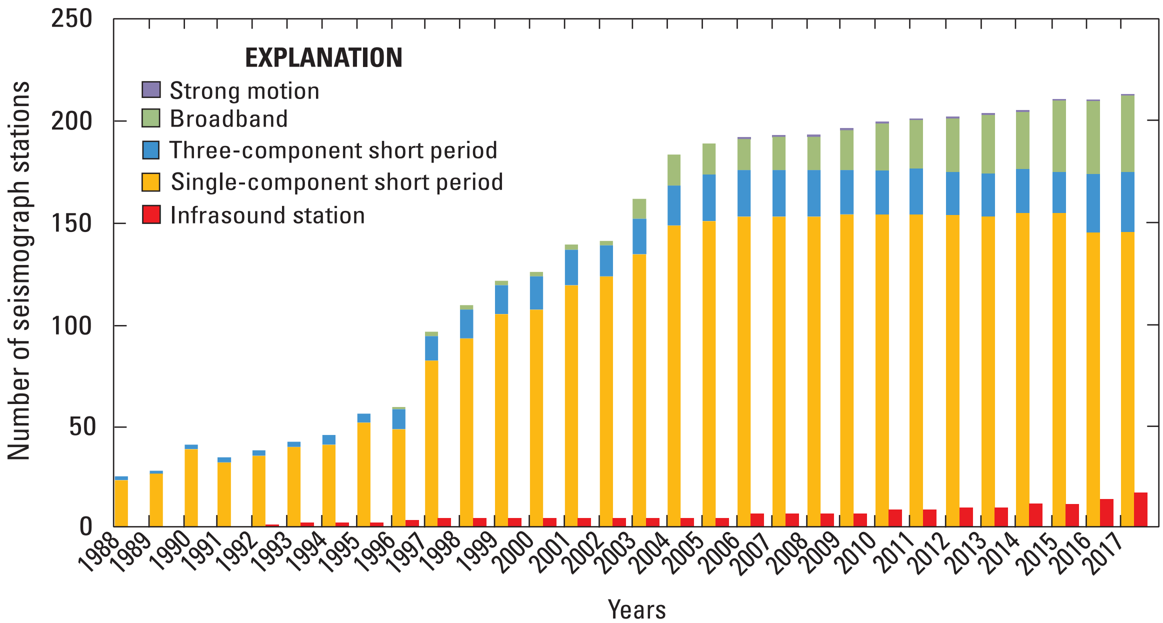

Figure 2. Graph showing the number of Alaska Volcano Observatory seismograph and infrasound stations by type and year.

infrasound installations that were established before 2007. Infrasound sample rates typically are 50 sps, although some stations record at 100 sps, including most arrays and CLES in the Cleveland subnetwork.

When available, calibration information in the form of poles and zeros, for each seismograph and infrasound sensor is included in the dataless SEED volume that can be found in the data supplement to this report and available from AVO offices and the Incorporated Research Institutions for Seismology (IRIS). A description of how instrument corrections are created for AVO seismograph stations can be found in Haney and others (2012). Instrument specifications are available online from the instrument manufacturers.

Data from AVO seismograph stations are increasingly telemetered with digital telemetry. Current analog telemetry links uses voltage-controlled oscillators (VCOs) to transform the signals generated by the seismometer from a voltage to a frequency-modulated carrier suitable for transmission over a radio link or telephone circuit. AVO uses VCOs developed by McChesney (1999) to modulate signals in the field with one exception—Mount Spurr seismograph station NCG uses an A1 voltage control oscillator (A1VCO) (Rogers and others, 1980). Signals are transmitted by ultrahigh frequency (UHF) and very high frequency (VHF) radio from station sites to communication hubs located throughout Alaska, where the signal is digitized and forwarded to the AVO in Anchorage. Digital telemetry links are accomplished with spread-spectrum radios, taking signals digitized at the field sites to AVO communication hubs. These data were forwarded to AVO offices in Anchorage through high-speed digital circuits. Progress moving from analog to digital telemetry is shown in figure 3.

Locations for all AVO stations are shown in appendix 1 with locations tabulated in appendix 2. A measure of each station's operational status for the catalog period is shown in appendix 3 using the IRIS Gap/Overlap Analysis Tool (Stromme, 2000) and in appendix 4 with data-use scores, a normalized measure of the number of P-wave phase arrivals by station in the AVO earthquake catalog developed by Matt Haney (AVO, written commun., 2018).

Data Acquisition and Processing

Data acquisition for the AVO seismograph and infrasound network for 2013–17 used the Advanced National Seismic System *(ANSS) Quake Monitoring System* (AQMS). AQMS is an integrated data acquisition and processing system derived from software developed as part of the TriNet project (Hauksson and others, 2003) that incorporates Earthworm modules (Johnson and others, 1995) for data acquisition and event detection. The Jiggle software package (Hauksson and others, 2003; U.S. Geological Survey, 2018) is used to time phase arrivals and determine magnitudes. Earthquake hypocenters were calculated using Hypoinverse (Klein, 2002).

Earthquakes were detected using the Earthworm modules *carlstatrig* and *carlsubtrig*, with the *carlstatrig* parameters set as follows—long-term-average time=8 seconds, ratio=2.3, and quiet=4. Three station triggers from the *carlstatrig* module are required for an event to trigger *carlsubtrig* to create an event record. *Carlsubtrig* was modified such that each triggered record is identified with the triggering network (table 3). If four or more subnetworks triggered on the same event, the trigger was tagged as a regional event. About one third of all triggers are auto located. All data is stored in mini-SEED format (International Federation of Digital Seismograph Networks, 2012). Infrasound signals were detected by in-house

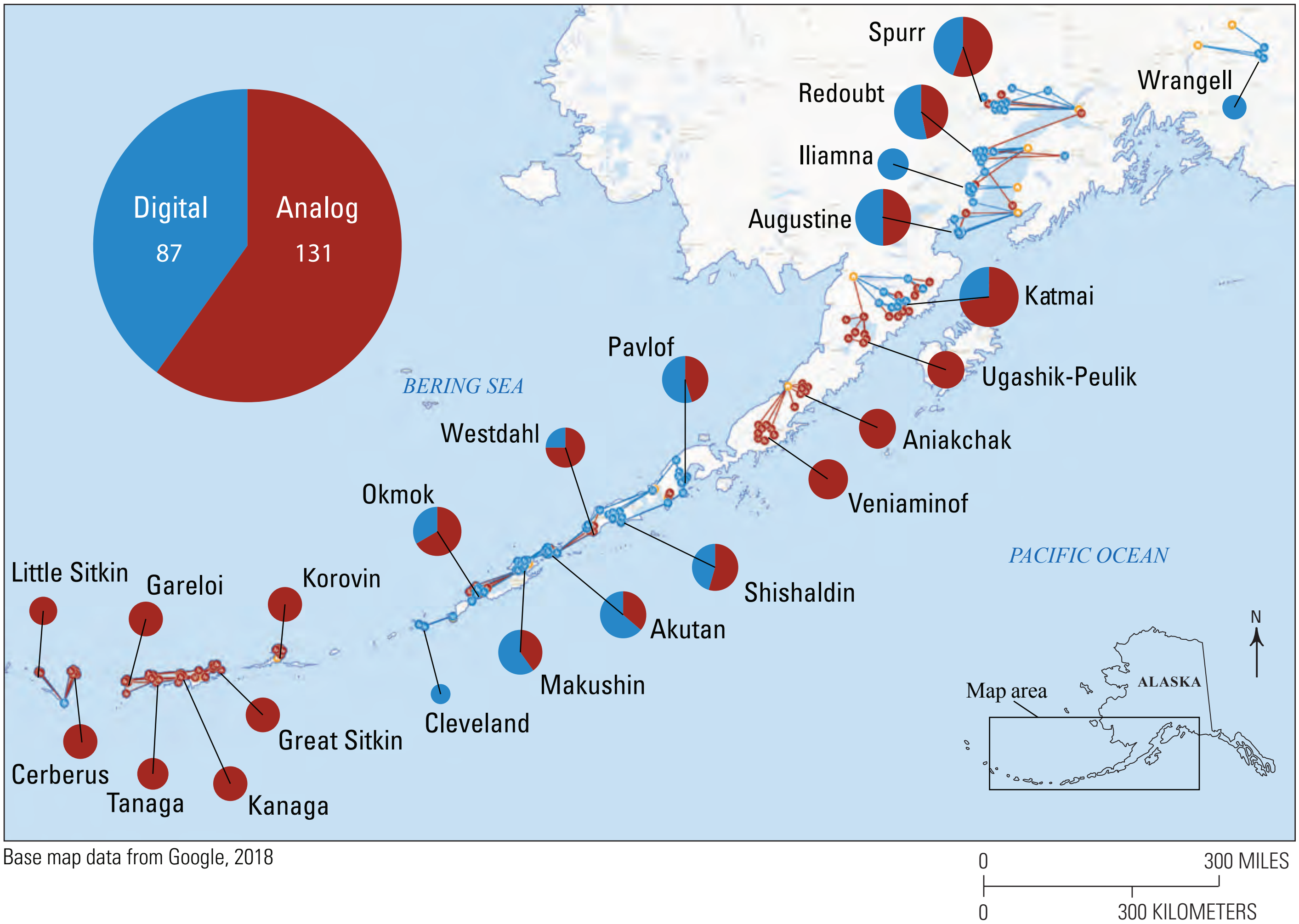

Figure 3. Map showing status of the transition from analog to digital telemetry for the Alaska Volcano Observatory volcano-monitoring network at the end of 2017. The progress for each subnetwork is shown by small circles with the percentage of stations with digital telemetry shown by the blue color. The overall progress is shown in the large circle with the number of sites using digital telemetry (87 sites) and those using analog telemetry (131 sites). Individual sites that record data digitally are shown by blue dots with digital links shown by blue lines. Red dots and lines show analog recording sites and links. The Fourpeaked Mountain network is not shown because the telemetry links are inoperable and will be replaced with digital links at some future date. The Mount Dutton seismograph network is not shown because the sites use either Pavlof Volcano or Shishaldin Volcano telemetry links. See table 3 for a listing of volcanoes being monitored in each subnetwork.

event detection algorithms, which triggered alarms that prompted AVO staff to determine the source.

Each event trigger was visually inspected, and false triggers were deleted. Earthquakes with a P- and S-wave separation of greater than 5 seconds on the closest station were assumed to come from regional sources and typically were not located; however, the trigger was preserved. Each finalized hypocenter meets three minimum parameters—three P-phases, two S-phases, and standard hypocentral errors less than 15 kilometers (km). If on reevaluation, the minimum parameters could not be met, the event was removed from the final catalog listing but retained in the AQMS database. Event picks and location information for events that met AVO minimum parameters were tagged as “finalized” and saved in the AQMS database. Waveforms for individual located events were saved in mini-SEED format. The average root-mean-square (RMS) travel-time error for earthquakes located in 2013–17 was 0.14 seconds, and the average vertical and horizontal hypocentral errors were 1.35 km and 0.94 km, respectively. For the earthquakes appearing in the 2013–17 AVO catalog, 95 percent had an average RMS travel-time error less than 0.32.

At the time of publication, all hypocentral locations of earthquakes in the AVO seismic catalog have been made available as part of the ANSS Comprehensive Earthquake Catalog, ComCat (see https://earthquake.usgs.gov/data/comcat/), and are added on a daily basis. An effort started in 2016 to relocate the entire AVO catalog with the aim of obtaining more consistent locations was completed in 2019 (Power and others, 2019). Continuous waveform data for the majority of AVO seismograph and infrasound stations, whose availability

Table 1. Number of permanent Alaska Volcano Observatory seismograph and infrasound stations/arrays by type and subnetwork at the end of 2017.

[See appendixies 1–4 for station details and operational status; See table 3 for a listing of volcanoes being monitored in each subnetwork.]

Volcano subnetwork	Seismograph stations	Station components	Single-component short-period stations	Three-component short-period stations	Three-component broadband stations	Three-component strong-motion stations	Infrasound stations or arrays
Akutan	12	33	3	1	9	0	1
Aniakchak	6	6	6	0	0	0	0
Augustine	15	39	7	1	8	1	1
Cerberus	6	8	5	1	0	0	0
Cleveland	2	8	2	0	2	0	2
Dutton	5	5	5	0	0	0	0
Fourpeaked	4	7	4	0	0	0	2
Gareloi	6	8	5	1	0	0	0
Great Sitkin	6	8	5	1	0	0	0
Iliamna	8	24	3	4	3	0	0
Kanaga	6	6	6	0	0	0	0
Katmai	20	34	13	2	5	0	0
Korovin	7	9	6	1	0	0	0
Little Sitkin	4	6	3	1	0	0	0
Makushin	7	24	3	0	7	0	1
Okmok	13	21	9	0	4	0	1
Pavlof	7	23	5	3	3	0	4
Redoubt	12	31	6	2	6	0	1
Shishaldin	7	23	5	2	4	0	1
Spurr	17	34	10	1	7	0	0
Tanaga	6	8	5	1	0	0	0
Ugashik-Peulik	7	9	6	1	0	0	0
Veniaminof	9	9	9	0	0	0	0
Westdahl	6	11	5	1	1	0	0
Wrangell	4	10	1	1	2	0	0
Regional Stations	10	15	9	1	1	0	2
Totals	212	419	146	26	62	1	16

Table 2. Number of Alaska Volcano Observatory seismograph and infrasound stations by type and year.

Year	Seismograph stations	Station components	Single-component short-period stations	Three-component short-period stations	Three-component broadband stations	Three-component strong-motion stations	Infrasound stations or arrays
1988	25	29	23	2	0	0	0
1989	28	32	26	2	0	0	0
1990	42	49	39	3	0	0	0
1991	36	42	33	3	0	0	0
1992	39	46	36	3	0	0	0
1993	44	51	41	3	0	0	1
1994	47	58	42	5	0	0	2
1995	57	67	52	5	0	0	2
1996	60	79	49	10	1	0	3
1997	92	125	83	12	2	0	4
1998	108	142	94	14	2	0	4
1999	121	156	106	14	2	0	4
2000	125	162	108	16	2	0	4
2001	138	177	120	17	3	0	4
2002	140	179	124	16	2	0	4
2003	160	217	135	18	9	0	4
2004	182	255	149	20	15	0	4
2005	188	266	151	23	15	0	4
2006	190	275	154	23	15	1	6
2007	193	281	154	22	17	1	6
2008	193	281	154	22	17	1	6
2009	196	291	155	22	19	1	6
2010	200	303	155	22	23	1	8
2011	201	319	158	22	29	1	8
2012	202	326	155	22	32	1	9
2013	204	338	155	22	36	1	9
2014	207	356	156	23	41	1	10
2015	211	377	156	23	48	1	10
2016	211	400	147	26	55	1	13
2017	212	419	146	26	62	1	16

is estimated using IRIS's Gap/Overlap Analysis Tool (GOAT) (Stromme, 2000; appendix 3), are archived and available through the IRIS Data Management Center (https://ds.iris.edu/ds/nodes/dmc/). All continuous data since 2002 are also available from AVO on a Winston server (https://volcanoes.usgs.gov/software/winston/index.shtml). Waveforms for all located events between October 12, 1989, and December 31, 2017, are contained within the AVO AQMS database.

Data from selected seismograph stations operated by the Alaska Earthquake Center (AEC; formerly the Alaska Earthquake Information Center, AEIC), Global Seismograph Network (GSN), Transportable Array (TA), and National Tsunami Warning Center (NTWC) were routinely used in event detection and location by AVO analysts. Station parameters for the AEIC, GSN, TA, and NTWC stations used by AVO are available from the respective agencies and IRIS.

Table 3. Volcanic centers associated with each of the volcano seismic-monitoring subnetworks used by the Alaska Volcano Observatory.

[Seismic-monitoring networks are abbreviated from the volcanoes being monitored. See figure 1 for the location of the volcanoes.]

Volcano subnetwork	Volcanoes monitored
Akutan	Akutan Peak
Aniakchak	Aniakchak Crater
Augustine	Augustine Volcano
Cerberus	Mount Cerberus
Cleveland	Mount Cleveland
Dutton	Mount Dutton
Iliamna	Iliamna Volcano
Fourpeaked	Fourpeaked Mountain
Gareloi	Mount Gareloi
Great Sitkin	Great Sitkin Volcano
Kanaga	Kanaga Volcano
Katmai	Mount Griggs, Mount Katmai, Mount Mageik and Mount Martin, Novarupta, Snowy Mountain, and Trident Volcano
Korovin	Korovin Volcano
Little Sitkin	Little Sitkin Volcano
Makushin	Makushin Volcano
Okmok	Okmok Caldera
Pavlof	Pavlof Volcano
Redoubt	Redoubt Volcano
Shishaldin	Fisher Caldera, Isanotski Peaks, and Shishaldin Volcano
Spurr	Mount Spurr
Tanaga	Tanaga Volcano
Ugashik-Peulik	Ugashik-Peulik Volcano and Ukinrek Maars
Veniaminof	Mount Veniaminof
Westdahl	Fisher Caldera, and Westdahl Peak
Wrangell	Mount Wrangell

Seismic-Velocity Models

AVO currently uses 13 local volcano-specific seismic-velocity models and a regional seismic-velocity model to locate earthquakes at Alaskan volcanoes. All velocity models are one-dimensional models using horizontal layers to approximate the local seismic-velocity structure. Each model, with one exception, assumes a series of constant velocity layers. The single exception is the Akutan velocity model (Power and others, 1996), which has a velocity gradient in a layer overlying a half-space of constant velocity.

One or more vertical cylindrical volumes were used to model the volcanic-source zones for all volcanoes where a local velocity model was used. Earthquakes within these cylindrical volumes were located using a local model, and earthquakes outside of the cylindrical volumes were located using the regional model. The top of each cylinder was set at the summit elevation of the highest volcanic peak located within the cylinder zone, and the bottom was set at a depth of 50 km below sea level. Most cylindrical volumes had a radius of 20 km with the exception of the cylinders centered on Shishaldin and Mount Veniaminof. The cylinder centered on Shishaldin had a radius of 30 km to encompass Fisher Caldera and Isanotski Volcano. The cylinder centered on Mount Veniaminof also had a radius of 30 km because of the large size of the volcanic edifice. The maximum elevation for the regional model was set at 3.2 km, the elevation of the highest volcano in the Aleutian arc.

The Akutan Peak, Augustine (Power, 1988), Iliamna (Roman and others, 2001), Makushin (Cheryl Searcy, USGS, written commun., 2010), Okmok Caldera (Masterlark and others, 2010), Tanaga (John Power, USGS, written commun., 2005), Mount Veniaminof (Sánchez, 2005), and Westdahl Peak (Dixon and others, 2005) velocity models were used to locate hypocenters that fell within cylindrical volumes described above, centered on each respective volcano. Five overlapping cylinders defined the volume in which the Mount Spurr velocity model (Jolly and others, 1994) was used, 4 overlapping cylinders defined the volume for the Redoubt Volcano velocity model (Lahr and others, 1994), and 4 overlapping cylinders defined the volume for the Mount Katmai model (Searcy, 2003). The Andreanof Islands velocity model, modified from that in Toth and Kisslinger (1984), was used to locate earthquakes within a volume defined by three cylinders centered on Kanaga Volcano, Mount Moffet (located near Adak), and Great Sitkin Volcano. The Cold Bay velocity model (McNutt and Jacob, 1986) was used to locate earthquakes that fell within cylindrical volumes centered on Mount Dutton, Pavlof Volcano, and Shishaldin Volcano. Earthquakes located at Fisher Caldera and Isanotski Volcano fell within the cylindrical volume centered on Shishaldin Volcano. Specific velocity models for the remaining monitored volcanoes were not available in the reporting period and the regional velocity model of Fogleman and others (1993) was used to locate earthquakes near these volcanoes. The regional velocity model and volcano-specific models used to locate earthquakes in this report are summarized in appendix 5. The cylindrical model parameters and figures showing the volcanic-source zones modeled by multiple cylinders are shown in appendix 6.

Seismicity

Between 2013 and 2017, AVO located 28,172 earthquakes, an average of 5,634 earthquakes per year (3,840 in 2013, 5,819 in 2014, 5,297 in 2015, 6,151 in 2016, and 7,065 in 2017) at 34 volcanic centers with seismograph subnetworks (fig. 4, appendix 1). Of the earthquakes located in 2013–17, 82 percent (4,628 earthquakes per year) were located within 20 km of a monitored volcanic center. The numbers of located earthquakes associated with volcanic centers for 2013–17 are shown in table 4. The numbers of located earthquakes in the AVO catalog by year are shown in figure 4 and table 5. A summary file of origin times, hypocenters, magnitudes, and location quality statistics for earthquakes located in 2013–17 is included in a data supplement to this report with data headers described in appendix 7.

Using the AVO earthquake catalog from the period in which an Earthworm based system was used for event detection (2002–17), the magnitude of completeness (M_c) for each subnetwork was calculated (table 4). M_c is the magnitude threshold above which we are reasonably certain that an event

Table 4. Number of earthquakes located by the Alaska Volcano Observatory within 20 kilometers of monitored volcanic centers in in 2013–17.

[Volcano names used for seismic-monitoring subnetworks are abbreviated; see figure 1 for complete names. M^c, magnitude of completeness for Alaska Volcano Observatory seismograph subnetworks during the period March 2002–December 2017; --, not enough data to calculate a M_c]

Volcano subnetwork	Earthquakes located in 2013	Earthquakes located in 2014	Earthquakes located in 2015	Earthquakes located in 2016	Earthquakes located in 2017	M_c
Akutan	147	293	117	238	228	0.3
Aniakchak	48	0	1	35	60	0.1
Augustine	102	125	162	836	367	0.1
Cerberus	0	1,722	903	57	96	0.5
Cleveland	--	1	1	1	1	--
Dutton	11	4	1	12	1	1.0
Fourpeaked	77	1	0	1	33	0.7
Gareloi	10	4	20	262	268	1.2
Great Sitkin	77	18	24	100	764	0.4
Iliamna	443	28	8	4	18	−0.2
Kanaga	143	143	57	127	53	1.2
Katmai-North	111	129	179	193	139	0.8
Katmai-Central	162	297	497	310	852	0.4
Katmai-South	223	381	454	139	323	0.3
Korovin	186	282	108	114	114	0.5
Little Sitkin	3	38	115	32	39	0.0
Makushin	458	413	707	692	857	0.5
Okmok	39	42	45	27	32	0.8
Pavlof	9	25	18	11	29	1.0
Redoubt	189	96	173	170	195	0.4
Shishaldin	3	18	33	38	32	0.6
Spurr	330	577	513	1,686	747	0.2
Tanaga	98	145	85	72	462	1.1
Ugashik-Peulik	19	36	9	7	7	0.9
Veniaminof	7	18	0	0	33	1.1
Westdahl	22	12	53	96	67	1.1
Wrangell	0	0	0	0	16	0.9
Totals	2,917	4,848	4,283	5,260	5,833	--

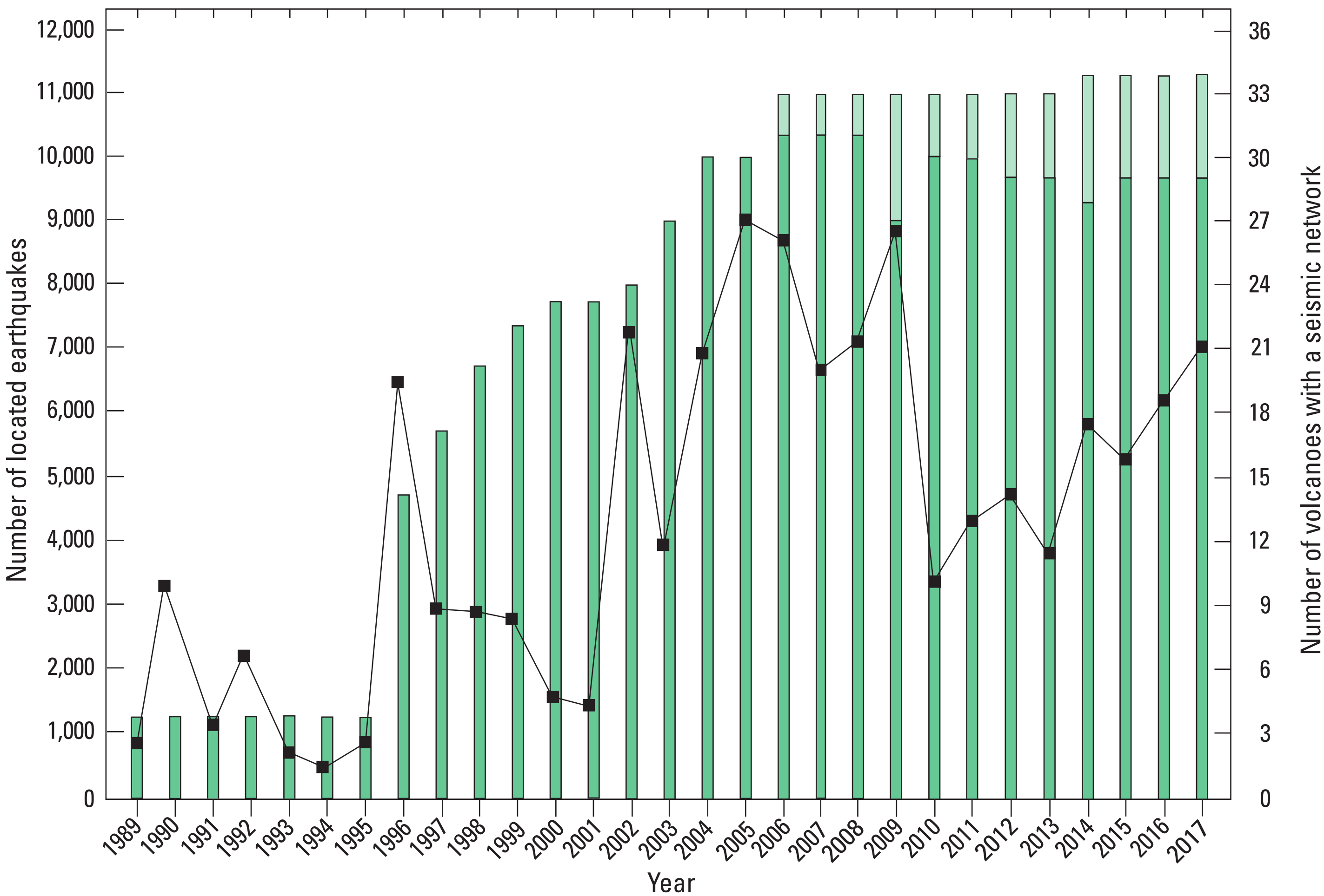

Figure 4. Number of earthquakes located per year in the Alaska Volcano Observatory earthquake catalog, 1989–2017 (black line), and number of volcanoes with a seismograph network per year (green bars). The lighter green color indicates the number of volcanoes with seismograph networks that are not included on the formal list of monitored volcanoes.

Table 5. Number of earthquakes located per year in the Alaska Volcano Observatory (AVO) earthquake catalog, 1989–2017.

Year	Number of earthquakes located per year	Number of earthquakes located per year within 20 kilometers of a monitored volcano	Volcanoes with an AVO seismograph network
1989	911	892	4
1990	3,285	3,148	4
1991	1,119	1,064	4
1992	2,184	2,104	4
1993	697	592	4
1994	441	407	4
1995	850	760	4
1996	6,466	4,259	14
1997	2,930	1,783	17
1998	2,873	1,886	20
1999	2,769	2,343	22
2000	1,551	1,225	22

Table 5. Number of earthquakes located per year in the Alaska Volcano Observatory (AVO) earthquake catalog, 1989–2017.—Continued

Year	Number of earthquakes located per year	Number of earthquakes located per year within 20 kilometers of a monitored volcano	Volcanoes with an AVO seismograph network
2001	1,427	1,122	23
2002	7,242	6,578	24
2003	3,911	3,264	27
2004	6,928	6,105	30
2005	9,012	8,146	32
2006	8,666	7,782	33
2007	6,664	5,660	33
2008	7,097	5,318	33
2009	8,829	7,438	33
2010	3,405	2,846	33
2011	4,364	3,651	33
2012	4,791	4,188	33
2013	3,840	2,917	33
2014	5,819	4,848	34
2015	5,297	4,283	34
2016	6,151	5,260	34
2017	7,065	5,833	34

of magnitude M_c or greater was detected. The M_c was determined using a maximum likelihood estimate of the inflection point in the frequency magnitude distribution using the seismology analysis software ZMAP (Wiemer, 2001). The M_c ranged from −0.2 to 1.2 for the individual subnetworks.

A summary of notable events located in the years covered by this AVO earthquake catalog were presented in past publications (appendix 8). Because a description of the AVO seismograph network is no longer an annual publication, notable seismic activity is included in the AVO annual summaries. Table 6 summarizes the notable seismic activity presented in detail in the annual AVO summaries of volcanic activity with references for the AVO summaries that cover the reporting period of this report in table 7.

Table 6. Summary of notable seismic activity at Alaskan volcanoes for 2013–17.

[Details can be found in the Alaska Volcano Observatory annual summaries of volcanic activity in Alaska referenced in table 7]

Volcano	Period of activity	Type of activity
Akutan Volcano	January 2013 July 2014	Triggered seismicity Earthquake swarm
Aniakchak Crater	Intermittent in 2013	Earthquake swarm
Augustine Volcano	February 2016–December 2017	Earthquake swarm
Bogoslof Island	December 2016–December 2017	Eruption
Mount Cerberus	June 2014 January–May 2015	Earthquake swarm Earthquake swarm
Mount Cleveland	Intermittent 2013–17	Explosions
Fourpeaked Mountain	April–May 2013 September-October, 2016	Seismic unrest Earthquake swarm
Mount Gareloi	July–August 2013	Felt earthquakes
Great Sitkin Volcano	July–August 2013 January, July 2017	Earthquake Swarm Earthquake swarms

Table 6. Summary of notable seismic activity at Alaskan volcanoes for 2013–17.—Continued

[Details can be found in the Alaska Volcano Observatory annual summaries of volcanic activity in Alaska referenced in table 7]

Volcano	Period of activity	Type of activity
Iliamna Volcano	July 2015	Large tectonic earthquake
Kanaga Volcano	March 2014	Earthquake swarm
Mount Katmai/ Mount Martin	October 2014	Earthquake swarm
Korovin Volcano	April–August 2016	Tremor
Makushin Volcano	Intermittent 2013–17	Earthquake swarms, tremor
Okmok Caldera	March, September, and October 2013 Intermittent in 2013 September 2016	Earthquake swarms Tremor Tremor
Pavlof Volcano	May–August 2013 May–June 2014 November 2014–January 2015 2016	Eruption Eruption Eruption Eruption
Mount Recheshnoi	Intermittent 2013–17	Earthquake swarm
Shishaldin Volcano	January 2013 March 2014–December 2017	Increased seismicity Small eruptions
Mount Spurr	June and September 2014 October–December 2015 Throughout 2015–17 June–July 2016	Earthquake swarm Earthquake swarm Earthquake swarm Earthquake swarm
Tanaga Volcano	February-August 2014	Earthquake swarm
Ugashik-Peulik Volcano	March 2015	Large tectonic earthquake
Mount Veniaminof	June 2013–January 2015 September–December 2015	Effusive eruption Seismic unrest

Table 7. Alaska Volcano Observatory Annual Summary reports for 2013–2015.

[Summary reports for 2016 and 2017 are not yet published]

Year	Report citation
2013	Dixon, J.P., Cameron, C.E., McGimsey, R.G., Neal, C.A., and Waythomas, C.F., 2015, 2013 Volcanic activity in Alaska—Summary of events and response of the Alaska Volcano Observatory: U.S. Geological Survey Scientific Investigations Report 2015–5110, 92 p., https://dx.doi.org/10.3133/sir20155110.
2014	Cameron, C.E., Dixon, J.P., Neal, C.A., Waythomas, C.F., Schaefer, J.R., and McGimsey, R.G., 2017, 2014 Volcanic activity in Alaska—Summary of events and response of the Alaska Volcano Observatory: U.S. Geological Survey Scientific Investigations Report 2017–5077, 81 p., https://doi.org/10.3133/sir20175077.
2015	Dixon, J.P., Cameron, C.E., Iezzi, A.M., and Wallace, K., 2017, 2015 Volcanic activity in Alaska—Summary of events and response of the Alaska Volcano Observatory: U.S. Geological Survey Scientific Investigations Report 2017–5104, 81 p., https://doi.org/10.3133/sir20175104.

Summary

Between January 1, 2013, and December 31, 2017, AVO located 28,172 earthquakes or an average of 5,634 earthquakes per year, of which an average of 4,628 occurred within 20 km of the 34 volcanoes with seismograph subnetworks. There was significant seismic activity at 22 volcanoes in 2013–17 (Akutan Peak, Aniakchak Crater, Augustine, Bogoslof Island, Mount Cerberus, Mount Cleveland, Fourpeaked Mountain, Mount Gareloi, Great Sitkin, Ilimana, Kanaga, Korovin, Makushin, Martin, Okmok Caldera, Pavlof, Mount Recheshnoi, Shishaldin, Mount Spurr, Tanaga, Ugashik-Peulik, and Mount Veniaminof). Instrumentation highlights for 2013–17 were the establishment of two seismograph and infrasound stations near Mount Cleveland, the start of a transition from analog to digital telemetry, and increased number of broadband seismometers and infrasound sensors. The operational highlight was the return of seismic monitoring at Korovin and Ugashik-Peulik Volcanoes and their return to the seismic monitored list following network repairs. This catalog includes locations, magnitudes, and statistics of the earthquakes located in 2013–17.

Earthquake epicenters at volcanic centers located in 2013–17 with the AVO seismograph network are shown in appendix 1. Locations for all AVO stations are contained in appendix 2 with maps showing the locations of stations with respect to individual volcanoes in appendix 1. Each station's operational status for the catalog period is shown in appendixes 3 and 4. Included with this report is a list of earthquakes located in 2013–17 in which a description of the data in the summary listing is in appendix 7. Previous AVO earthquake catalogs are listed in appendix 8. Selected papers that used data from the AVO seismograph and infrasound networks are listed in appendix 9.

Available for download with this report is a data supplement (available only online at https://doi.org/10.3133/ds1115) that is a compressed file containing a summary listing of earthquake hypocenters and a metadata file in the form of a dataless SEED volume for the AVO seismograph network. Continuous waveform data for the majority of AVO seismograph stations, whose availability is displayed using IRIS's Gap/Overlap Analysis Tool (appendix 3), are archived and available through IRIS (http://www.iris.edu/). Archives of waveform data are also maintained at AVO offices.

References Cited

Cameron, C.E., and Schaefer, J.R., 2016, Historically active volcanoes of Alaska: Alaska Division of Geological & Geophysical Surveys Miscellaneous Publication 133, v. 2, 1 sheet, scale 1:3,000,000, https://doi.org/10.14509/20181.

Cameron, C.E., Dixon, J.P., Neal, C.A., Waythomas, C.F., Schaefer, J.R., and McGimsey, R.G., 2017, 2014 Volcanic activity in Alaska—Summary of events and response of the Alaska Volcano Observatory: U.S. Geological Survey Scientific Investigations Report 2017–5077, 81 p., https://doi.org/10.3133/sir20175077.

Dixon, J.P., Power, J.A., and Stihler, S.D., 2005, Seismic observations of Westdahl Volcano and Western Unimak Island, Alaska—1999–2005: EOS, Transactions American Geophysical, v. 86, no. 52, fall meeting supplement, abstract S11B-0169.

Dixon, J.P., Cameron, C.E., McGimsey, R.G., Neal, C.A., and Waythomas, C.F., 2015, 2013 Volcanic activity in Alaska—Summary of events and response of the Alaska Volcano Observatory: U.S. Geological Survey Scientific Investigations Report 2015–5110, 92 p., https://doi.org/10.3133/sir20155110.

Dixon, J.P., Cameron, C.E., Iezzi, A.M., and Wallace, K., 2017, 2015 Volcanic activity in Alaska—Summary of events and response of the Alaska Volcano Observatory: U.S. Geological Survey Scientific Investigations Report 2017–5104, 61 p., https://doi.org/10.3133/sir20175104.

Fogleman, K.A., Lahr, J.C., Stephens, C.D., and Page, R.A., 1993, Earthquake locations determined by the southern Alaska seismograph network for October 1971 through May 1989: U.S. Geological Survey Open-File Report 93–309, 54 p., https://doi.org/10.3133/ofr93309.

Johnson, C.E., Bittenbinder, A., Bogaert, D., Dietz, L., and Kohler, W., 1995, Earthworm—A flexible approach to seismograph network processing: Incorporated Research Institutions for Seismology Newsletter, v. 14, no. 2, p. 1–4.

Jolly, A.D., Page, R.A., and Power, J.A., 1994, Seismicity and stress in the vicinity of Mt. Spurr volcano, south-central Alaska: Journal of Geophysical Research, v. 99, no. B8, p. 15305–15318, https://doi.org/10.1029/94JB00136.

Haney, M.M., Power, J.A., West, M., and Michaels, P., 2012, Causal instrument corrections for short-period and broadband seismometers: Seismological Research Letters, v. 83, no. 5, p. 834-845, https://doi.org/10.1785/0220120031.

Hauksson, E., Jones, L.M., and Shakal, A., 2003, TriNet—A modern ground motion seismic network, *in* Jennings, P., Kanamori, H., and Lee, W., eds., International handbook of earthquake and engineering seismology, vol. 81B: International Association of Seismology and Physics of the Earth's Interior centennial publication, p. 1275–1284.

International Federation of Digital Seismograph Networks, 2012, SEED reference manual—Standard for the Exchange of Earthquake Data, version 2.4: International Federation of Digital Seismograph Networks, 224 p., accessed April 9, 2019, at https://www.fdsn.org/seed_manual/SEEDManual_V2.4.pdf.

Klein, F.W., 2002, User's Guide to HYPOINVERSE-2000, a Fortran program to solve for earthquake locations and magnitudes, U.S. Geological Survey Open-File Report 02–171, 123 p., https://doi.org/10.3133/ofr02171.

Lahr, J.C., Chouet, B.A., Stephens, C.D., Power, J.A., and Page, R.A., 1994, Earthquake classification, location, and error analysis in a volcanic environment—Implications for the magmatic system of the 1989–90 eruptions at Redoubt Volcano, Alaska: Journal of Volcanology and Geothermal Research, v. 62, no. 1–4, p. 137–151, https://doi.org/10.1016/0377-0273(94)90031-0.

Masterlark, T., Haney, M., Dickinson, H., Fournier, T., and Searcy, C.K., 2010, Rheological and structural controls on the deformation of Okmok Volcano, Alaska—FEMs, InSAR, and ambient noise tomography: Journal of Geophysical Research. v. 115, no. B2, https://doi.org/10.1029/2009JB006324.

McChesney, P.J., 1999, McVCO handbook 1999: U.S. Geological Survey Open-File Report 99–361, 51 p., https://doi.org/10.3133/ofr99361.

McNutt, S.R., and Jacob, K.H, 1986, Determination of large-scale velocity structure of the crust and upper mantle in the vicinity of Pavlof Volcano, Alaska: Journal of Geophysical Research, v. 91, no. B5, p. 5013–5022., https://doi.org/10.1029/JB091iB05p05013.

Power, J.A., 1988, Seismicity associated with the 1986 eruption of Augustine Volcano, Alaska: Fairbanks, University of Alaska Fairbanks, Master's thesis, 149 p.

Power, J.A., Paskievitch, J.F., Richter, D.H., McGimsey, R.G., Stelling, P., Jolly, A.D., and Fletcher, H.J., 1996, 1996 seismicity and ground deformation at Akutan Volcano, EOS, Transactions American Geophysical Union, v. 77, no. 46, fall meeting supplement, p. 514.

Power, J.A., Friberg, P.A., Haney, M.M., Parker, T., Stihler, S.D., and Dixon, J.P., 2019, A unified catalog of earthquake hypocenters and magnitudes at volcanoes in Alaska—1989 to 2018: U.S. Geological Survey Scientific Investigations Report 2019–5037, 17 p., https://doi.org/10.3133/sir20195037.

Rogers, J.A., Maslak, S., Lahr, J.C., 1980, A seismic electronic system with automatic calibration and crystal reference: U.S. Geological Survey Open-File Report 80–324, 48 p.

Roman, D.C., Power, J.A., Moran, S.C., Cashman, K.V., and Stihler, S.D., 2001, Unrest at Iliamna Volcano, Alaska in 1996—Evidence for a magmatic intrusion: EOS, Transactions American Geophysical Union, v. 82, no. 47, fall meeting supplement, p. 1329.

Sánchez, J.J., 2005, Volcano seismology from around the World—Case studies from Mount Pinatubo (Philippines), Galeras (Columbia), Mount Wrangell and Mount Veniaminof (Alaska): Fairbanks, University of Alaska Fairbanks, Ph.D. dissertation, 208 p.

Stromme, S., 2000, Gap/Overlap Analysis Tool (GOAT): Incorporated Research Institutions for Seismology DMS Newsletter, v. 2, no. 1.

Searcy, C.K., 2003, Station corrections for the Katmai Region seismograph network: U.S. Geological Survey Open-File Report 03–403, 16 p., https://doi.org/10.3133/ofr03403.

Toth, T., and Kisslinger, C., 1984, Revised focal depths and velocity model for local earthquakes in the Adak seismic zone: Bulletin of the Seismological Society of America, v. 74, no. 4, p. 1349–1360.

U.S. Geological Survey, 2018, Jiggle—A graphical earthquake analysis tool: U.S. Geological Survey web page, accessed October 1, 2018, at http://pasadena.wr.usgs.gov/jiggle/.

Wiemer, S., 2001, A software package to analyze seismicity—ZMAP: Seismological Research Letters, v. 72, no. 3, p. 373–382, https://doi.org/10.1785/gssrl.72.3.373.

Appendix 1. Maps of Monitored Volcanoes with Earthquake Hypocenters in 2013–17

The location of earthquake hypocenters and the seismograph stations used by the Alaska Volcano Observatory to locate earthquakes by seismograph subnetwork, showing their relation to the monitored volcanic centers, are included in appendix 1. The seismograph subnetwork that covers the Katmai volcanic cluster is broken into two figures, one covering the northern end of the group and the other the southern end.

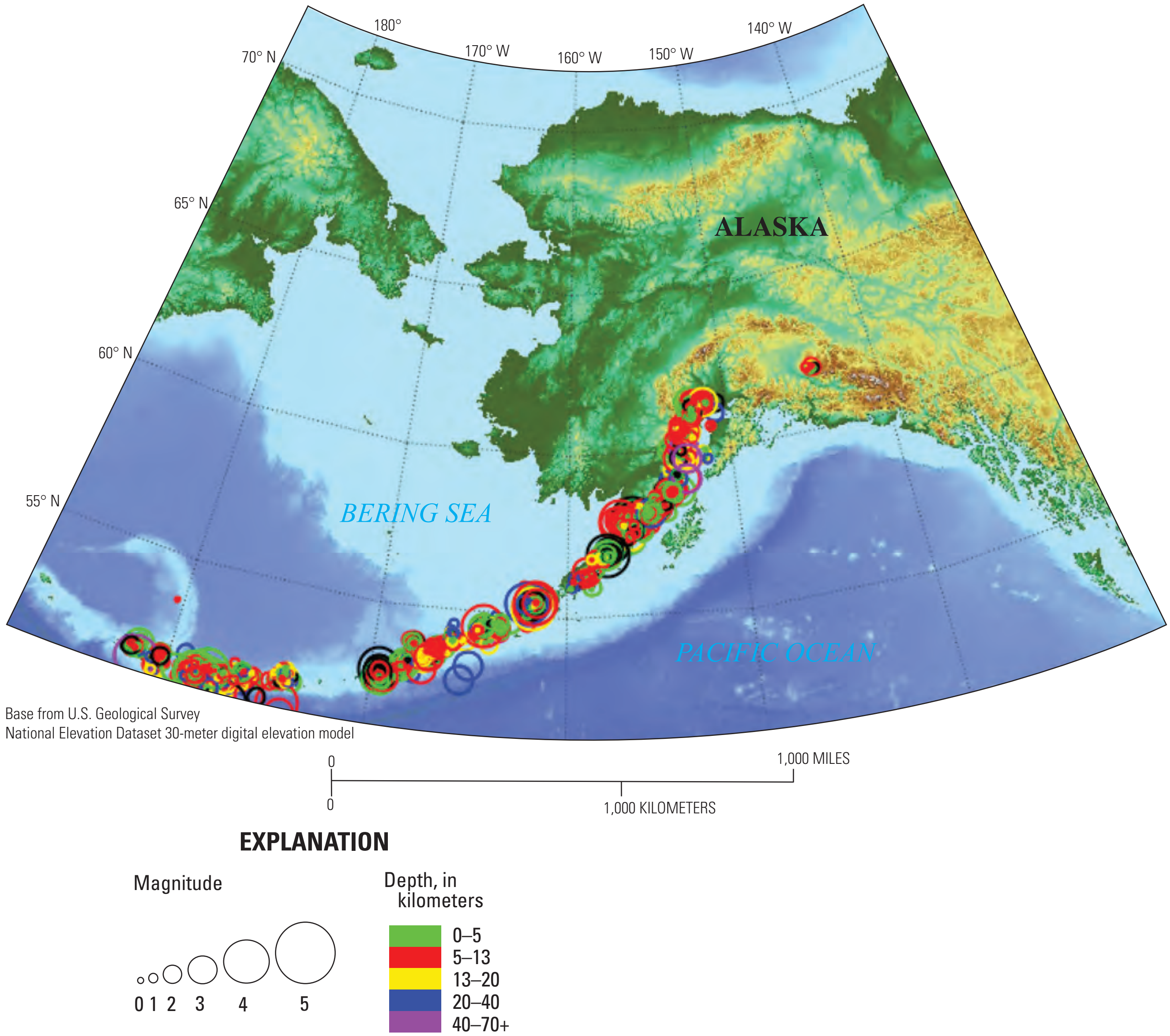

Figure 1.1. Map of Alaska showing all earthquakes (open circles) located by the Alaska Volcano Observatory in 2013–17. Earthquakes are scaled by magnitude and the color of the symbols varies with depth.

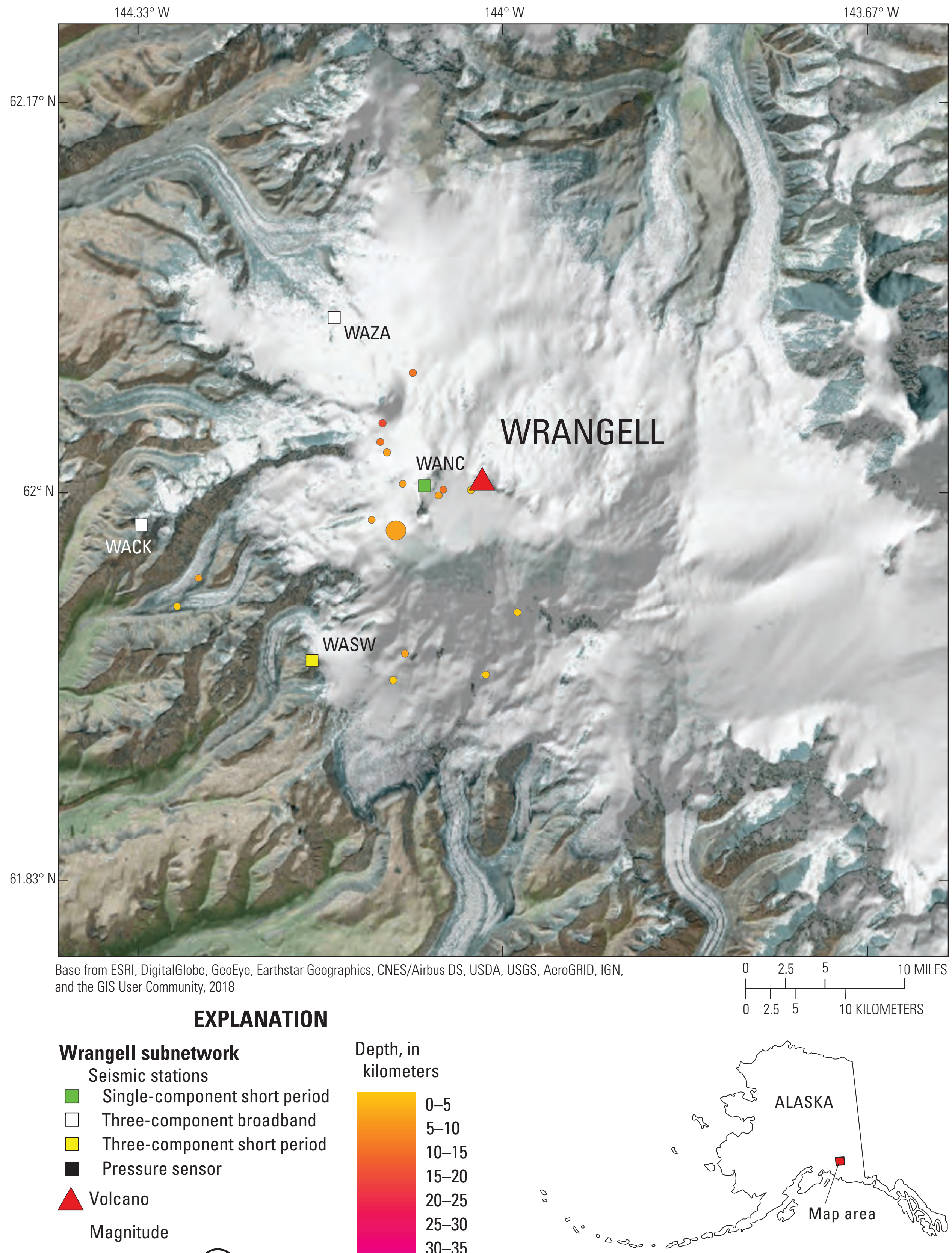

Figure 1.2. Map showing summary plot of earthquakes located by the Alaska Volcano Observatory with the seismic-monitoring subnetwork at Mount Wrangell in 2013–17.

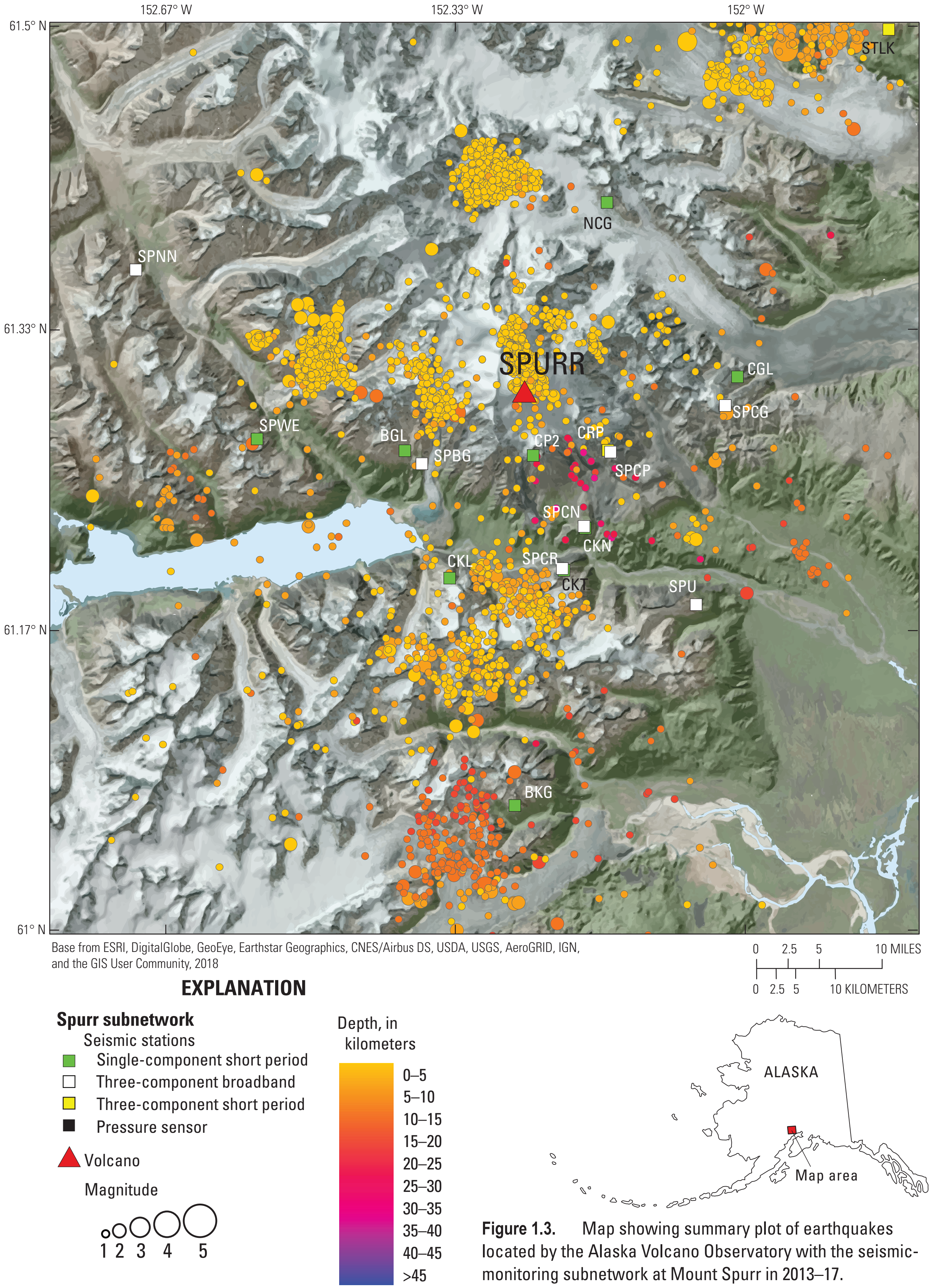

Figure 1.3. Map showing summary plot of earthquakes located by the Alaska Volcano Observatory with the seismic-monitoring subnetwork at Mount Spurr in 2013–17.

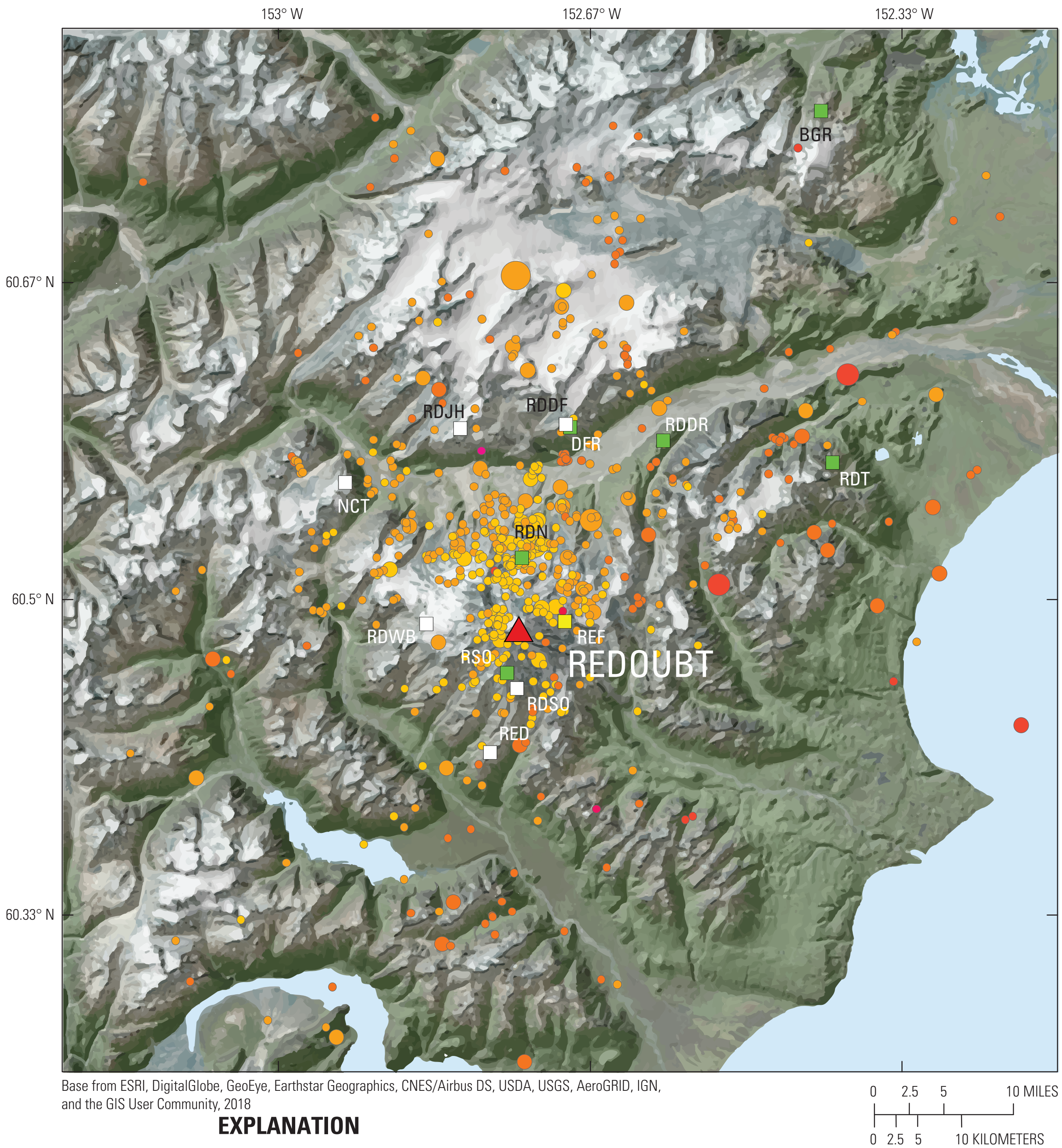

Base from ESRI, DigitalGlobe, GeoEye, Earthstar Geographics, CNES/Airbus DS, USDA, USGS, AeroGRID, IGN, and the GIS User Community, 2018

EXPLANATION

Redoubt subnetwork

Seismic stations
- Single-component short period
- Three-component broadband
- Three-component short period
- Pressure sensor

Volcano

Magnitude

1 2 3 4 5

Depth, in kilometers

0–5
5–10
10–15
15–20
20–25
25–30
30–35
35–40
40–45
>45

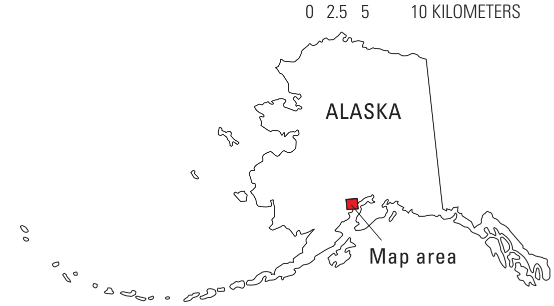

Figure 1.4. Map showing summary plot of earthquakes located by the Alaska Volcano Observatory with the seismic-monitoring subnetwork at Redoubt Volcano in 2013–17.

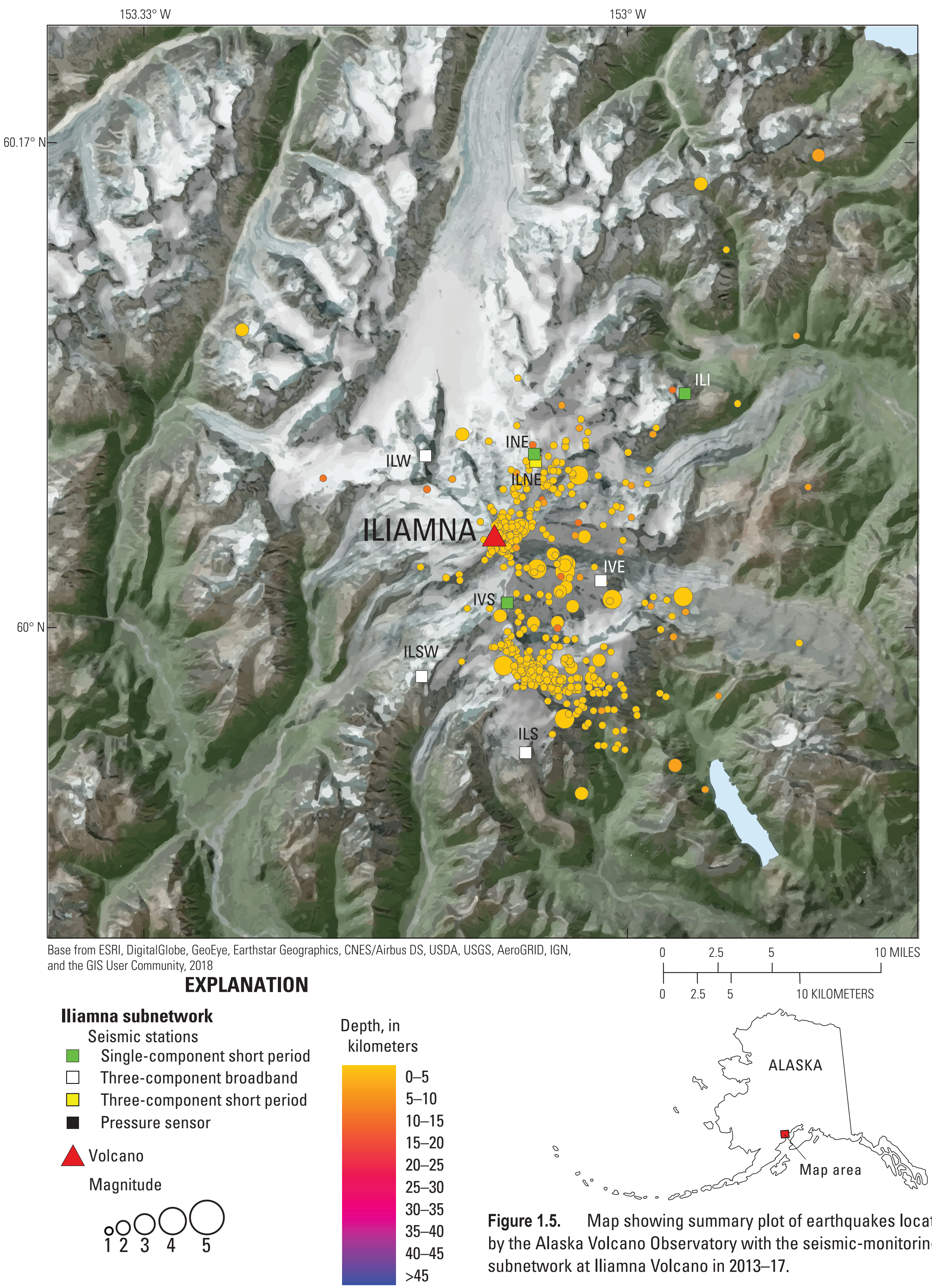

Figure 1.5. Map showing summary plot of earthquakes located by the Alaska Volcano Observatory with the seismic-monitoring subnetwork at Iliamna Volcano in 2013–17.

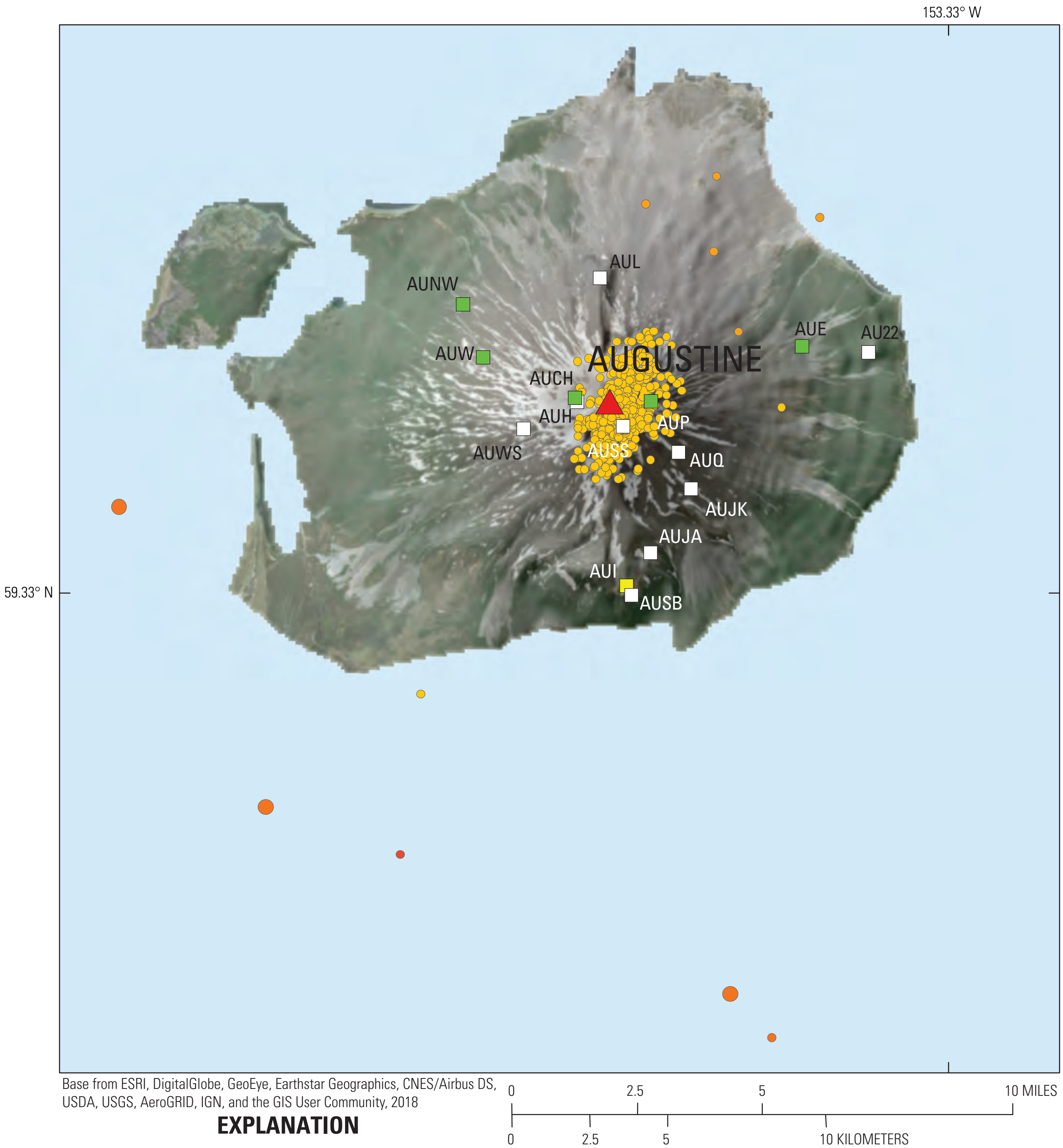

Base from ESRI, DigitalGlobe, GeoEye, Earthstar Geographics, CNES/Airbus DS, USDA, USGS, AeroGRID, IGN, and the GIS User Community, 2018

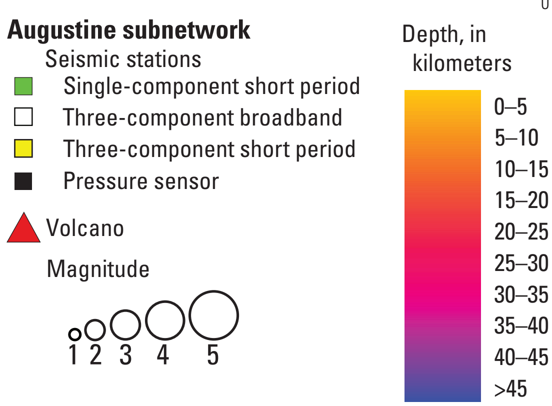

Figure 1.6. Map showing summary plot of earthquakes located by the Alaska Volcano Observatory with the seismic-monitoring subnetwork at Augustine Volcano in 2013–17.

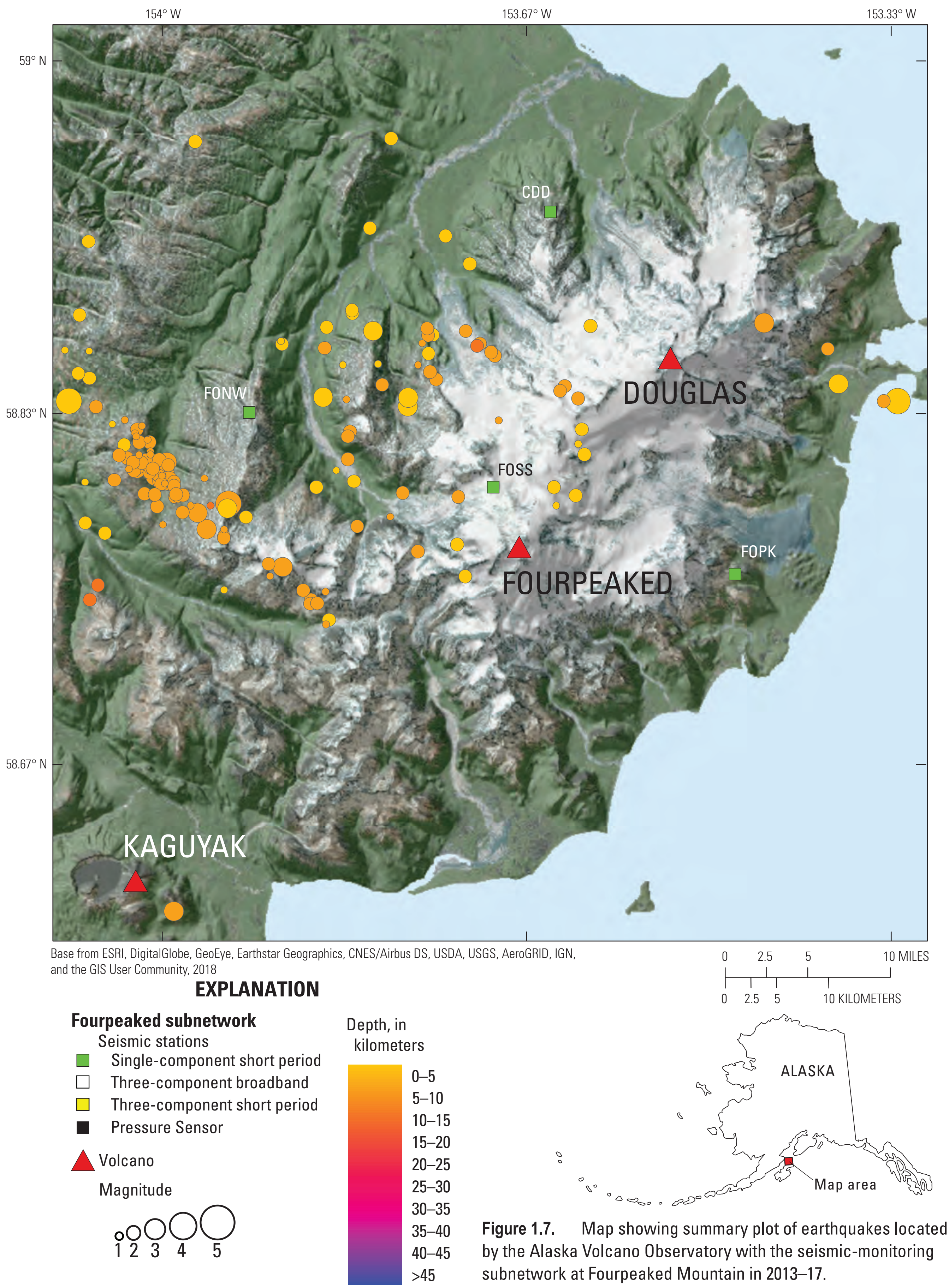

Figure 1.7. Map showing summary plot of earthquakes located by the Alaska Volcano Observatory with the seismic-monitoring subnetwork at Fourpeaked Mountain in 2013–17.

Figure 1.7

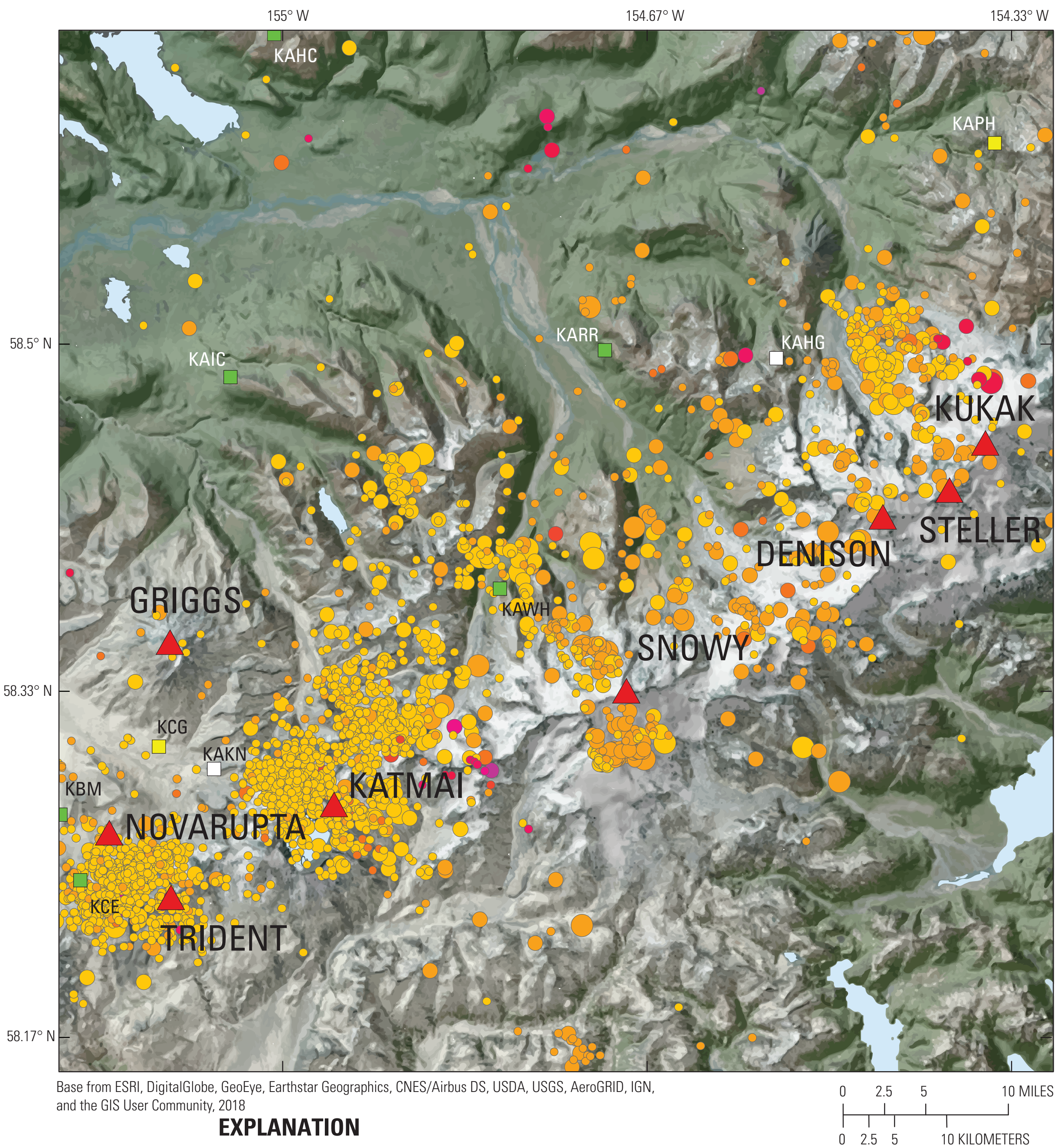

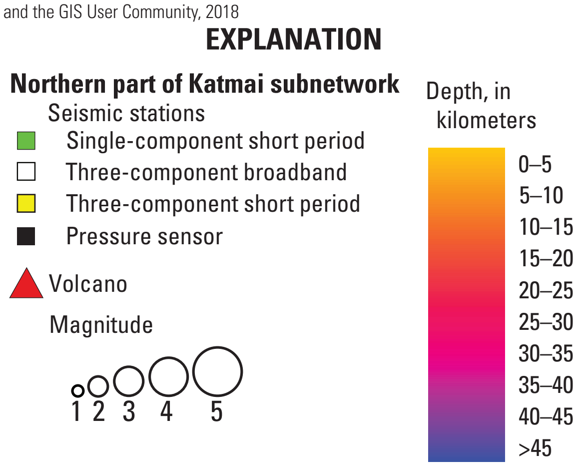

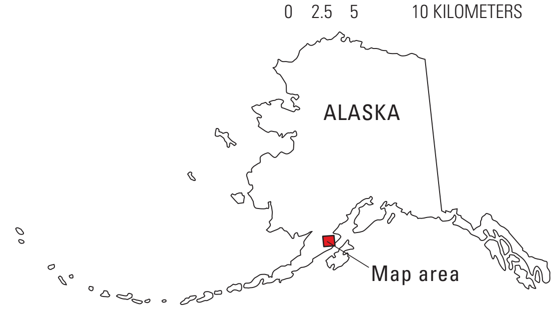

Figure 1.8. Map showing summary plot of earthquakes located by the Alaska Volcano Observatory with the seismic-monitoring subnetwork for the northern part of the Katmai volcanic cluster in 2013–17.

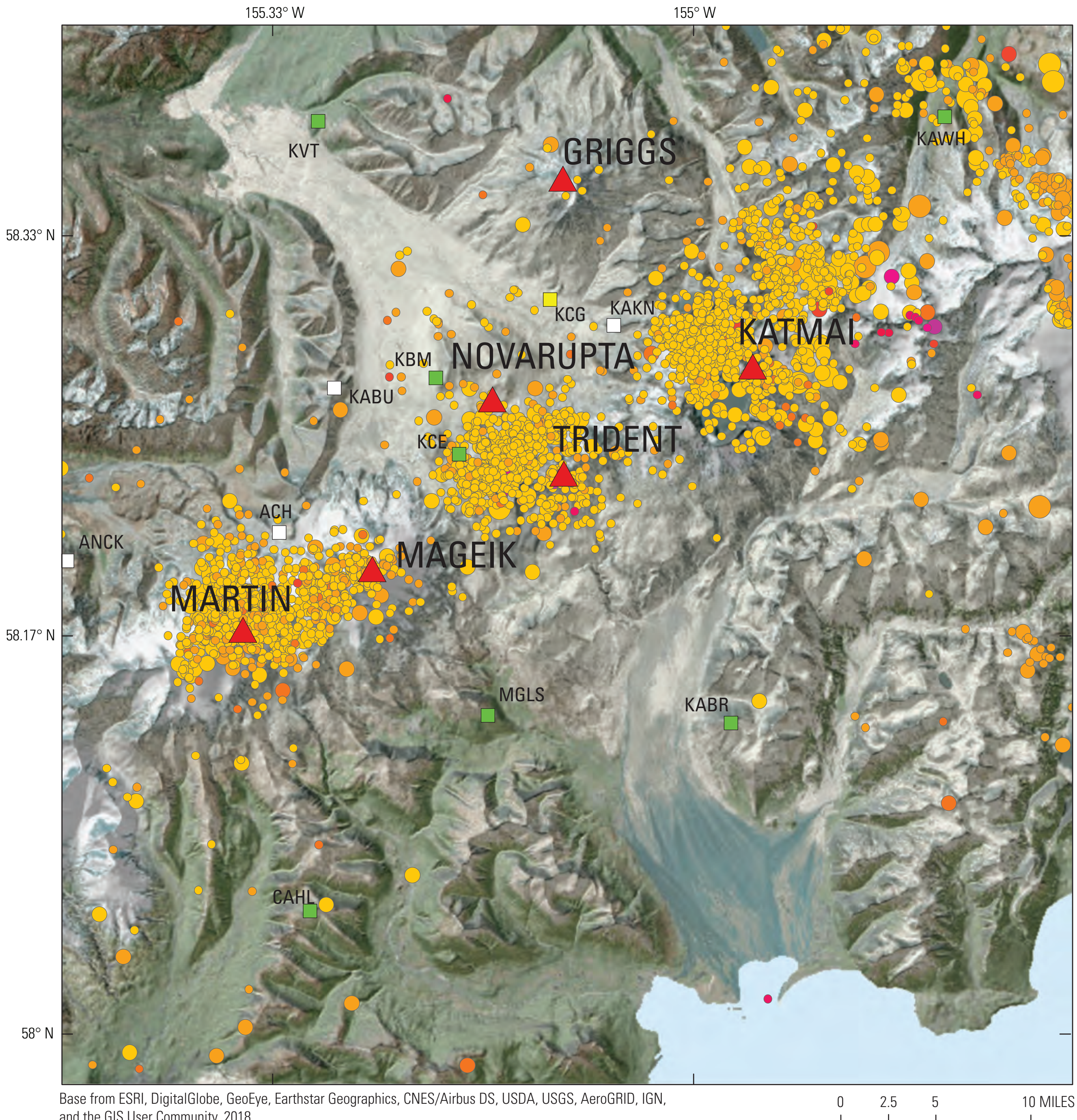

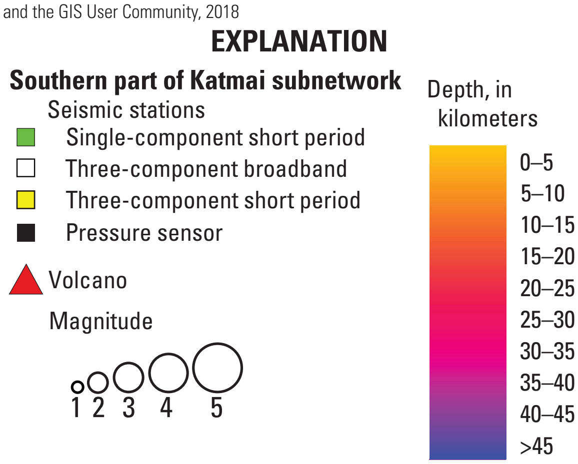

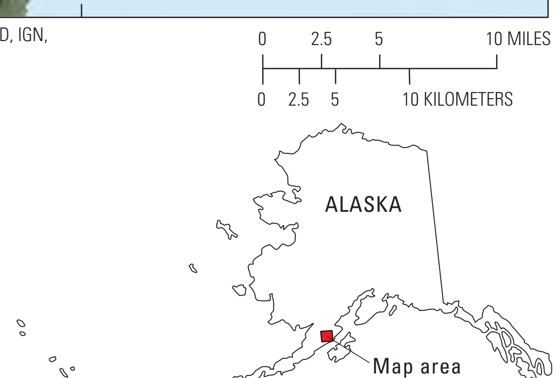

Figure 1.9. Map showing summary plot of earthquakes located by the Alaska Volcano Observatory with the seismic-monitoring subnetwork for the southern part of the Katmai volcanic cluster in 2013–17.

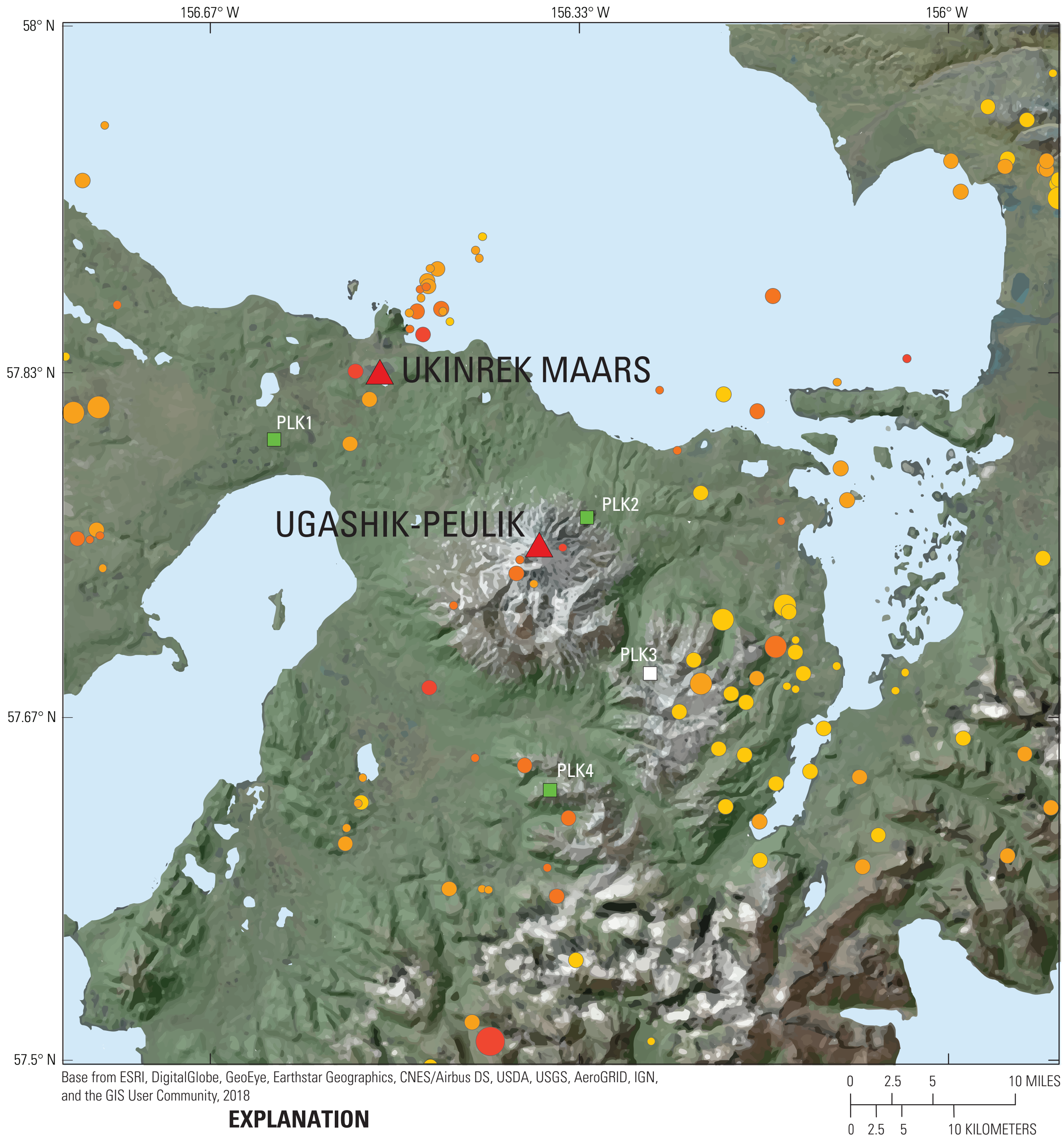

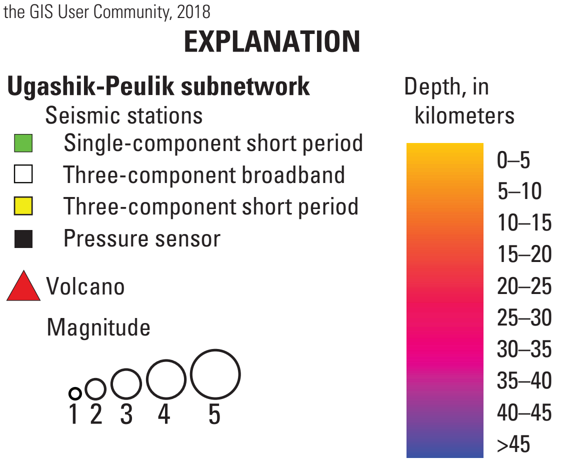

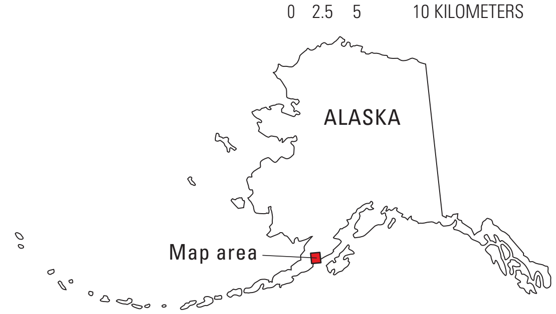

Figure 1.10. Map showing summary plot of earthquakes located by the Alaska Volcano Observatory with the seismic-monitoring subnetwork at Ugashik-Peulik Volcano in 2013–17.

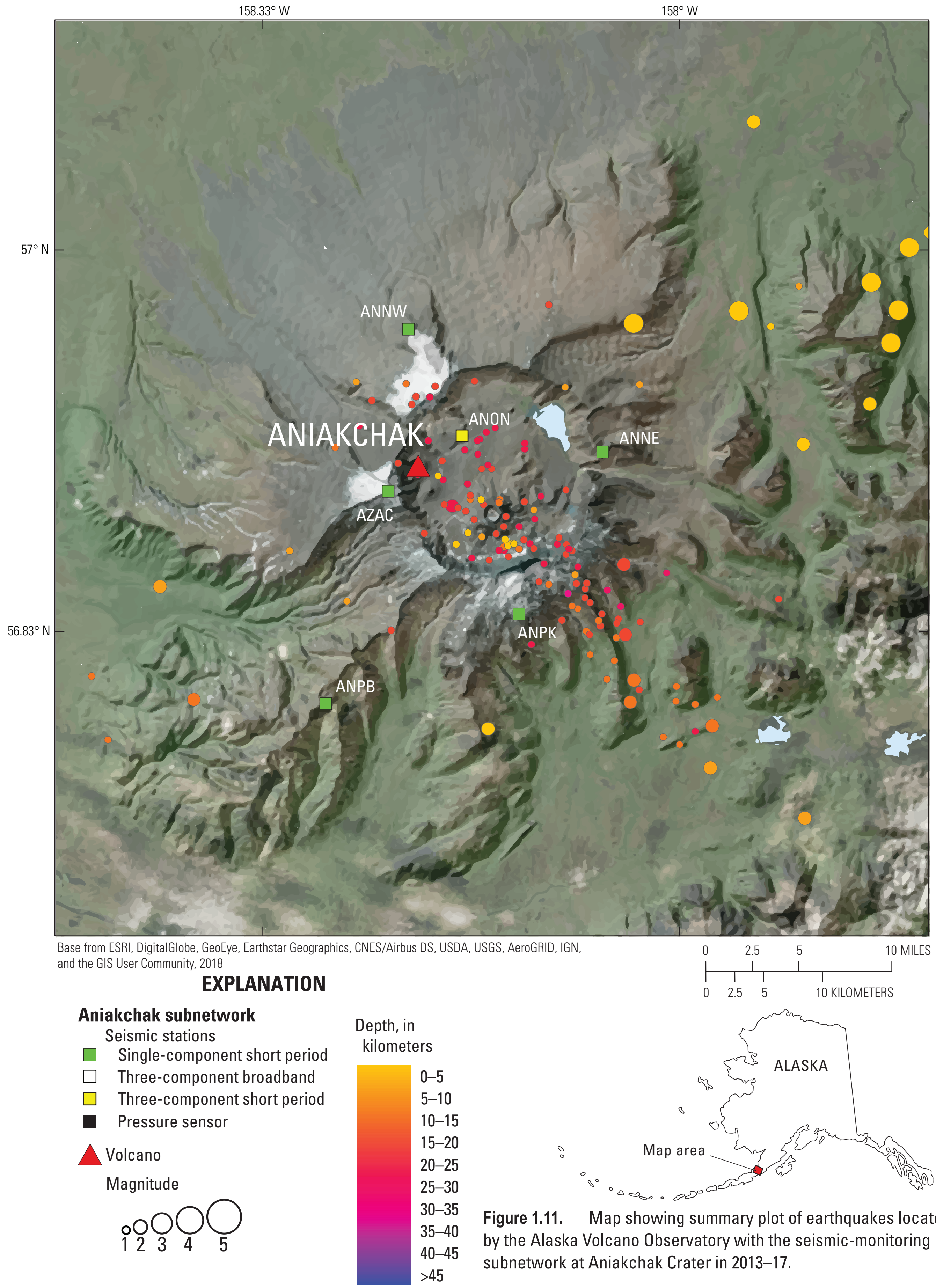

Figure 1.11. Map showing summary plot of earthquakes located by the Alaska Volcano Observatory with the seismic-monitoring subnetwork at Aniakchak Crater in 2013–17.

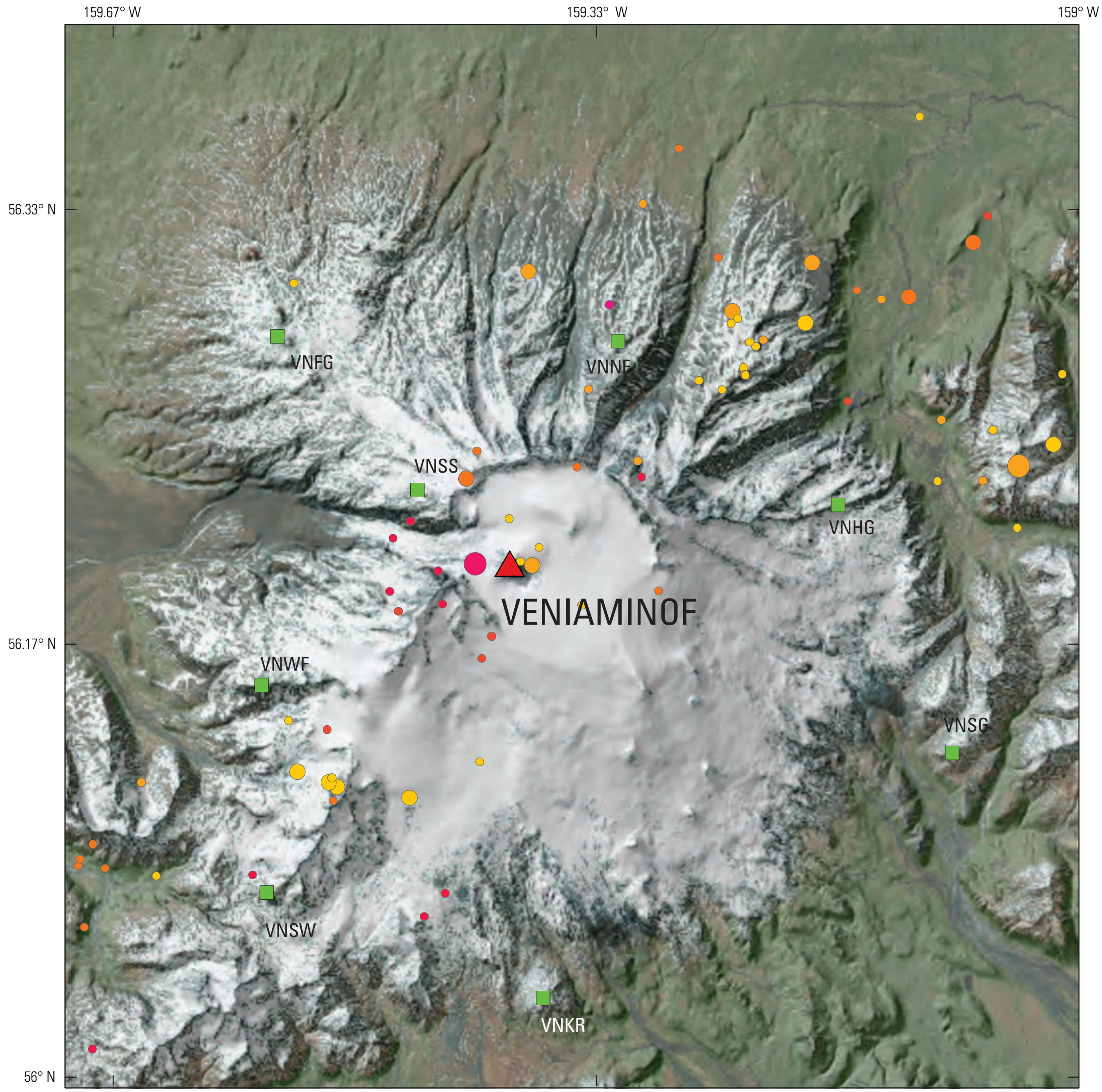

Base from ESRI, DigitalGlobe, GeoEye, Earthstar Geographics, CNES/Airbus DS, USDA, USGS, AeroGRID, IGN, and the GIS User Community, 2018

EXPLANATION

Veniaminof subnetwork

Seismic stations
- Single-component short period
- Three-component broadband
- Three-component short period
- Pressure sensor

Volcano

Magnitude
1 2 3 4 5

Depth, in kilometers
0–5
5–10
10–15
15–20
20–25
25–30
30–35
35–40
40–45
>45

Figure 1.12. Map showing summary plot of earthquakes located by the Alaska Volcano Observatory with the seismic-monitoring subnetwork at Mount Veniaminof in 2013–17.

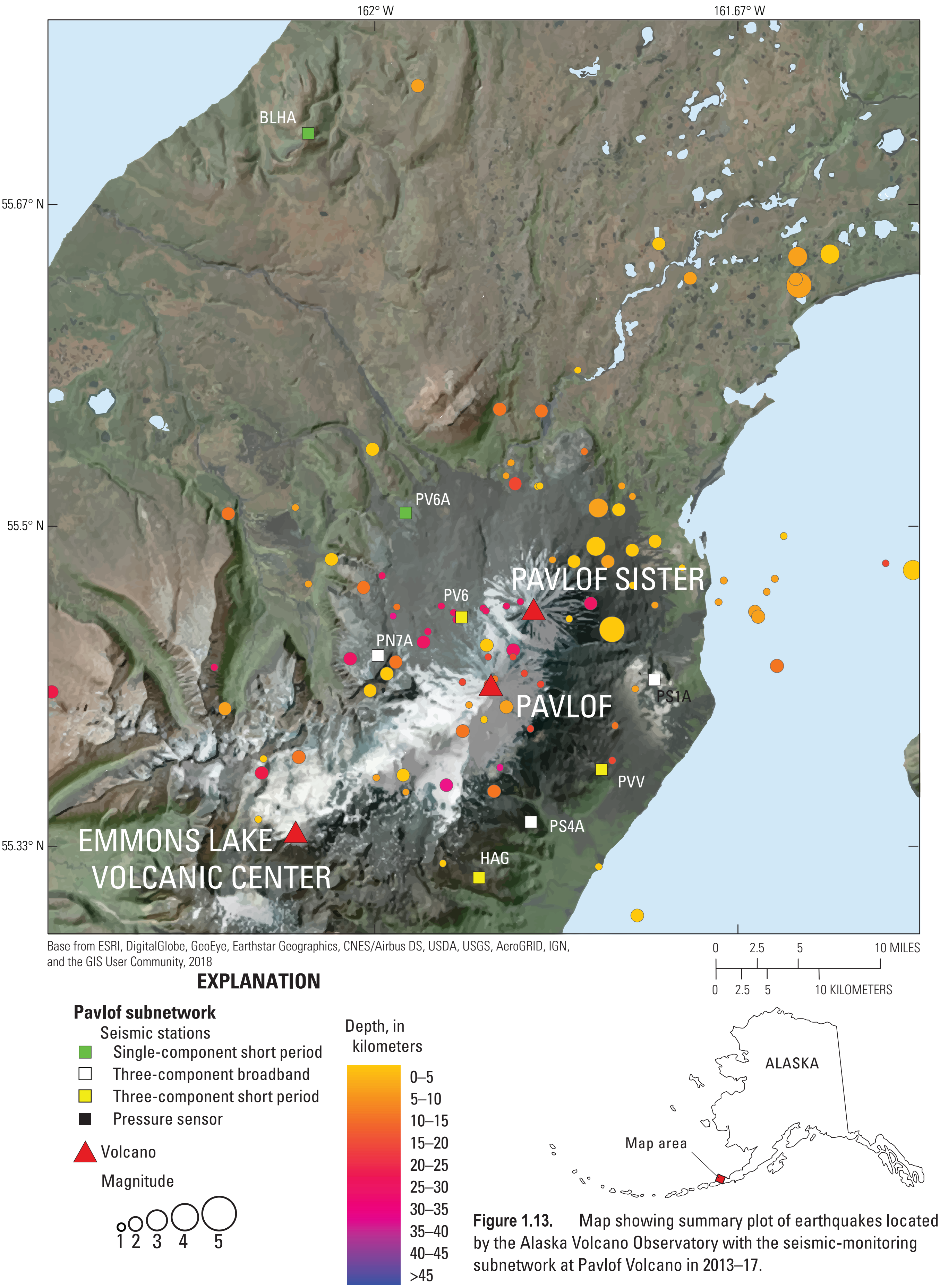

Figure 1.13. Map showing summary plot of earthquakes located by the Alaska Volcano Observatory with the seismic-monitoring subnetwork at Pavlof Volcano in 2013–17.

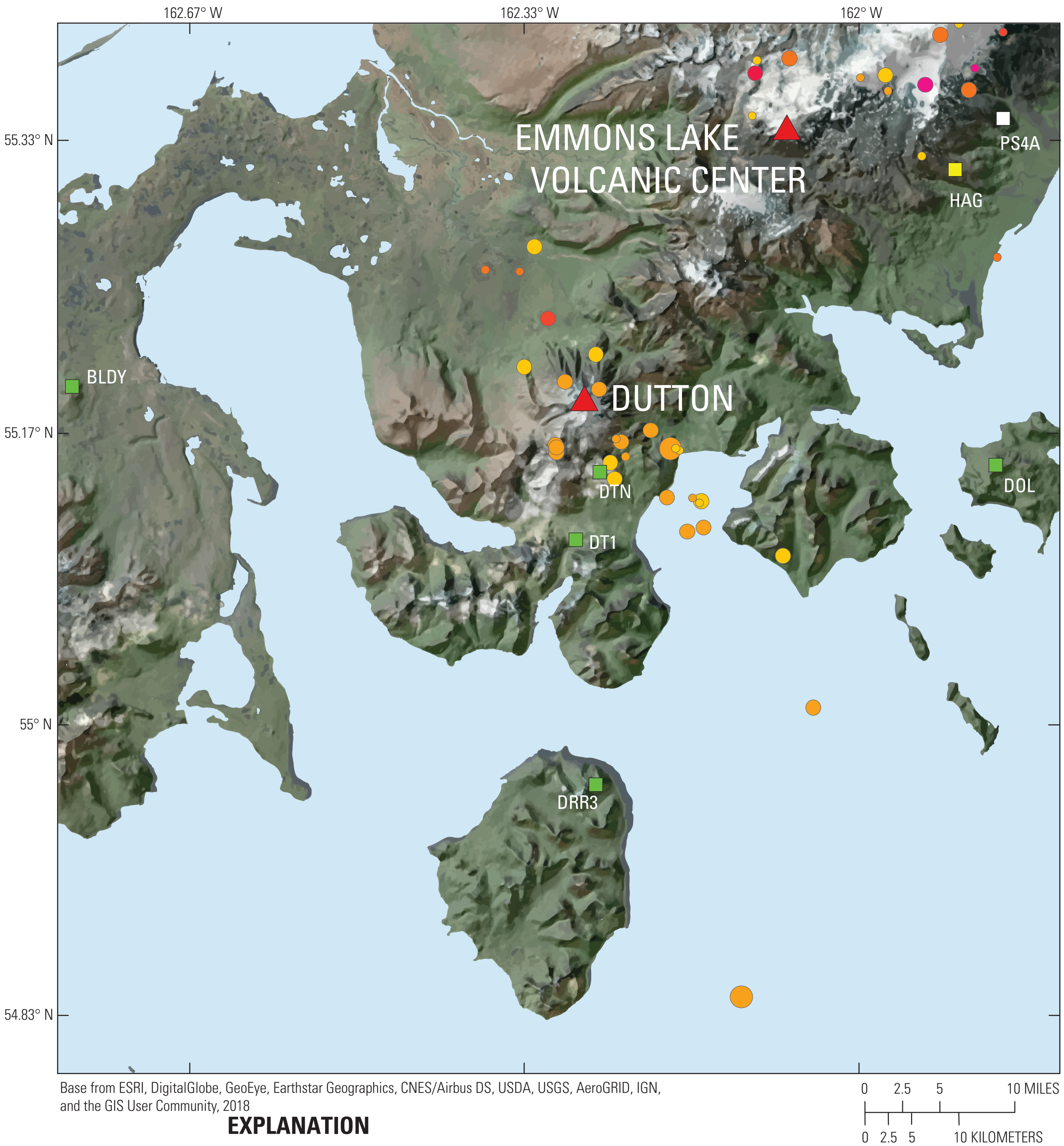

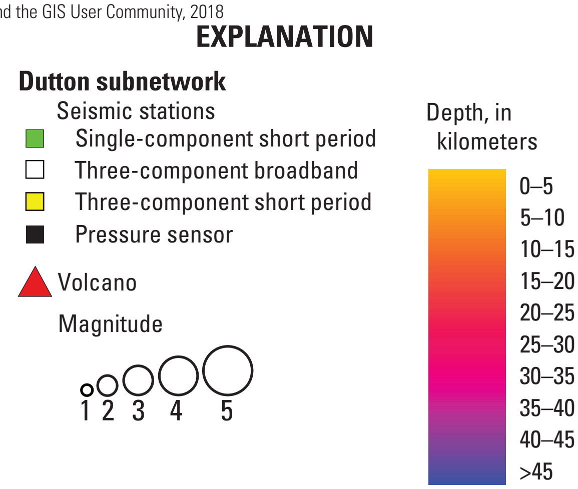

Figure 1.14. Map showing summary plot of earthquakes located by the Alaska Volcano Observatory with the seismic-monitoring subnetwork at Mount Dutton in 2013–17.

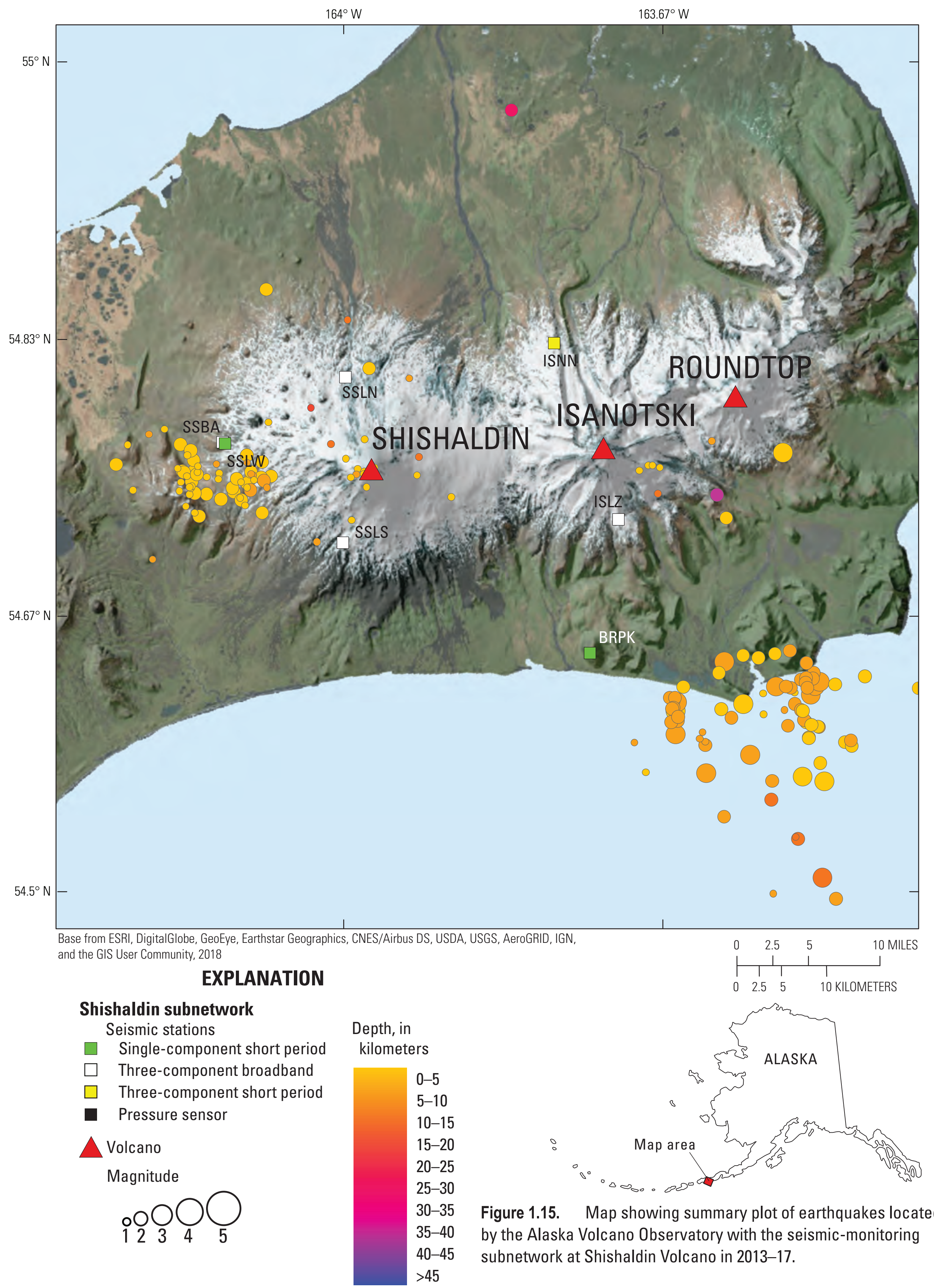

Figure 1.15. Map showing summary plot of earthquakes located by the Alaska Volcano Observatory with the seismic-monitoring subnetwork at Shishaldin Volcano in 2013–17.

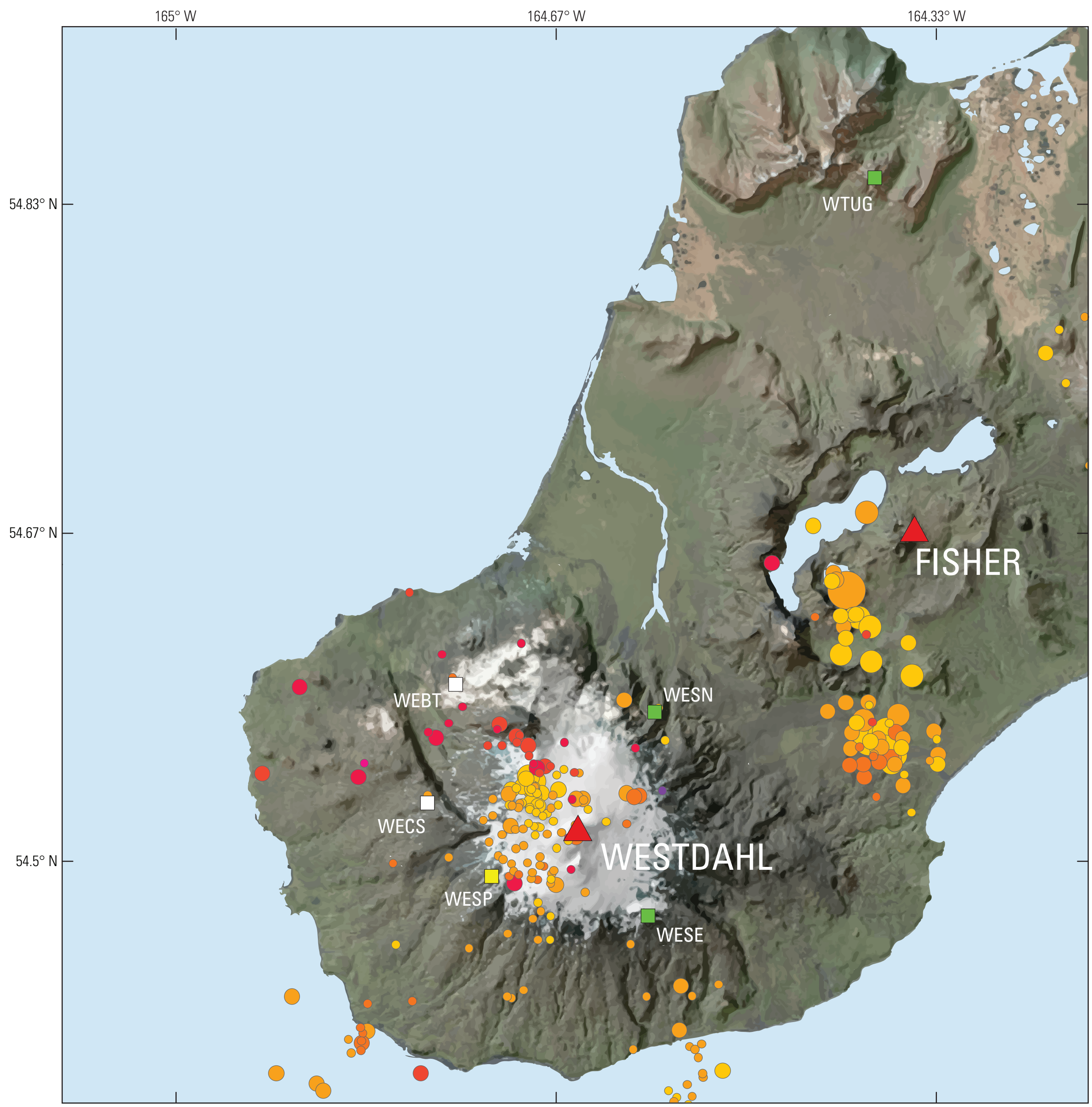

Base from ESRI, DigitalGlobe, GeoEye, Earthstar Geographics, CNES/Airbus DS, USDA, USGS, AeroGRID, IGN, and the GIS User Community, 2018

EXPLANATION

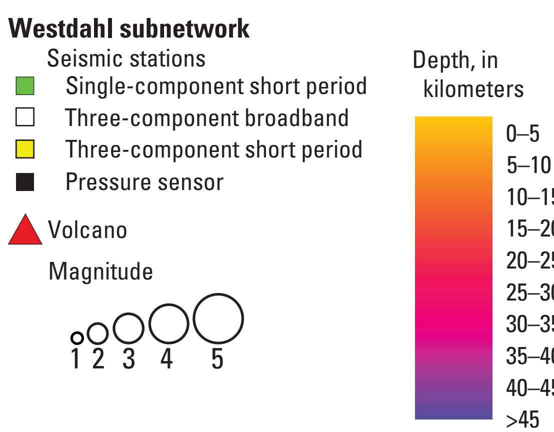

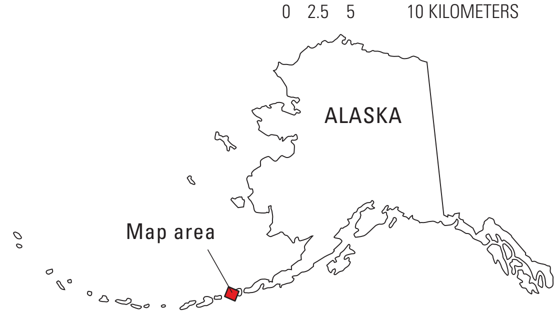

Figure 1.16. Map showing summary plot of earthquakes located by the Alaska Volcano Observatory with the seismic-monitoring subnetwork at Westdahl Peak in 2013–17.

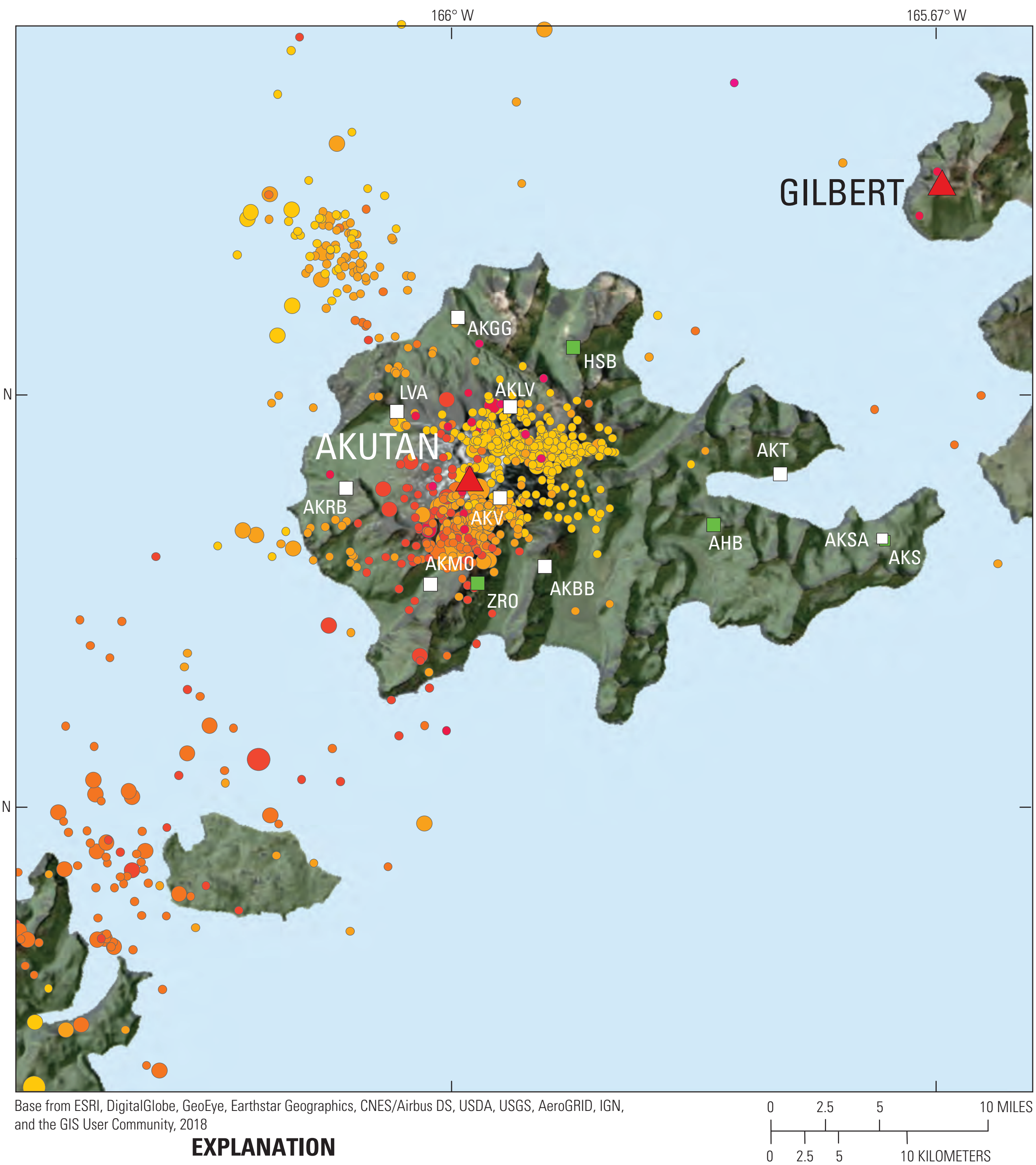

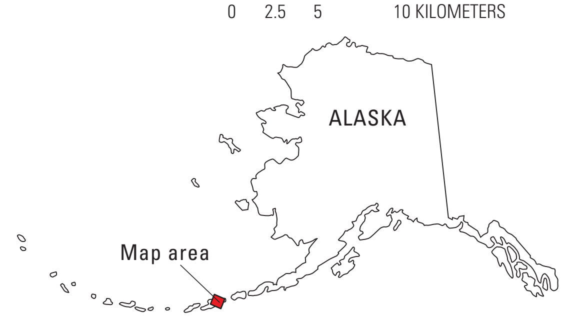

Figure 1.17. Map showing summary plot of earthquakes located by the Alaska Volcano Observatory with the seismic-monitoring subnetwork at Akutan Peak in 2013–17.

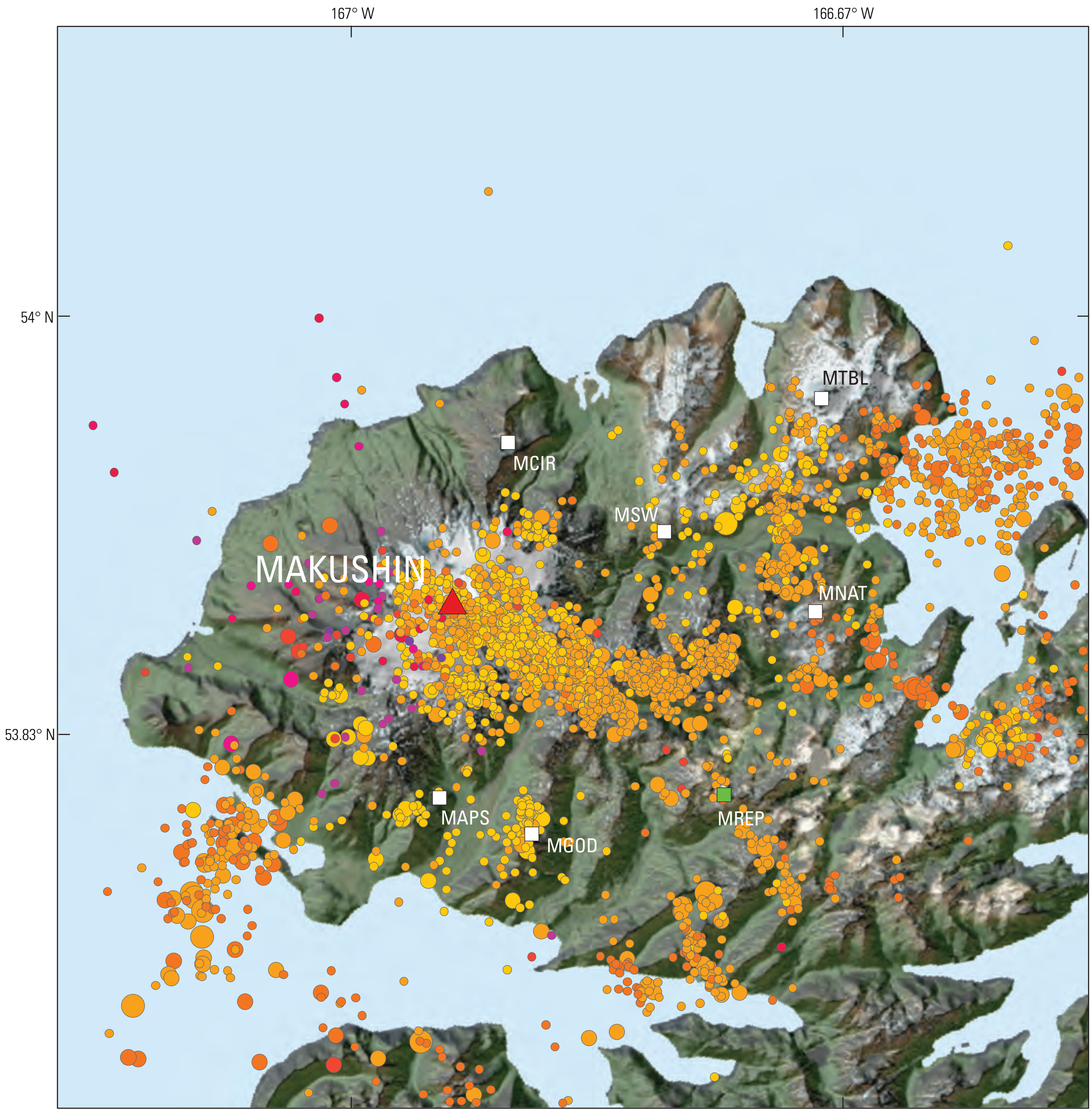

Figure 1.18. Map showing summary plot of earthquakes located by the Alaska Volcano Observatory with the seismic-monitoring subnetwork at Makushin Volcano in 2013–17.

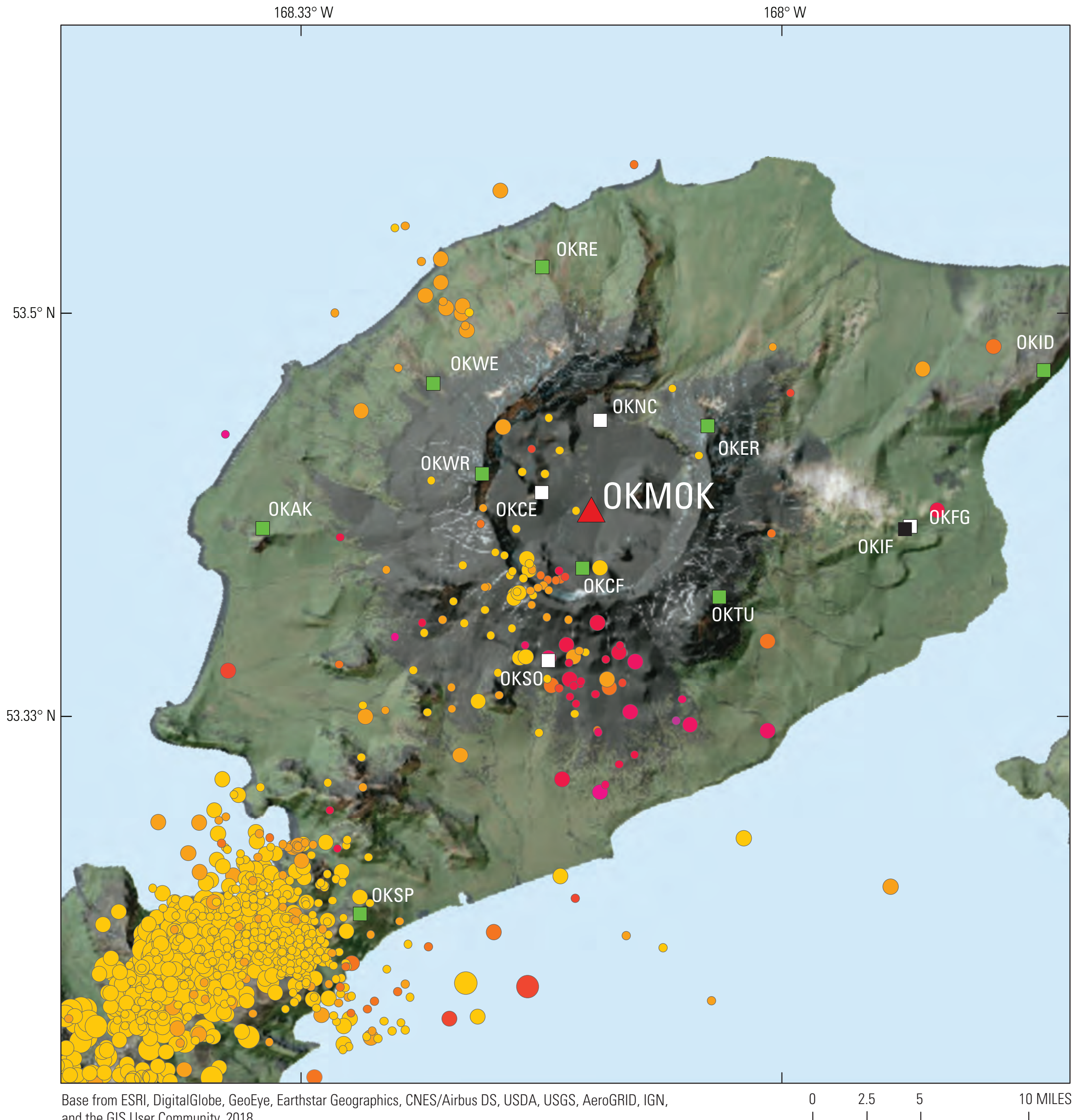

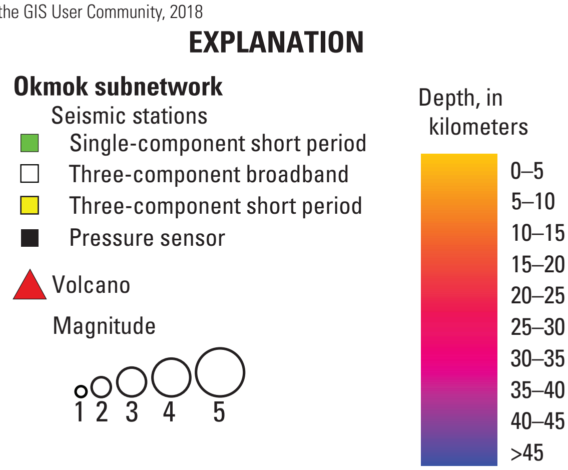

Figure 1.19. Map showing summary plot of earthquakes located by the Alaska Volcano Observatory with the seismic-monitoring subnetwork at Okmok Caldera in 2013–17.

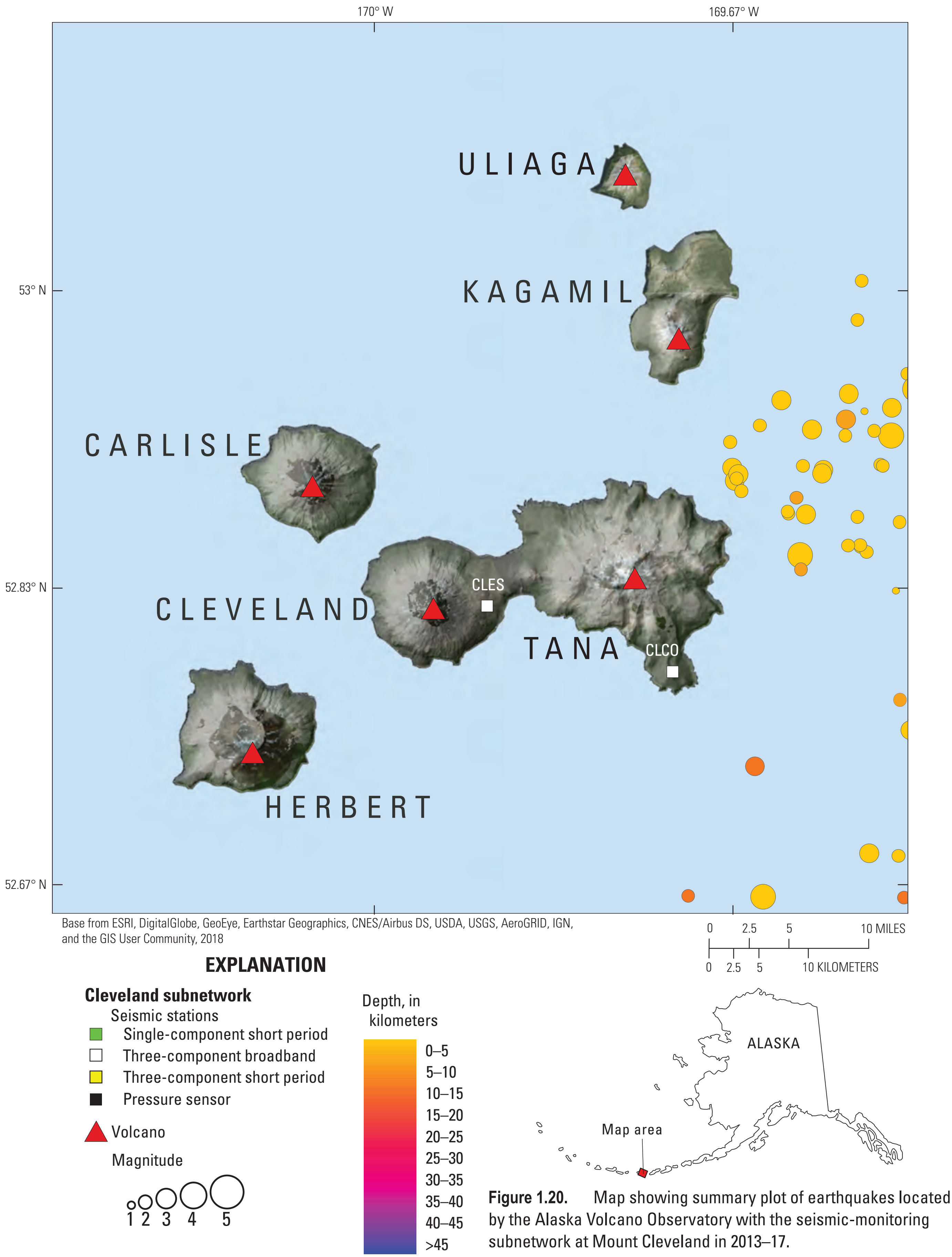

Figure 1.20. Map showing summary plot of earthquakes located by the Alaska Volcano Observatory with the seismic-monitoring subnetwork at Mount Cleveland in 2013–17.

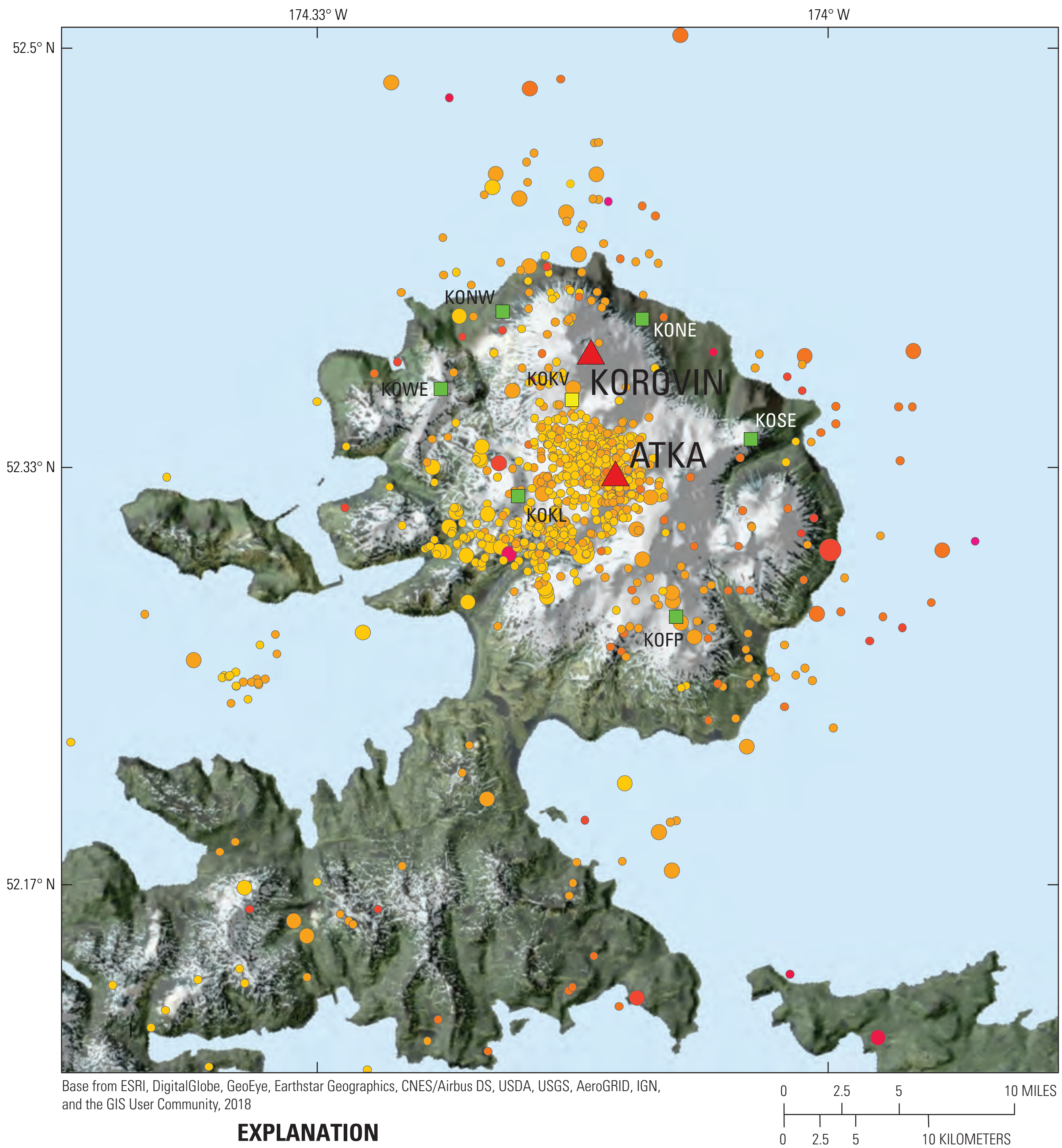

Figure 1.21. Map showing summary plot of earthquakes located by the Alaska Volcano Observatory with the seismic-monitoring subnetwork at Korovin Volcano in 2013–17.

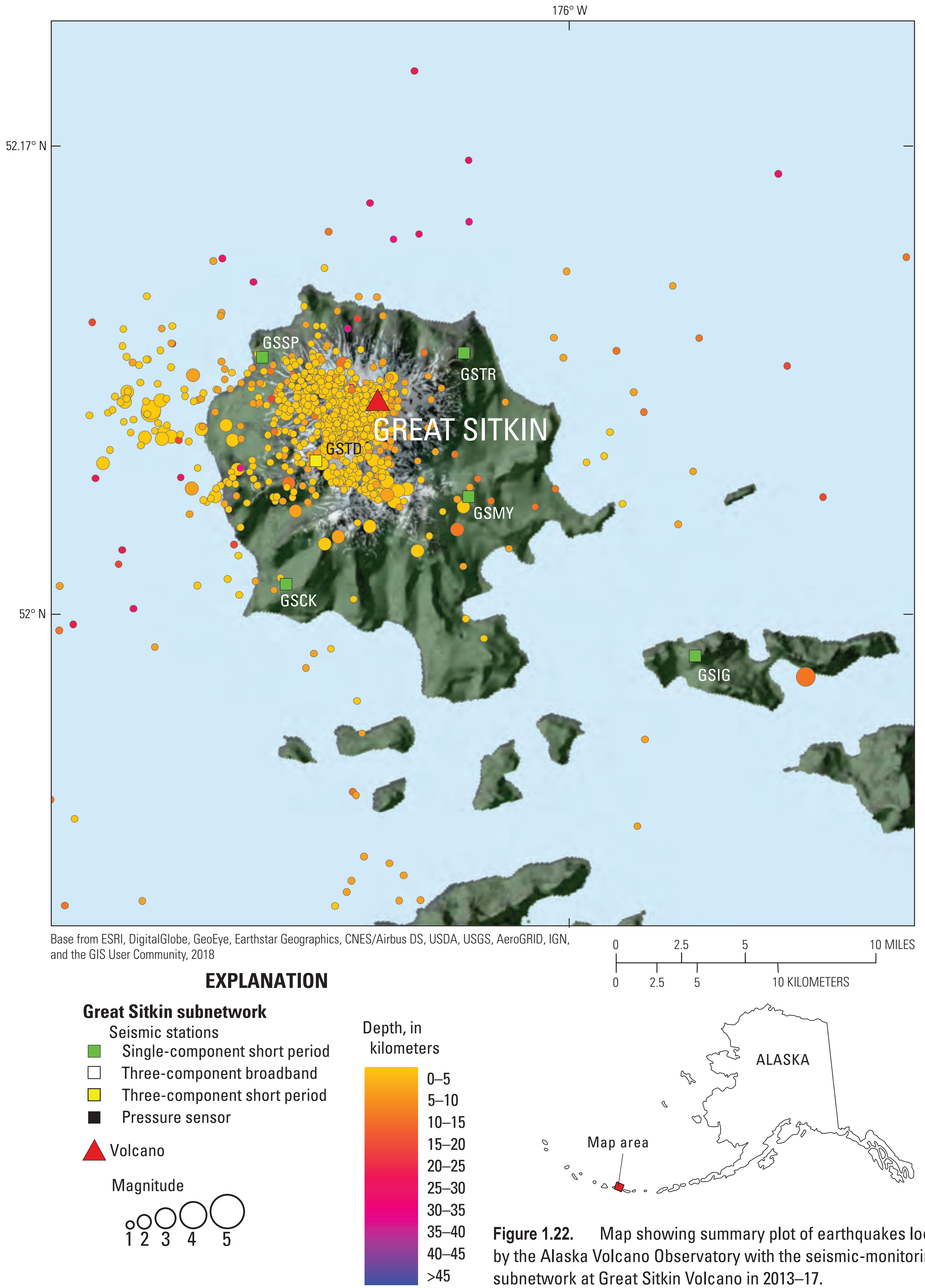

Figure 1.22. Map showing summary plot of earthquakes located by the Alaska Volcano Observatory with the seismic-monitoring subnetwork at Great Sitkin Volcano in 2013–17.

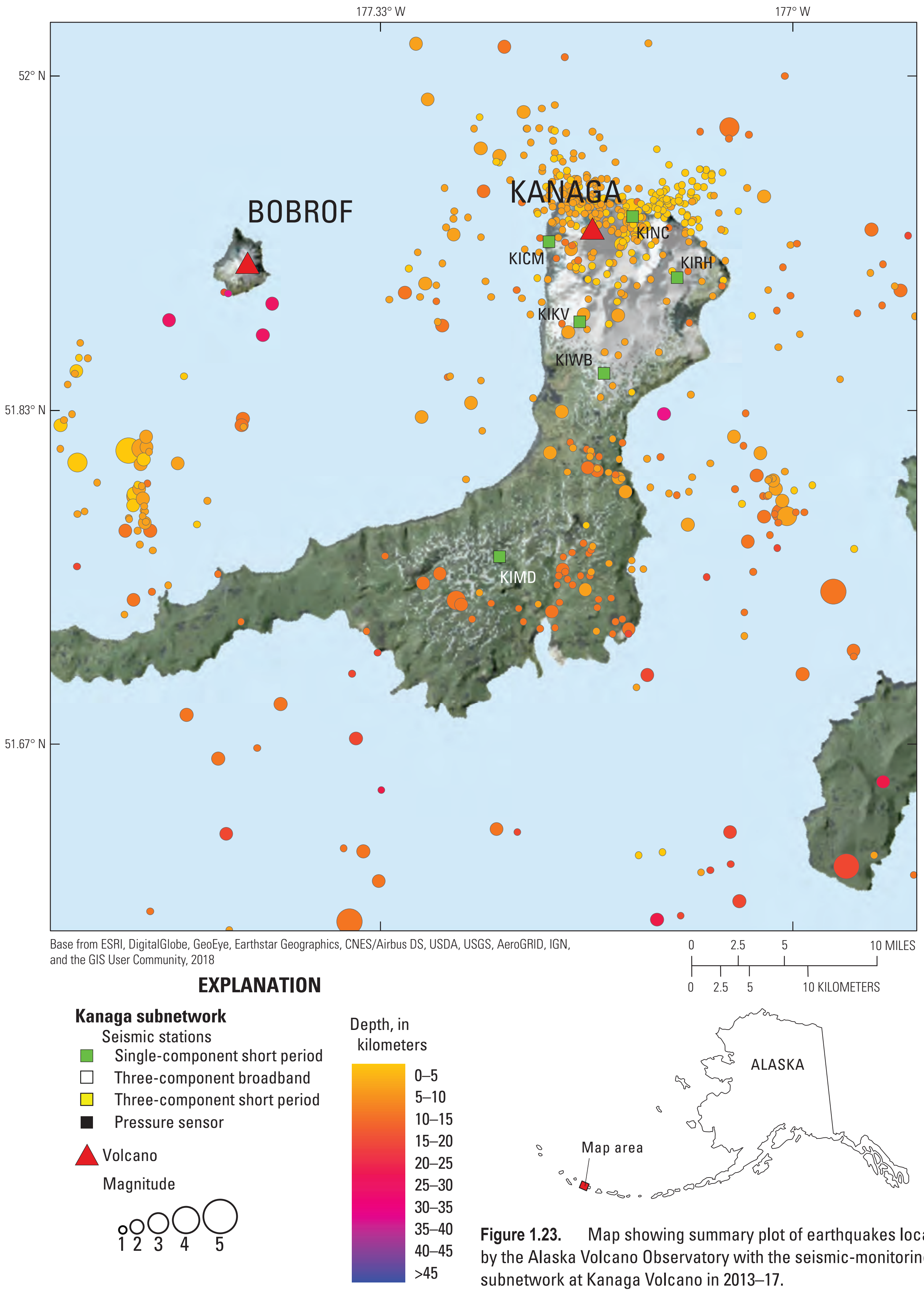

Figure 1.23. Map showing summary plot of earthquakes located by the Alaska Volcano Observatory with the seismic-monitoring subnetwork at Kanaga Volcano in 2013–17.

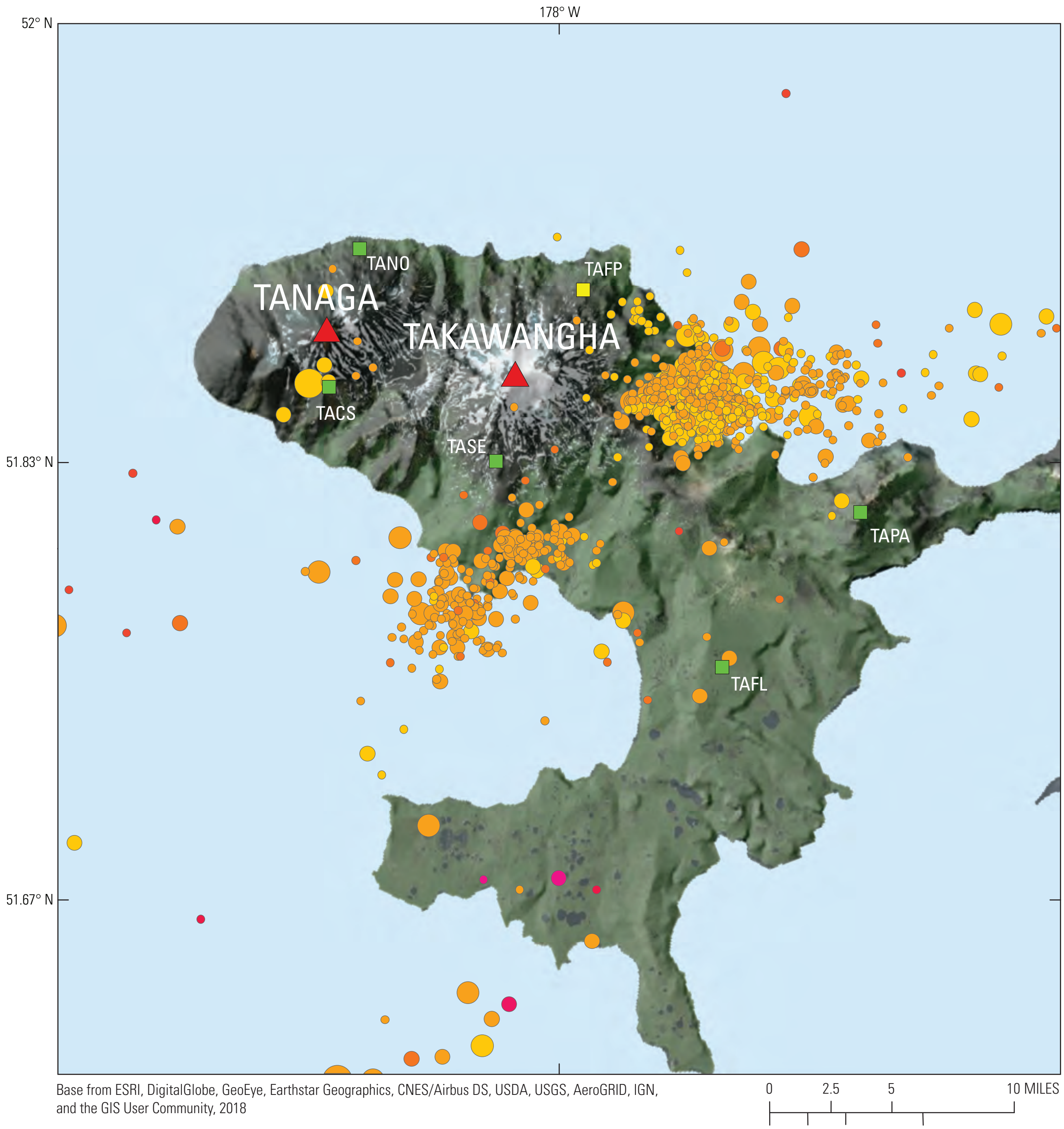

Figure 1.24. Map showing summary plot of earthquakes located by the Alaska Volcano Observatory with the seismic-monitoring subnetwork at Tanaga Volcano in 2013–17.

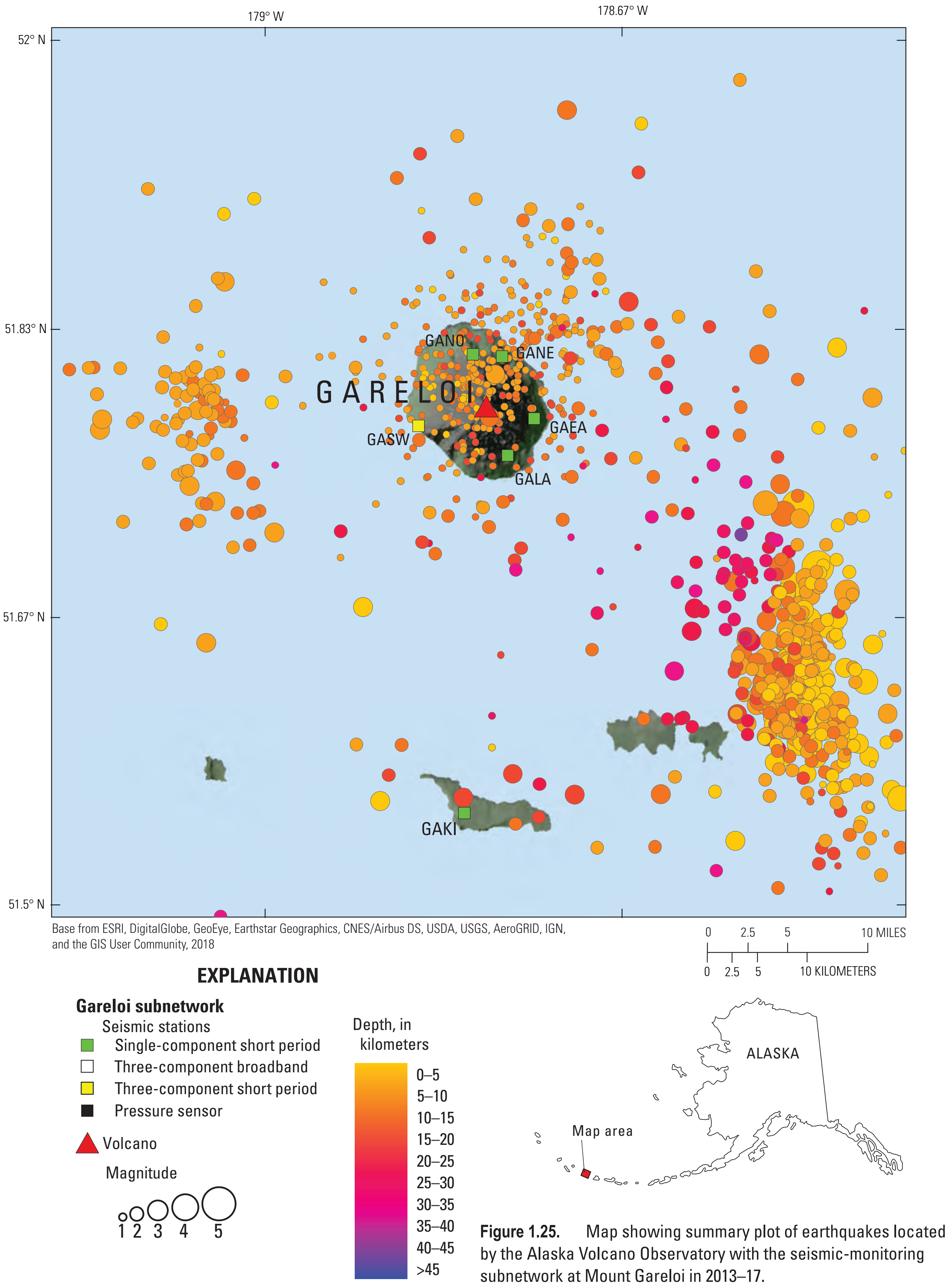

Figure 1.25. Map showing summary plot of earthquakes located by the Alaska Volcano Observatory with the seismic-monitoring subnetwork at Mount Gareloi in 2013–17.

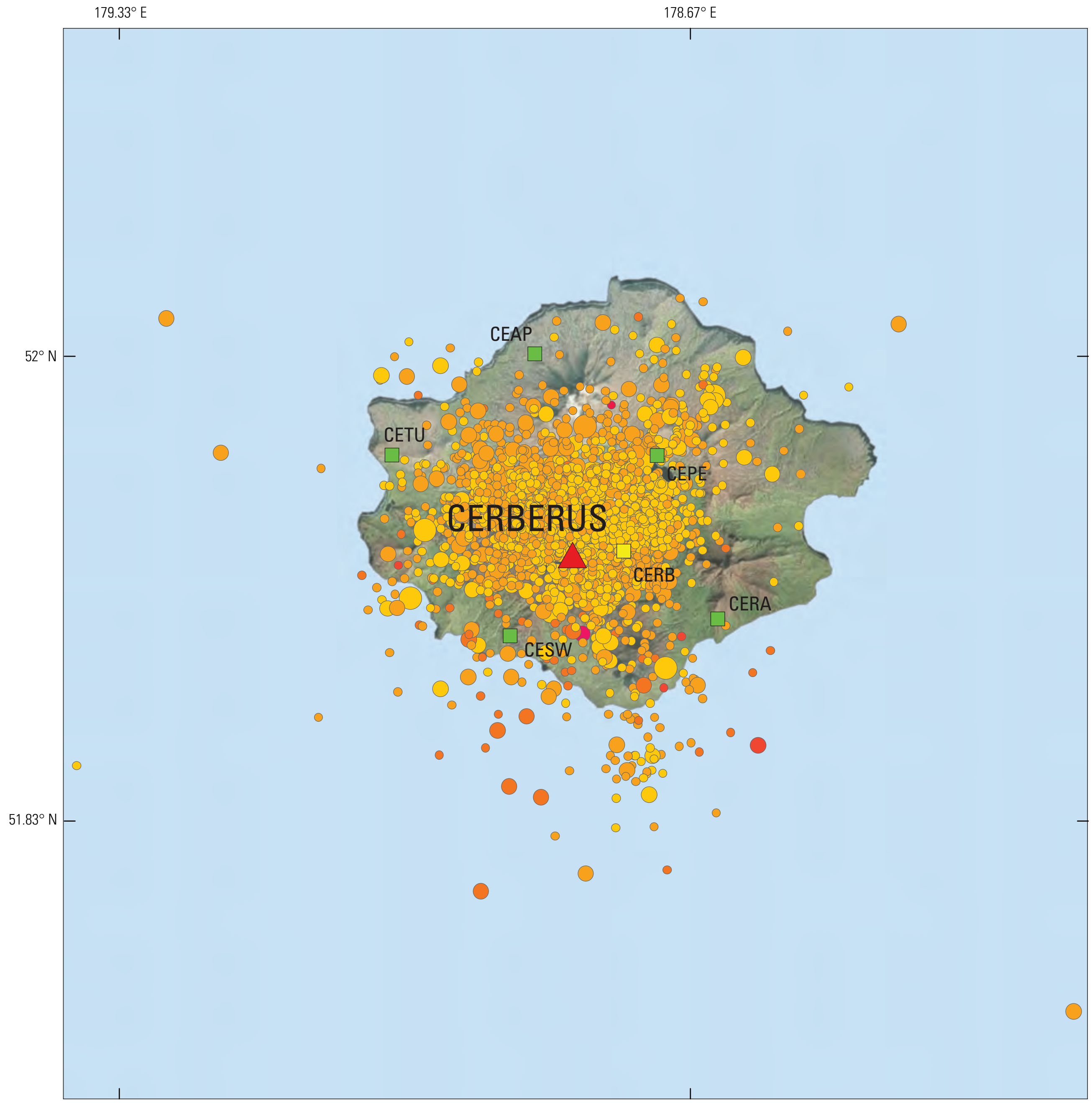

Base from ESRI, DigitalGlobe, GeoEye, Earthstar Geographics, CNES/Airbus DS, USDA, USGS, AeroGRID, IGN, and the GIS User Community, 2018

0 2.5 5 10 MILES
0 2.5 5 10 KILOMETERS

EXPLANATION

Cerberus subnetwork

Seismic stations

- Single-component short period
- Three-component broadband
- Three-component short period
- Pressure sensor

Volcano

Magnitude

1 2 3 4 5

Depth, in kilometers

0–5
5–10
10–15
15–20
20–25
25–30
30–35
35–40
40–45
>45

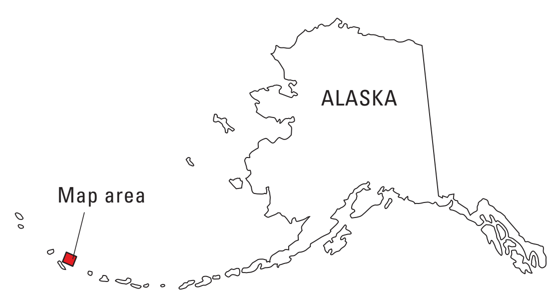

Figure 1.26. Map showing summary plot of earthquakes located by the Alaska Volcano Observatory with the seismic-monitoring subnetwork at Mount Cerberus in 2013–17.

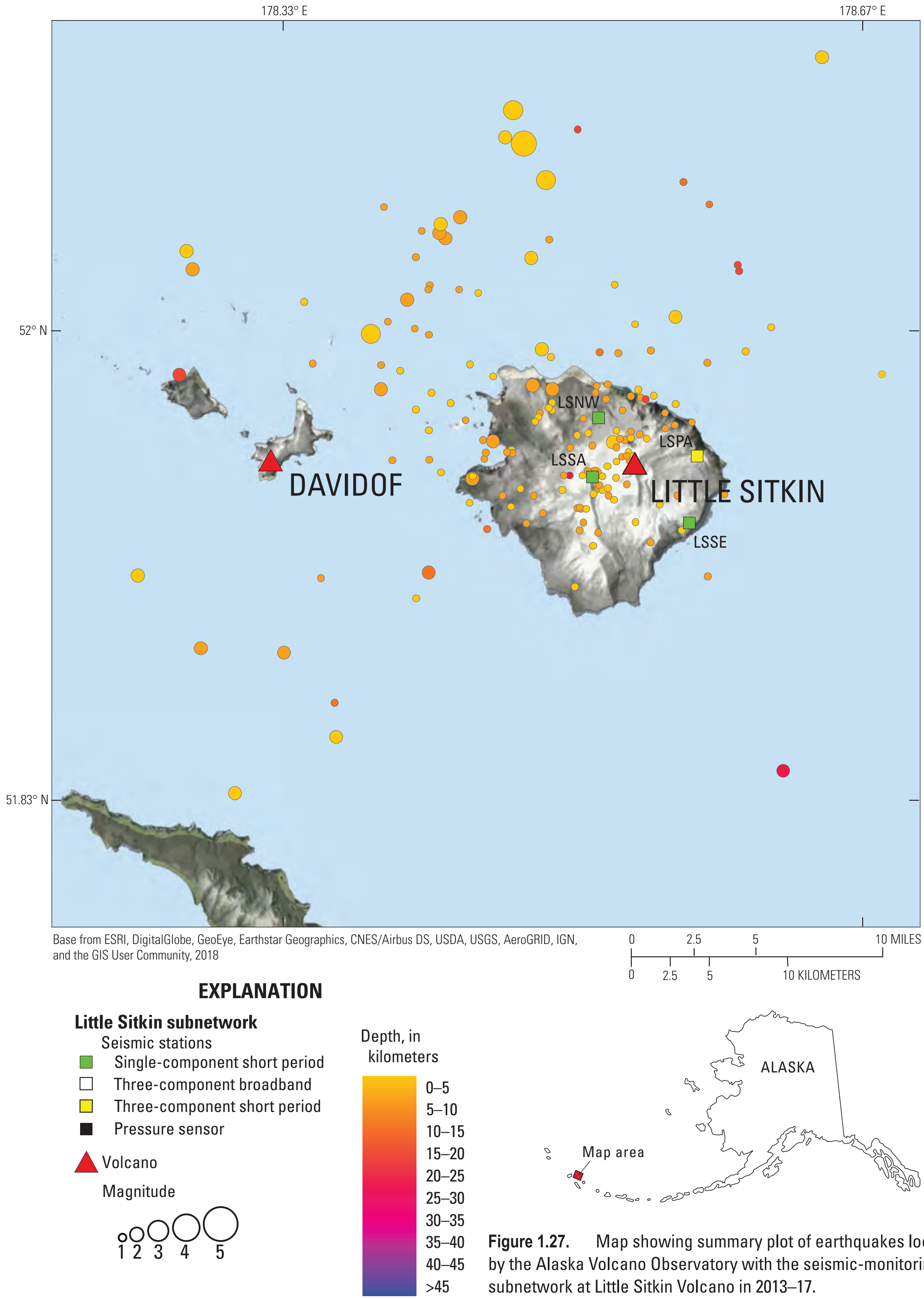

Figure 1.27. Map showing summary plot of earthquakes located by the Alaska Volcano Observatory with the seismic-monitoring subnetwork at Little Sitkin Volcano in 2013–17.

Appendix 2. Alaska Volcano Observatory Seismograph and Infrasound Stations in 2013–17

This list includes station parameters for seismograph and infrasound stations operated by the Alaska Volcano Observatory. Metadata for all stations is included with this report. The open date is the date that data were first recorded, and the close date is the date that recording was stopped. Discounting temporary data outages, data are available for each listed station between the open and close date. Stations still in operation are indicated by a dash in the close date column. Unless noted, stations are single-component short-period seismograph stations. If a station has multiple elements, the location code is added to the station name—for example, AKS_01. Station locations in relation to volcanic centers are shown in appendix 1.

Table 2.1. Seismograph and infrasound stations of the Akutan Peak subnetwork, operated by the Alaska Volcano Observatory.

[Date format is year/two-digit month/two-digit day; -, station is still in operation]

Station[1]	Latitude	Longitude	Elevation, in meters	Sensor[2]	Open date	Close date
AHB	54.1144	−165.8177	447	L-4	1996/07/24	-
AKBB[B]	54.0975	−165.9338	310	CMG-6T	2005/07/05	-
AKGG[B]	54.1979	−165.9936	326	CMG-6T	2003/06/27	-
AKLV[B]	54.1618	−165.9576	551	CMG-6T	2003/07/02	-
AKMO[B]	54.0903	−166.0126	277	CMG-6T	2003/06/25	-
AKRB[B]	54.1292	−166.0708	334	CMG-6T	2003/06/29	-
AKS[3]	54.1095	−165.6987	213	L-22	1996/07/24	-
AKS_01[I]	54.1105	−165.6977	22	Chap-M21/25	2011/07/14	-
AKS_02[I]	54.1103	−165.6962	224	Chap-M21/25	2011/07/14	-
AKS_03[I]	54.1110	−165.6970	218	Chap-M21/25	2011/07/14	-
AKS_04[I]	54.1105	−165.6968	219	Chap-M21/25	2011/07/14	-
AKSA[B]	54.1095	−165.6987	213	CMG-6T	2011/07/14	-
AKT[B]	54.1349	−165.7720	12	CMG-40T	1996/03/18	-
AKV	54.1253	−165.9647	863	L-4	1996/07/24	2016/08/08
AKV[B]	54.1253	−165.9647	863	TC120	2016/08/08	-
HSB	54.1859	−165.9144	497	L-4	1996/07/24	-
LVA	54.1600	−166.0358	457	L-4	1996/07/24	2016/08/08
LVA[B]	54.1600	−166.0358	457	TC120	2016/08/08	-
ZRO	54.0907	−165.9800	446	L-4	1996/07/24	-

[1]Station codes:

[3]Three-component short-period seismograph station.

[B]Three-component broadband seismograph station.

[I]Infrasound station array element.

[L]Low-gain component of the seismograph station.

[P]Single Infrasound sensor collocated with a seismometer.

[R]Station removed in 2013–17.

[S]Three-component strong-motion seismograph station.

[TA]Seismograph station collocated with an U.S. Transportable Array station.

[2]Sensor codes:

Chap-M2: Chaparral Physics Model 2 infrasound sensors.

Chap-M21/25: Chaparral Physics Model 21/25 infrasound sensor.

Chap-M60/64: Chaparral Physics Model 60/64 infrasound sensor.

CMG-40T: Güralp CMG-40T three-component broadband seismometer.

CMG-6T: Güralp CMG-6TD three-component broadband seismometer.

ES-T: Kinemetrics Episensor ES-T strong-motion seismometer.

L-4: Sercel L-4 single-component vertical short-period seismometer (1 hertz).

L-4-3D: Sercel L-4 three component short-period seismometers (1 hertz).

L-22: Sercel L-22 three-component short-period seismometer (2 hertz).

S-13: Teledyne Geotech S-13 single-component vertical short-period seismometer (1 hertz).

TC120-PH2: Nanometrics Trillium Compact three-component posthole broadband sensor.

TC120: Nanometrics Trillium Compact three-component broadband seismometer.

T-40: Nanometrics Trillium 40 three-component broadband seismometer.

VDP-5: U.S. Geological Survey Cascades Volcano Observatory VDP5 infrasound sensor.

VDP-10: U.S. Geological Survey Cascades Volcano Observatory VDP10 infrasound sensor.

Table 2.2. Seismograph stations of the Aniakchak Crater subnetwork, operated by the Alaska Volcano Observatory.

[See table 2.1 for explanation of superscripted footnotes. Date format is year/two-digit month/two-digit day; -, station is still in operation.]

Station[1]	Latitude	Longitude	Elevation, in meters	Sensor[2]	Open date	Close date
ANNE	56.9119	−158.0610	705	L-4	1997/07/18	-
ANNW	56.9656	−158.2170	816	L-4	1997/07/18	-
ANON[3]	56.9190	−158.1737	445	L-22	2000/07/09	2017/07/05
ANON	56.9190	−158.1737	445	L-4	2017/07/05	-
ANPB	56.8016	−158.2829	658	L-4	1997/07/18	-
ANPK	56.8409	−158.1283	972	L-4	1997/07/18	-
AZAC	56.8947	−158.2328	1,057	L-4	2003/07/12	-

Table 2.3. Seismograph stations of the Augustine Volcano subnetwork, operated by the Alaska Volcano Observatory.

[See table 2.1 for explanation of superscripted footnotes. Date format is year/two-digit month/two-digit day; -, station is still in operation]

Station[1]	Latitude	Longitude	Elevation, in meters	Sensor[2]	Open date	Close date
AU22[SB]	59.3702	−153.3573	105	CMG-6T,ES-T	2007/09/01	-
AUCH[B]	59.3626	−153.4447	916	CMG-6T	2014/08/20	-
AUE[LP]	59.3711	−153.3773	168	S-13, Chap-M2	1980/10/29	-
AUH	59.3632	−153.4454	890	S-13	1978/12/01	-
AUI[3]	59.3345	−153.4299	293	S-13	1978/04/06	-
AUJA[B]	59.3395	−153.4227	376	CMG-6T	2013/08/20	-
AUJK	59.3493	−153.4106	377	L-4	2011/08/16	-
AUL	59.3816	−153.4379	360	S-13	1978/08/27	-
AUL[B]	59.3816	−153.4379	360	CMG-6T	1997/08/27	-
AUNW[L]	59.3775	−153.4790	160	L-4	2006/03/15	-
AUP	59.3627	−153.4226	1,033	L-4	1977/09/22	-
AUQ[B]	59.3549	−153.4143	647	CMG-6T	2013/08/20	-
AUSB[B]	59.3330	−153.4284	230	CMG-6T	2015/08/29	-
AUSS[B]	59.3539	−153.4309	1,235	CMG-6T	2015/06/14	-
AUW	59.3694	−153.4730	276	S-13	1986/10/17	-
AUWS[B]	59.3585	−153.4609	487	CMG-6T	2015/06/14	-

Table 2.4. Seismograph stations of the Mount Cerberus subnetwork, operated by the Alaska Volcano Observatory.

[See table 2.1 for explanation of superscripted footnotes. Date format is year/two-digit month/two-digit day; -, station is still in operation]

Station[1]	Latitude	Longitude	Elevation, in meters	Sensor[2]	Open date	Close date
CEAP	52.0012	179.5758	244	L-4	2005/09/17	-
CEPE	51.9646	179.6472	335	L-4	2005/09/17	-
CERA	51.9058	179.6826	305	L-4	2005/09/26	-
CERB[3]	51.9302	179.6277	305	L-22	2005/09/18	-
CESW	51.8998	179.5613	238	L-4	2005/09/18	-
CETU	51.9649	179.4922	335	L-4	2005/09/22	-

Table 2.5. Seismograph stations of the Mount Cleveland subnetwork, operated by the Alaska Volcano Observatory.

[See table 2.1 for explanation of superscripted footnotes. Date format is year/two-digit month/two-digit day; -, station is still in operation]

Station[1]	Latitude	Longitude	Elevation, in meters	Sensor[2]	Open date	Close date
CLCO[I]	52.7866	−169.7229	137	L-4	2014/08/09	-
CLCO[B]	52.7866	−169.7229	137	CMG-6T	2014/08/09	-
CLCO_01[I]	52.7864	−169.7229	136	VDP-5	2014/08/09	-
CLCO_02[I]	52.7871	−169.7244	125	VDP-5	2014/08/09	-
CLCO_03[I]	52.7875	−169.7210	107	VDP-5	2014/08/09	-
CLCO_04[I]	52.7861	−169.7204	113	VDP-5	2014/08/09	-
CLCO_05[I]	52.7851	−169.7250	113	VDP-5	2014/08/09	-
CLES[P]	52.8235	−169.8951	146	L-4, Chap-M21/25, Chap-M60/64	2014/08/09	-
CLES[B]	52.8235	−169.8951	146	TC120	2014/08/09	-

Table 2.6. Seismograph stations of the Mount Dutton subnetwork, operated by the Alaska Volcano Observatory.

[See table 2.1 for explanation of superscripted footnotes. Date format is year/two-digit month/two-digit day; -, station is still in operation]

Station[1]	Latitude	Longitude	Elevation, in meters	Sensor[2]	Open date	Close date
BLDY	55.1936	−162.7856	259	L-4	1996/07/11	-
DOL	55.1488	−161.8638	439	L-4	1996/07/11	-
DRR3	54.9660	−162.2631	457	L-4	1996/07/11	-
DT1	55.1062	−162.2830	198	L-4	1991/06/21	-
DTN	55.1448	−162.2590	396	S-13	1988/07/16	-

Table 2.7. Seismograph stations of the Fourpeaked Mountain subnetwork, operated by the Alaska Volcano Observatory.

[See table 2.1 for explanation of superscripted footnotes. Date format is year/two-digit month/two-digit day; -, station is still in operation]

Station[1]	Latitude	Longitude	Elevation, in meters	Sensor[2]	Open date	Close date
CDD[TA]	58.9289	−153.6449	622	S-13	1981/08/17	-
FONW[LP]	58.8341	−153.9204	905	L-4, Chap-M2	2006/10/19	-
FOPK[L]	58.7574	−153.4762	546	L-4	2006/09/25	-
FOSS[LP]	58.7987	−153.6971	1,268	L-4, Chap-M2	2006/10/19	-

Table 2.8. Seismograph stations of the Mount Gareloi subnetwork, operated by the Alaska Volcano Observatory.

[See table 2.1 for explanation of superscripted footnotes. Date format is year/two-digit month/two-digit day; -, station is still in operation]

Station[1]	Latitude	Longitude	Elevation, in meters	Sensor[2]	Open date	Close date
GAEA	51.7819	−178.7488	326	L-4	2003/08/30	-
GAKI	51.5534	−178.8140	99	L-4	2003/09/01	-
GALA	51.7606	−178.7735	315	L-4	2003/08/30	-
GANE	51.8178	−178.7787	325	L-4	2003/09/02	-
GANO	51.8192	−178.8058	451	L-4	2003/09/02	-
GASW[3]	51.7778	−178.8566	248	L-22	2003/08/30	-

Table 2.9. Seismograph stations of the Great Sitkin Volcano subnetwork, operated by the Alaska Volcano Observatory.

[See table 2.1 for explanation of superscripted footnotes. Date format is year/two-digit month/two-digit day; -, station is still in operation]

Station[1]	Latitude	Longitude	Elevation, in meters	Sensor[2]	Open date	Close date
GSCK	52.0108	−176.1640	384	L-4	1999/09/15	-
GSIG	51.9853	−175.9270	407	L-4	1999/09/03	-
GSMY	52.0421	−176.0583	418	L-4	1999/09/03	-
GSSP	52.0917	−176.1777	295	L-4	1999/09/15	-
GSTD[3]	52.0548	−176.1468	873	L-22	1999/09/03	-
GSTR	52.0932	−176.0611	536	L-4	1999/09/03	-

Table 2.10. Seismograph stations of the Iliamna Volcano subnetwork, operated by the Alaska Volcano Observatory.

[See table 2.1 for explanation of superscripted footnotes. Date format is year/two-digit month/two-digit day; -, station is still in operation]

Station[1]	Latitude	Longitude	Elevation, in meters	Sensor[2]	Open date	Close date
ILI	60.0807	−152.9606	771	L-4	1987/09/15	-
ILNE[3]	60.0573	−153.0635	1,614	L-22	2016/09/27	
ILS[3]	59.9570	−153.0703	1,125	S-13	1996/08/28	-
ILS[B]	59.9570	−153.0703	1,125	CMG-6T	2015/09/01	2017/08/22
ILS[B]	59.9570	−153.0703	1,125	TC120-PH2	2017/08/22	-
ILSW[B]	59.9832	−153.1420	1,318	TC120	2015/09/10	
ILW	60.0592	−153.1392	1,646	S-13	1994/09/09	-
ILW[B]	60.0592	−153.1392	1,646	CMG-6T	2013/08/20	2016/09/27
ILW[3]	60.0592	−153.1392	1,646	L-22	2016/09/27	-
INE	60.0599	−153.0644	1,634	S-13	1990/08/29	2016/08/31
IVE[3]	60.0163	−153.0185	1,173	S-13, L-22	1996/08/29	-
IVE[B]	60.0163	−153.0185	1,173	CMG-6T	2013/08/20	
IVS	60.0086	−153.0830	2,332	S-13	1990/08/29	-

Table 2.11. Seismograph stations of the Kanaga Volcano subnetwork, operated by the Alaska Volcano Observatory.

[See table 2.1 for explanation of superscripted footnotes. Date format is year/two-digit month/two-digit day; -, station is still in operation]

Station[1]	Latitude	Longitude	Elevation, in meters	Sensor[2]	Open date	Close date
KICM	51.9178	−177.1973	183	L-4	1999/09/15	-
KIKV	51.8777	−177.1724	411	L-4	1999/09/15	-
KIMD	51.7605	−177.2369	183	L-4	1999/09/15	-
KINC	51.9303	−177.1296	198	L-4	1999/09/15	-
KIRH	51.8985	−177.0955	309	L-4	1999/09/03	-
KIWB	51.8520	−177.1528	244	L-4	1999/09/03	-

Table 2.12. Seismograph stations of the Katmai volcanic cluster subnetwork, operated by the Alaska Volcano Observatory.

[See table 2.1 for explanation of superscripted footnotes. Date format is year/two-digit month/two-digit day; -, station is still in operation]

Station[1]	Latitude	Longitude	Elevation, in meters	Sensor[2]	Open date	Close date
ACH[3]	58.2100	−155.3281	960	L-22	1996/07/25	2017/08/18
ACH[B]	58.2100	−155.3281	960	TC120-PH2	2017/08/21	-
ANCK	58.1981	−155.4961	869	L-4	1996/07/25	2016/08/16
ANCK[B]	58.1981	−155.4961	869	TC120	2016/07/16	-
CAHL	58.0518	−155.3036	807	L-4	1996/07/25	-
CNTC[TA]	58.2638	−155.8858	1,158	L-4	1996/07/25	-
KABR	58.1304	−154.9716	940	L-4	1998/08/12	-
KABU[B]	58.2702	−155.2843	1,065	CMT-6T	2004/08/01	2017/08/17
KABU[B]	58.2702	−155.2843	1,065	TC120-PH2	2017/08/17	-
KAHC[TA]	58.6483	−155.0081	1,250	L-4	1998/10/12	-
KAHG	58.4933	−154.5484	923	L-4	1998/10/12	2017/08/21
KAHG[B]	58.4933	−154.5484	923	TC120-PH2	2017/08/21	-
KAIC	58.4843	−155.0479	734	L-4	1998/10/12	-
KAKN[B]	58.2963	−155.0623	1,049	CMG-6T	2004/08/01	2017/08/23
KAKN[B]	58.2963	−155.0623	1,049	TC120-PH2	2017/08/23	-
KAPH[3]	58.5961	−154.3489	907	L-22	1998/10/12	-
KARR	58.4971	−154.7054	610	L-4	1998/10/12	-
KAWH	58.3830	−154.8013	777	L-4	1998/10/12	-
KBM	58.2743	−155.2038	732	L-4	1991/07/22	-
KCE	58.2426	−155.1854	777	L-4	1991/07/22	-
KCG[3]	58.3069	−155.1135	762	L-22	1988/08/01	-
KEL	58.4393	−155.7428	975	L-4	1988/08/01	-
KJL	58.0533	−155.5753	792	L-4	1996/07/25	-
KVT	58.3810	−155.2971	457	L-4	1988/08/01	-
MGLS	58.1336	−155.1629	472	L-4	1996/07/25	-

Table 2.13. Seismograph stations of the Korovin Volcano subnetwork, operated by the Alaska Volcano Observatory.

[See table 2.1 for explanation of superscripted footnotes. Date format is year/two-digit month/two-digit day; -, station is still in operation]

Station[1]	Latitude	Longitude	Elevation, in meters	Sensor[2]*	Open date	Close date
KOFP	52.2740	−174.0992	662	L-4	2004/07/02	-
KOKL	52.3221	−174.2022	758	L-4	2004/07/05	-
KOKV[3]	52.3603	−174.1673	776	L-22	2004/07/05	-
KONE	52.3925	−174.1213	253	L-4	2004/07/10	-
KONW	52.3954	−174.2125	334	L-4	2004/07/04	-
KOSE	52.3447	−174.0505	625	L-4	2004/07/07	-
KOWE	52.3646	−174.2527	527	L-4	2004/07/06	-

Table 2.14. Seismograph stations of the Little Sitkin Volcano subnetwork, operated by the Alaska Volcano Observatory.

[See table 2.1 for explanation of superscripted footnotes. Date format is year/two-digit month/two-digit day; -, station is still in operation]

Station[1]	Latitude	Longitude	Elevation, in meters	Sensor[2]	Open date	Close date
LSNW	51.9693	178.5148	290	L-4	2005/09/30	-
LSPA[3]	51.9557	178.5714	335	L-22	2005/09/30	-
LSSA	51.9484	178.5112	549	L-4	2005/09/28	-
LSSE	51.9320	178.5670	335	L-4	2005/09/27	-

Table 2.15. Seismograph stations of the Makushin Volcano subnetwork, operated by the Alaska Volcano Observatory.

[See table 2.1 for explanation of superscripted footnotes. Date format is year/two-digit month/two-digit day; -, station is still in operation]

Station[1]	Latitude	Longitude	Elevation, in meters	Sensor[2]	Open date	Close date
MAPS[B]	53.8082	−166.9407	333	CMG-6TD	2012/08/03	-
MCIR	53.9505	−166.8942	800	L-4	1996/07/25	2016/08/08
MCIR[B]	53.9505	−166.8942	800	TC120	2016/08/08	-
MGOD	53.7938	−166.8780	650	L-4	1996/07/25	-
MGOD[B]	53.7938	−166.8780	650	CMG-6T	2012/08/03	-
MNAT	53.8829	−166.6856	390	L-4	1996/07/25	-
MNAT[B]	53.8829	−166.6856	390	CMG-6T	2012/08/03	-
MREP	53.8096	−166.7476	785	L-4	2002/01/01	-
MSW[3]	53.9148	−166.7880	423	L-22	1996/07/25	2016/08/07
MSW[B]	53.9148	−166.7880	423	CMG-6T	2011/08/04	-
MSW[BP]	53.9148	−166.7880	423	TC120, Chap-M21/25	2016/08/07	-
MTBL	53.9680	−166.6813	810	L-4	1996/07/25	2016/08/07
MTBL[B]	53.9680	−166.6813	810	TC120	2016/07/07	-

Table 2.16. Seismograph and infrasound stations of the Okmok Caldera subnetwork, operated by the Alaska Volcano Observatory.

[See table 2.1 for explanation of superscripted footnotes. Date format is year/two-digit month/two-digit day; -, station is still in operation]

Station[1]	Latitude	Longitude	Elevation, in meters	Sensor[2]	Open date	Close date
OKAK	53.4113	−168.3600	165	L-4	2005/07/11	-
OKCE[B]	53.4260	−168.1663	515	CMG-6T	2003/01/09	-
OKCF	53.3948	−168.1382	685	L-4	2003/01/09	-
OKER	53.4536	−168.0513	956	L-4	2003/01/09	-
OKFG[B]	53.4107	−167.9115	201	CMG-6T	2003/01/09	-
OKID	53.4764	−167.8182	437	L-4	2003/01/09	-
OKIF_01[I]	53.4108	−167.9143	210	Chap-M21/25	2010/09/01	-
OKIF_02[I]	53.4100	−167.9137	212	Chap-M21/25	2010/09/01	-
OKIF_03[I]	53.4100	−167.9150	213	Chap-M21/25	2010/09/01	-
OKIF_04[I]	53.4103	−167.9144	215	Chap-M21/25	2010/09/01	-
OKNC[B]	53.4559	−168.1257	404	CMG-6T	2010/09/01	-
OKRE	53.5192	−168.1661	422	L-4	2003/01/09	-
OKSO[B]	53.3565	−168.1619	460	CMG-6T	2004/09/01	-
OKSP	53.2516	−168.2925	608	L-4	2003/01/09	-
OKTU	53.3829	−168.0431	646	L-4	2003/01/09	-
OKWE	53.4711	−168.2418	445	L-4	2003/01/09	-
OKWR	53.4337	−168.2076	1,017	L-4	2003/01/09	-

Table 2.17. Seismograph stations of the Pavlof Volcano subnetwork, operated by the Alaska Volcano Observatory.

[See table 2.1 for explanation of superscripted footnotes. Date format is year/two-digit month/two-digit day; -, station is still in operation]

Station[1]	Latitude	Longitude	Elevation, in meters	Sensor[2]	Open date	Close date
BLHA[TA]	55.7038	−162.0611	411	L-4	1996/07/11	-
HAG	55.3170	−161.9045	516	L-4	1996/07/11	-
HAG[3]	55.3170	−161.9045	516	L-22	2017/07/08	-
PN7A	55.4329	−161.9973	838	L-4	1996/07/11	2016/07/04
PN7A[3]	55.4329	−161.9973	838	L-22	2016/07/04	2017/07/09
PN7A[BP]	55.4329	−161.9973	838	TC120-PH2, Chap-M60/64	2017/07/09	-
PS1A	55.4201	−161.7437	283	L-4	1996/07/11	-
PS1A[BP]	55.4201	−161.7437	283	TC120-PH2, Chap-M60/64	2017/07/06	-
PS4A	55.3460	−161.8567	322	L-4	1996/07/11	-
PS4A[BP]	55.3460	−161.8567	322	TC120-PH2, Chap-M60/64	2017/07/04	-
PV6[3]	55.4528	−161.9205	747	L-22	1996/07/11	2016/07/04
PV6A[3p]	55.5070	−161.9714	352	L-22, Chap-M60/64	2016/07/04	-
PVV	55.3732	−161.7919	173	L-4	1996/07/11	-
PVV[3]	55.3732	−161.7919	173	L-22	2017/07/07	-

Table 2.18. Seismograph stations of the Redoubt Volcano subnetwork, operated by the Alaska Volcano Observatory.

[See table 2.1 for explanation of superscripted footnotes. Date format is year/two-digit month/two-digit day; -, station is still in operation]

Station[1]	Latitude	Longitude	Elevation, in meters	Sensor[2]	Open date	Close date
DFR[P]	60.5913	−152.6882	1,090	L-4, Chap-M2	1988/08/15	-
NCT	60.5615	−152.9316	1,120	L-4	1988/08/14	-
NCT[B]	60.5621	−152.9293	1,136	CMG-6T	2011/08/24	-
RDDF[B]	60.5912	−152.6883	1,134	CMG-6T	2010/01/11	-
RDDR	60.5843	−152.5887	905	L-4	2009/07/01	-
RDJH[B]	60.5905	−152.8058	1,414	CMG-6T	2009/02/04	-
RDN	60.5224	−152.7401	1,400	L-4	1988/08/13	-
RDSO[B]	60.4536	−152.7453	1,557	CMG-6T	2011/08/29	-
RDT	60.5726	−152.4075	930	L-4	1971/08/09	-
RDWB[B]	60.4875	−152.8424	1,546	CMG-6T	2009/02/24	-
RED[3]	60.4196	−152.7742	1,071	L-4	1990/08/30	2014/07/12
RED[3]	60.4196	−152.7742	1,071	L-22	2014/07/12	-
RED[B]	60.4196	−152.7742	1,071	CMG-6T	2011/08/24	-
REF[3L]	60.4888	−152.6940	1,641	L-22	1990/03/14	-
RSO	60.4616	−152.7560	1,921	L-4	1990/03/01	-

Table 2.19. Seismograph stations of the Shishaldin Volcano subnetwork, operated by the Alaska Volcano Observatory.

[See table 2.1 for explanation of superscripted footnotes. Date format is year/two-digit month/two-digit day; -, station is still in operation]

Station[1]	Latitude	Longitude	Elevation, in meters	Sensor[2]	Open date	Close date
BRPK	54.6446	−163.7428	393	L-4	1997/07/27	-
ISLZ	54.7251	−163.7130	631	L-4	2008/08/17	-
ISLZ[B]	54.7251	−163.7130	631	CMG-6T	2015/06/26	-
ISNN	54.8314	−163.7804	466	L-4	1997/07/27	-
ISNN[3]	54.8314	−163.7804	466	L-22	2016/07/29	-
SSBA[B]	54.7718	−164.1265	766	CMG-6T	2008/08/01	-
SSLN[P]	54.8109	−163.9979	637	L-4, Chap-M2	1997/07/27	-
SSLN[B]	54.8109	−163.9979	637	CMG-6T	2014/08/07	-
SSLS[3]	54.7111	−164.0008	817	L-22	1997/07/27	-
SSLS[B]	54.7111	−164.0008	817	CMG-6T	2014/08/07	-
SSLW	54.7709	−164.1234	636	L-4	1997/07/27	-

Table 2.20. Seismograph stations of the Mount Spurr subnetwork, operated by the Alaska Volcano Observatory.

[See table 2.1 for explanation of superscripted footnotes. Date format is year/two-digit month/two-digit day; -, station is still in operation]

Station[1]	Latitude	Longitude	Elevation, in meters	Sensor[2]	Open date	Close date
BGL	61.2663	−152.3913	1,127	L-4	1989/08/13	-
BKG	61.0696	−152.2650	1,009	L-4	1991/07/01	-
CGL	61.3071	−152.0090	1,082	L-4	1981/09/22	-
CKL	61.1958	−152.3400	1,281	L-4	1989/08/05	-
CKN	61.2234	−152.1838	735	L-4	1991/09/19	-
CKT	61.2002	−152.2085	975	L-4	1992/09/16	-
CP2	61.2636	−152.2441	1,981	L-4	1992/10/23	-
CRP[3]	61.2664	−152.1578	1,622	L-4	1981/08/26	-
NCG	61.4031	−152.1590	1,244	L-4	1989/08/06	-
SPBG[B]	61.2591	−152.3722	1,087	CMG-6T	2004/09/09	-
SPCG[B]	61.2913	−152.0228	1,329	CMG-6T	2004/09/08	-
SPCN[B]	61.2244	−152.1854	735	CMG-6T	2010/09/01	-
SPCP[B]	61.2655	−152.1550	1,616	TC120-PH2	2010/10/02	-
SPCR[B,TA]	61.2003	−152.2091	984	CMG-6T	2004/09/08	-
SPNN[B]	61.3662	−152.7012	1,666	CMG-6T	2011/08/01	-
SPU	61.1811	−152.0566	800	L-4	1971/08/10	-
SPU[B]	61.1811	−152.0566	800	TC120-PH2	2017/08/10	-
SPWE	61.2728	−152.5614	1,327	L-4	2004/08/18	-

Table 2.21. Seismograph stations of the Tanaga Volcano subnetwork, operated by the Alaska Volcano Observatory.

[See table 2.1 for explanation of superscripted footnotes. Date format is year/two-digit month/two-digit day; -, station is still in operation]

Station[1]	Latitude	Longitude	Elevation, in meters	Sensor[2]	Open date	Close date
TACS	51.8621	−178.1414	918	L-4	2003/08/28	-
TAFL	51.7555	−177.8998	186	L-4	2003/08/28	-
TAFP[3]	51.8990	−177.9853	440	L-22	2003/08/27	-
TANO	51.9146	−178.1228	269	L-4	2003/08/24	-
TAPA	51.8144	−177.8148	640	L-4	2003/08/27	-
TASE	51.8339	−178.0390	682	L-4	2003/08/24	-

Table 2.22. Seismograph stations of the Ugashik-Peulik Volcano subnetwork, operated by the Alaska Volcano Observatory.

[See table 2.1 for explanation of superscripted footnotes. Date format is year/two-digit month/two-digit day; -, station is still in operation]

Station[1]	Latitude	Longitude	Elevation, in meters	Sensor[2]	Open date	Close date
PLBL	57.6991	−156.8210	461	L-4	2004/08/01	-
PLK1	57.8012	−156.6093	78	L-4	2004/08/01	-
PLK2	57.7635	−156.3264	401	L-4	2004/08/01	-
PLK3[3]	57.6880	−156.2695	494	L-22	2004/08/01	-
PLK4	57.6314	−156.3598	1,031	L-4	2004/08/01	-
PLK5	57.9970	−156.8798	49	L-4	2004/08/01	-
PLWL	58.0442	−156.3434	585	L-4	2004/08/01	-

Table 2.23. Seismograph stations of the Mount Veniaminof subnetwork, operated by the Alaska Volcano Observatory.

[See table 2.1 for explanation of superscripted footnotes. Date format is year/two-digit month/two-digit day; -, station is still in operation]

Station[1]	Latitude	Longitude	Elevation, in meters	Sensor[2]	Open date	Close date
BPBC	56.5889	−158.4547	584	L-4	2002/10/03	-
VNFG[TA]	56.2849	−159.5532	1,068	L-4	2002/06/20	-
VNHG	56.2203	−159.1663	966	L-4	2002/02/06	-
VNKR	56.0304	−159.3699	620	L-4	2002/02/06	-
VNNF	56.2829	−159.3181	1,153	L-4	2002/06/20	-
VNSG	56.1250	−159.0875	761	L-4	2002/02/06	-
VNSS	56.2259	−159.4569	1,733	L-4	2002/02/06	-
VNSW	56.0712	−159.5606	716	L-4	2002/06/20	-
VNWF	56.1509	−159.5643	1,095	L-4	2002/02/06	-

Table 2.24. Seismograph stations of the Westdahl Peak subnetwork, operated by the Alaska Volcano Observatory.

[See table 2.1 for explanation of superscripted footnotes. Date format is year/two-digit month/two-digit day; -, station is still in operation]

Station[1]	Latitude	Longitude	Elevation, in meters	Sensor[2]	Open date	Close date
WEBT	54.5902	−164.7550	467	L-4	2008/08/02	-
WEBT[B]	54.5902	−164.7550	467	TC120-PH2	2017/06/27	-
WECS	54.5300	−164.7796	642	L-4	2008/08/04	-
WECS[B]	54.5300	−164.7796	642	CMG-6T	2015/06/29	-
WESE	54.4723	−164.5860	953	L-4	1998/08/28	-
WESN	54.5761	−164.5804	549	L-4	1998/10/17	-
WESP[3]	54.4926	−164.7233	937	L-22	2008/07/31	-
WTUG	54.8466	−164.3873	636	L-4	1998/10/17	-

Table 2.25. Seismograph stations of the Mount Wrangell subnetwork, operated by the Alaska Volcano Observatory.

[See table 2.1 for explanation of superscripted footnotes. Date format is year/two-digit month/two-digit day; -, station is still in operation]

Station[1]	Latitude	Longitude	Elevation, in meters	Sensor[2]	Open date	Close date
WACK[3]	61.9858	−144.3305	2,280	L-22	2000/07/31	2016/07/17
WACK[B]	61.9858	−144.3305	2,280	TC120	2016/07/17	-
WANC	62.0027	−144.0720	4,190	L-4	2000/07/31	-
WASW	61.9277	−144.1745	2,196	L-4	2001/08/03	2016/07/17
WASW[3]	61.9277	−144.1745	2,196	L-22	2016/07/17	-
WAZA	62.0746	−144.1544	2,531	L-4	2001/08/03	2016/10/05
WAZA[B]	62.0746	−144.1544	2,531	TC120	2017/07/29	-

Table 2.26. Regional seismograph and infrasound stations operated by the Alaska Volcano Observatory.

[See table 2.1 for explanation of superscripted footnotes. Date format is year/two-digit month/two-digit day; -, station is still in operation]

Station[1]	Latitude	Longitude	Elevation, in meters	Sensor[2]	Open date	Close date
ADAG	51.9791	−176.6037	286	L-4	1999/09/15	-
ADAK[P]	51.8620	−176.6449	5	Chap-M21/25	2012/06/25	2017/06/23
ADKI_01[I]	51.8619	−176.6439	5	Chap-M21/25	2017/06/23	-
ADKI_02[I]	51.8632	−176.6436	5	Chap-M21/25	2017/06/23	-
ADKI_03[I]	51.8623	−176.6446	5	Chap-M21/25	2017/06/23	-
ADKI_04[I]	51.8625	−176.6458	5	Chap-M21/25	2017/06/23	-
ADKI_05[I]	51.8633	−176.6461	5	Chap-M21/25	2017/06/23	-
ADKI_06[I]	51.8616	−176.6469	5	Chap-M21/25	2017/06/23	-
AMKA[B]	51.3771	179.3000	116	T-40	2005/10/14	-
BGM	59.3920	−155.2315	625	L-4	1978/09/08	-
BGR	60.7569	−152.4199	985	L-4	1991/07/01	-
ETKA	51.8608	−176.4079	290	L-4	1999/09/15	-
MMN	59.1845	−154.3389	442	S-13	1981/08/22	-
OPT[TA]	59.6526	−153.2321	602	S-13	1974/01/01	-
PDB	59.7841	−154.1917	360	L-4	1978/09/09	-
SDPI_01[I]	55.3490	−160.4764	200	VDP-10	2016/10/17	-
SDPI_02[I]	55.3487	−160.4768	200	VDP-10	2016/10/17	-
SDPI_03[I]	55.3493	−160.4773	200	VDP-10	2016/10/17	-
SDPI_04[I]	55.3495	−160.4766	200	VDP-10	2016/10/17	-
SDPI_05[I]	55.3492	−160.4765	200	VDP-10	2016/10/17	-
SDPI_06[I]	55.3492	−160.4771	200	VDP-10	2016/10/17	-
STLK	61.4982	−151.8349	945	L-4	1997/09/01	-
STLK[3]	61.4982	−151.8349	945	L-22	2016/08/31	2017/08/14
STLK[B]	61.4982	−151.8349	945	TC120-PH2	2017/08/14	-
SYI[TA]	58.6094	−152.3935	149	L-4	1997/09/01	-

Appendix 3. Operational Status for Alaska Volcano Observatory Stations in 2013–17

The operational status of Alaska Volcano Observatory seismograph stations for 2013–17 is shown using the Incorporated Research Institutions for Seismology (IRIS) Gap/Overlap Analysis Tool (GOAT) (Stromme, 2000). GOAT is a web-based tool which graphically displays gaps, overlaps, and continuous time spans of time series data in the IRIS Data Management Center's database. GOAT cannot determine the quality of the data, just the presence of data on the archived channel.

In figures 3.1–3.7, the plots display a color-coded graph showing gaps in red and continuous data in green. A summary of the station availability is shown in table 3.1.

Table 3.1. Summary of data availability for Alaska Volcano Observatory (AVO) stations in 2013–17 determined using to the Incorporated Research Institutions for Seismology Gap/Overlap Analysis Tool (Stromme, 2000).

Data availability, in percent	AVO seismograph stations sorted by data availability
100	ADKI, BPBC, CKL, CKN, CKT, CP2, CRP, ISNN, KAIC, KOFP, KOKL, KOKV, KONE, KNOW, KOSE, KOWE, MAPS, MREP, MSW, NCG, NCT, OKAK, OKCF, OKER, OKID, OKRE, OKSP, OKTU, OKWE, OKWR, PV6A, RDT, RSO, SPU, SPWE, STLK, SYI, VNFG, VNHG, WACK.
90–99	ADAG, AHB, AKGG, AKMO, AKRB, AKSA, AKS, AU22, AUE, AUH, AUI, AUJA, AUL, AUNW, AUP, AUSB, AUWS, AUW, BGL, BLDY, BLHA, BRPK, CDD, CGL, CLCO, CLES, CNTC, DFR, DRR3, DT1, DTN, ETKA, GAEA, GAKI, GALA, GANE, GANO, GASW, GSCK, GSIG, GSMY, GSSP, GSTD, GSTR, HAG, HSB, ILI, ILSW, ILS, ILW, INE, ISLZ, IVE, KICM, KIKV, KIMD, KINC, KIRH, KIWB, MCIR, MGOD, MNAT, MTBL, OKCE, OKFG, OPT, PN7A, PS1A, PS4A, PV6, PVV, RDDF, RED, SPBG, SPCG, SSLS, SSLW, TAFL, TAFP, TANO, TAPA, TASE, VNSG, WEBT, WECS, WESE, WESN, WESP, ZRO.
80–89	ACH, AKV, ANCK, AUQ, AUSS, BGM, CAHL, CEAP, CEPE, CERA, CERB, CESW, CETU, FONW, FOPK, FOSS, ILNE, IVS, KABR, KAHC, KAHG, KAPH, KARR, KAWH, KBM, KCE, KCG ,KEL, KJL, KVT, LSNW, LSPA, LSSA, LSSE, LVA, MMN, OKSO, PBD, PLBL, PLK1, PLK2, PLK3, PLK4, PLK5, PLWL, RDJH, RDSO, SPCN, SPCP, SSBA.
70–79	AKBB, AKLV, ANNE, ANNW, ANPB, ANPK, KAKN, RDN, REF, SSLN, VNSS, VNWF.
60–69	AMKA, ANON, AUCH, AZAC, DOL, KABU, MGLS, OKNC, VNKR, VNNF, VNSW, WAZA.
50–59	RDWB, SPNN, WASW.
40–49	WTUG.
30–39	no stations
20–29	no stations
10–19	AUJK.
0–9	no stations
Unavailable at IRIS	AKT, BGR, BKG, OKIF, RDDR, SDPI, TACS,WANC.

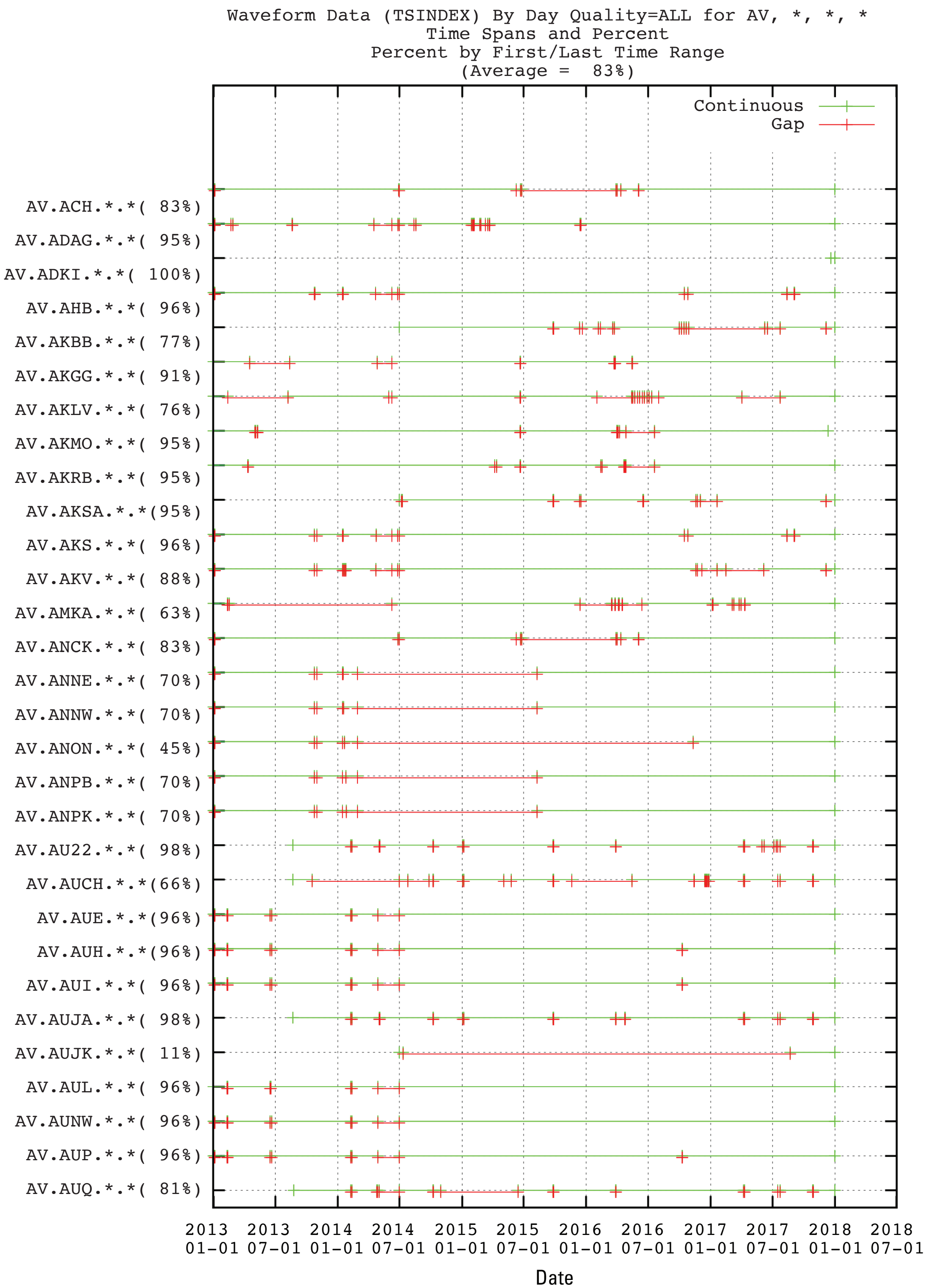

Figure 3.1. Image showing data availability for Alaska Volcano Observatory seismograph stations ACH to AUQ determined using the Incorporated Research Institutions for Seismology Gap/Overlap Analysis Tool (Stromme, 2000). Gaps are shown in red, and continuous data is shown in green. %, percent. Date format is year, two-digit month and day.

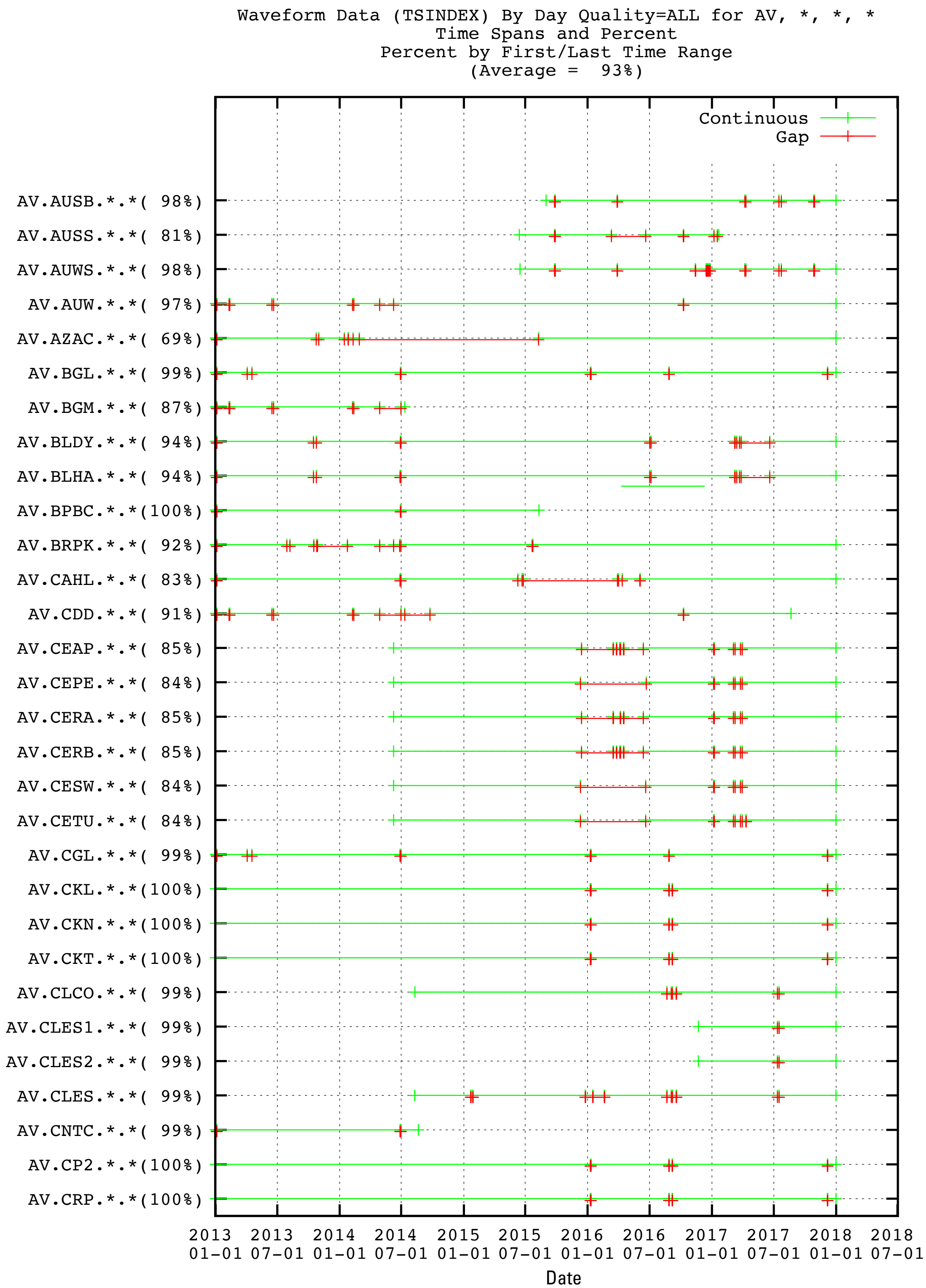

Figure 3.2. Image showing data availability for Alaska Volcano Observatory seismograph stations AUSB to CRP determined using the Incorporated Research Institutions for Seismology Gap/Overlap Analysis Tool (Stromme, 2000). Gaps are shown in red, and continuous data is shown in green. %, percent. Date/time format is year, two-digit month and day.

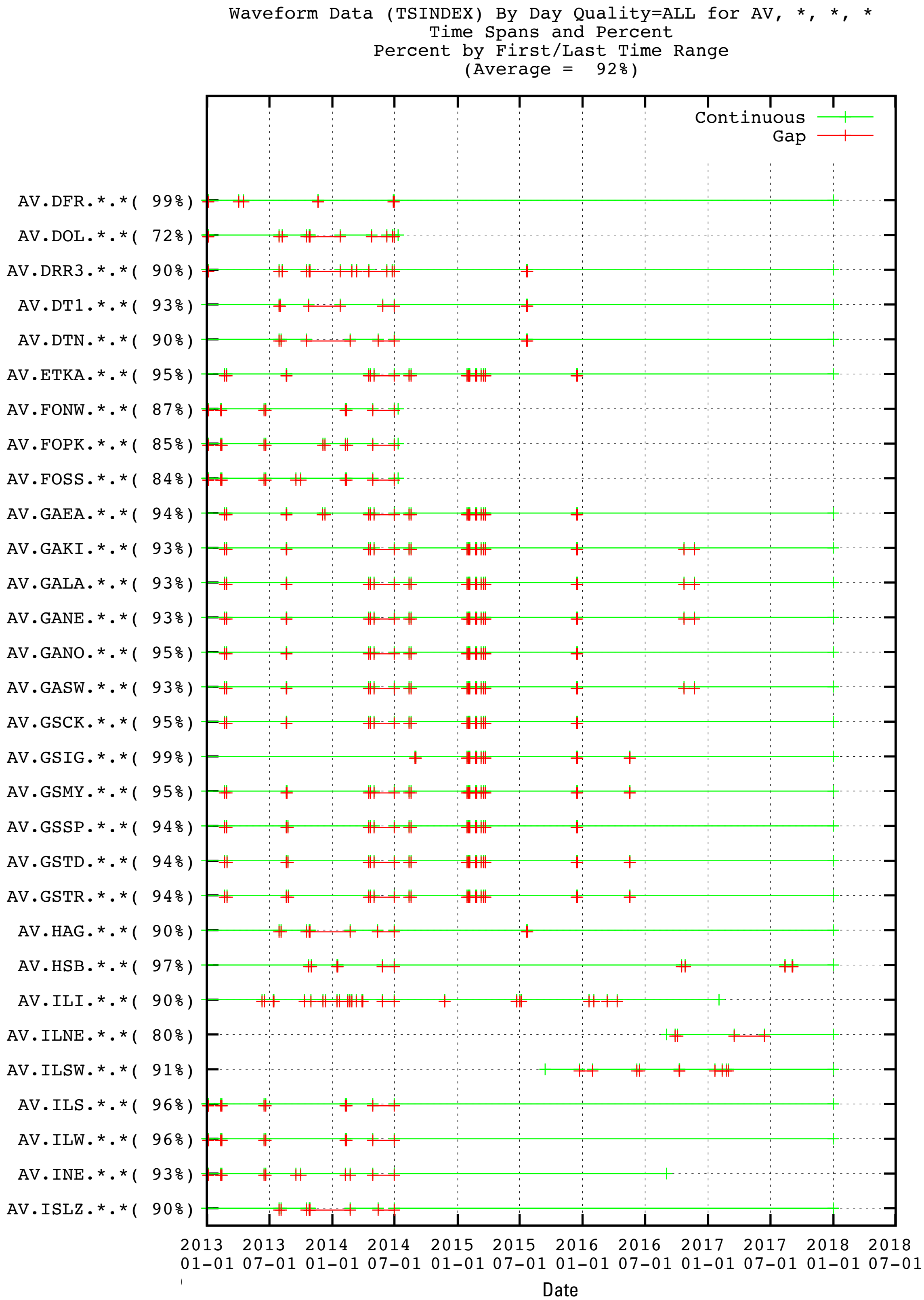

Figure 3.3. Image showing data availability for Alaska Volcano Observatory seismograph stations DFR to ISLZ determined using the Incorporated Research Institutions for Seismology Gap/Overlap Analysis Tool (Stromme, 2000). Gaps are shown in red, and continuous data is shown in green. %, percent. Date/time format is year, two-digit month and day.

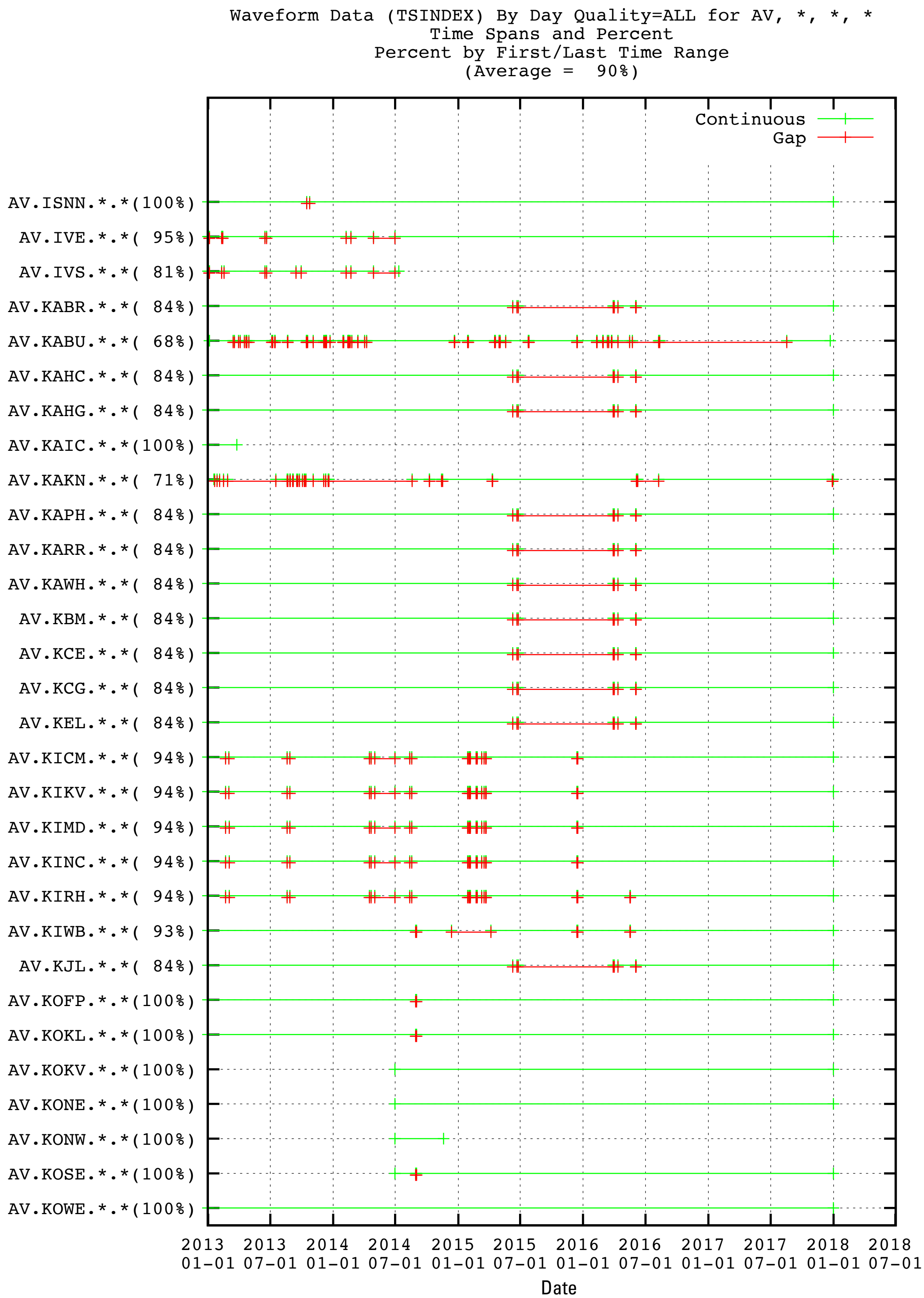

Figure 3.4. Image showing data availability for Alaska Volcano Observatory seismograph stations ISNN to KOWE determined using the Incorporated Research Institutions for Seismology Gap/Overlap Analysis Tool (Stromme, 2000). Gaps are shown in red, and continuous data is shown in green. %, percent. Date/time format is year, two-digit month and day

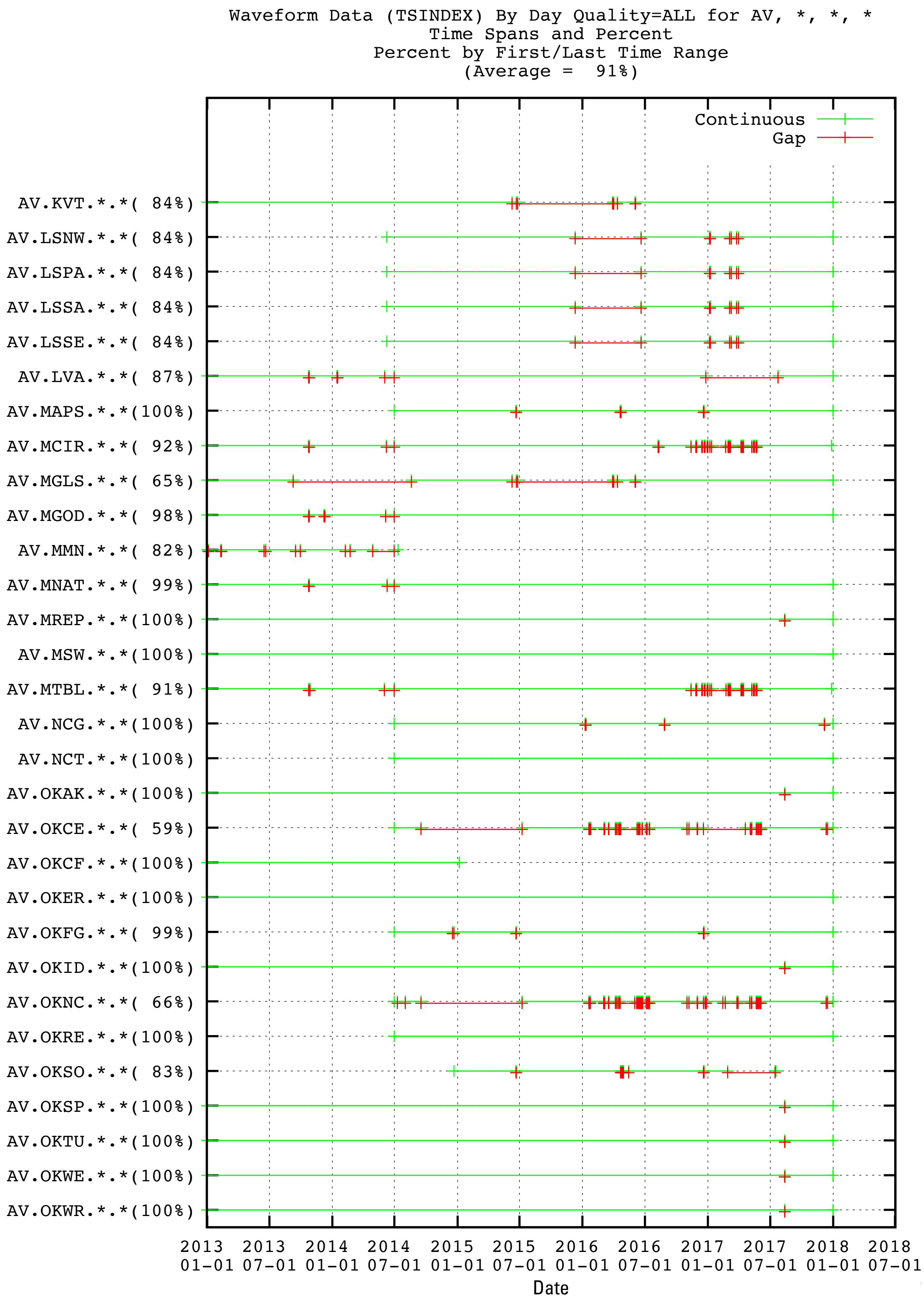

Figure 3.5. Image showing data availability for Alaska Volcano Observatory seismograph stations KVT to OKWR determined using the Incorporated Research Institutions for Seismology Gap/Overlap Analysis Tool (Stromme, 2000). Gaps are shown in red, and continuous data is shown in green. %, percent. Date/time format is year, two-digit month and day

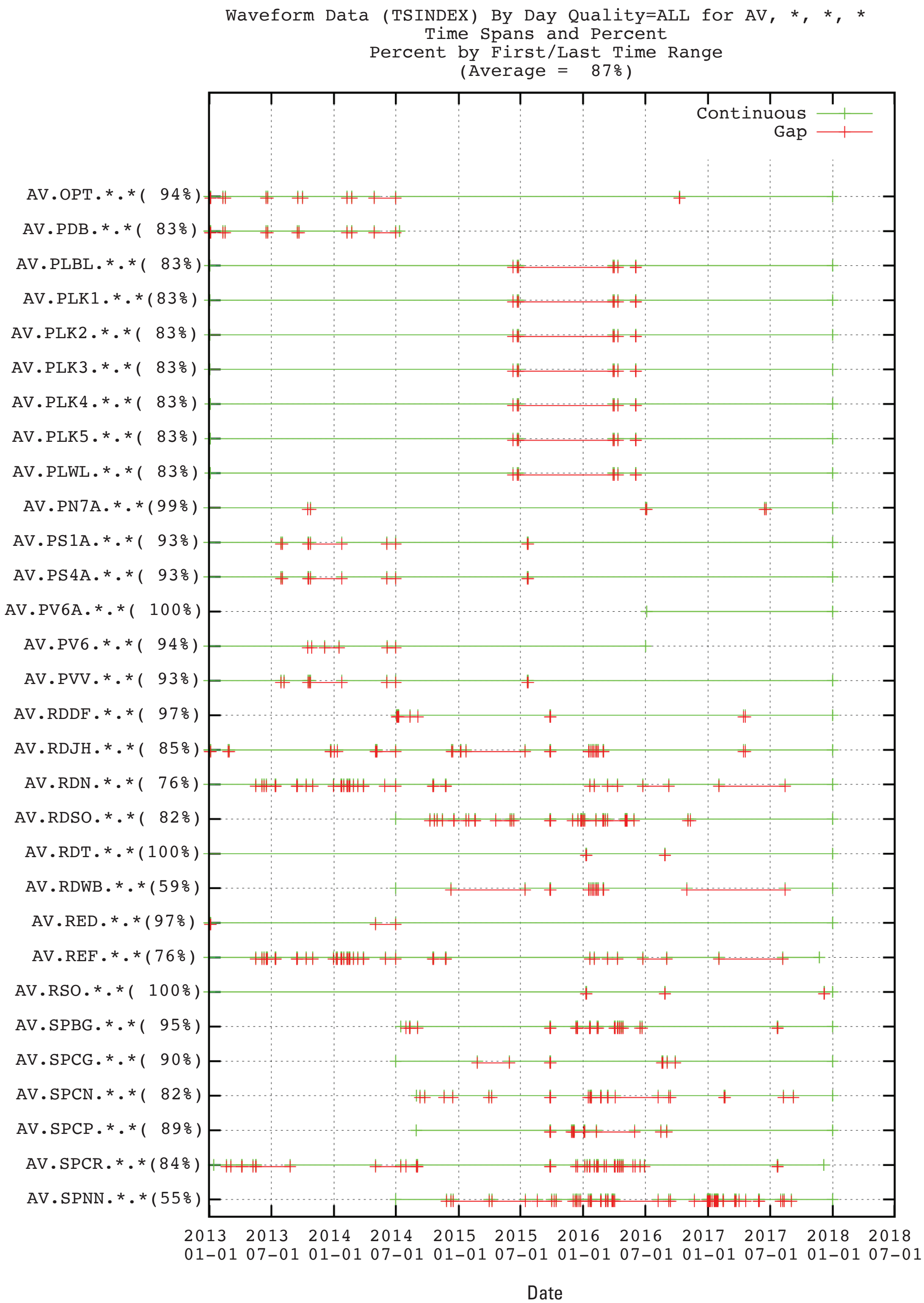

Figure 3.6. Image showing data availability for Alaska Volcano Observatory seismograph stations OPT to SPNN determined using the Incorporated Research Institutions for Seismology Gap/Overlap Analysis Tool (Stromme, 2000). Gaps are shown in red, and continuous data is shown in green. %, percent. Date/time format is year, two-digit month and day

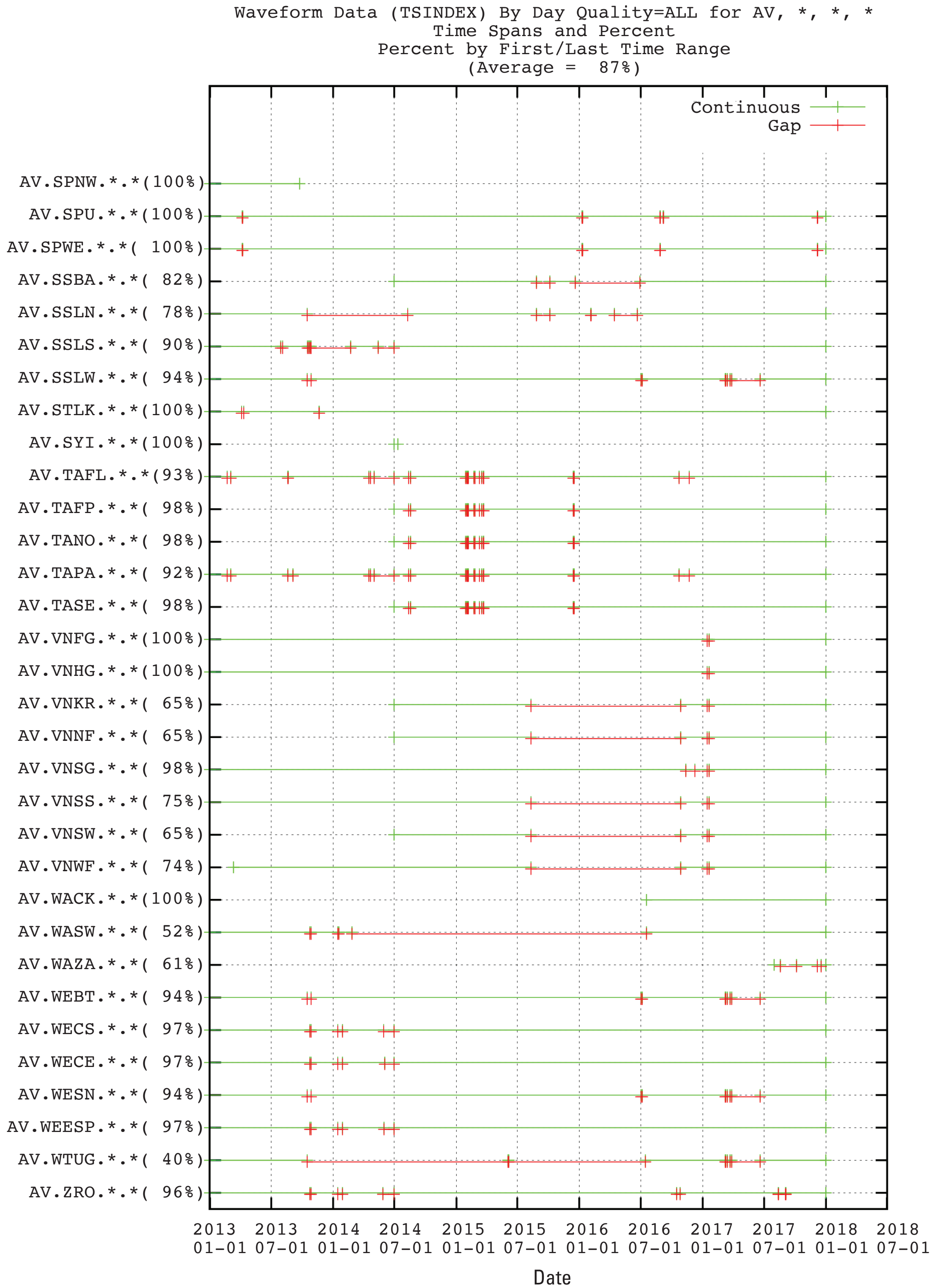

Figure 3.7. Image showing data availability for Alaska Volcano Observatory seismograph stations SPNW to ZRO determined using the Incorporated Research Institutions for Seismology Gap/Overlap Analysis Tool (Stromme, 2000). Gaps are shown in red, and continuous data is shown in green. %, percent. Date/time format is year, two-digit month and day

This page left blank intentionally

Appendix 4. Data Use Scores for Alaska Volcano Observatory Stations in 2013–17

Data-use scores developed by Matthew Haney are a normalized measure of the number of P-phases picks on a seismograph station in the Alaska Volcano Observatory (AVO) earthquake catalog. They represent a combination of data availability, data quality, and picking preference of the analyst in the case of co-located instruments at a site. The normalization seeks to remove, as much as possible, the effect of frequency of earthquake occurrence near a particular station.

The scores given in the tables 4.1–4.26 are based on an empirical relation derived from the AVO catalog between local magnitude (M_L) and the distance to the farthest P-phase pick (*dmax*):

$$M_L = 0.8494 \times \log10(dmax) + 0.0036 dmax - 0.7112$$

The relationship quantifies the fact that larger earthquakes register on stations at farther distances and in general are picked to greater range from the epicenter. For example, the above relation predicts that an earthquake with a magnitude of approximately 1.5 should be picked to distances of about 100 km. The regression model consists of three coefficients in the above equation which can be related to average values of geometrical spreading, attenuation, and site conditions in the Aleutian arc.

Given the above relation between M_L and *dmax*, whether a station should have been picked or not can be established for a located earthquake in the AVO catalog with a certain magnitude. Thus, the number of times a station should have been picked for the earthquakes in the AVO catalog can be determined, and this quantity can be compared to the number of times the station was actually picked. The ratio of the actual number of P-phase picks to the predicted number multiplied by 100 is the data use score. A score of 100 means a station was picked the same number of times it should have been picked based on the M_L-*dmax* relation. Stations that are picked more often than they should be have data-use scores higher than 100, whereas stations picked less often than they should be have scores below 100.

Table 4.1. Data-use scores by year for Alaska Volcano Observatory seismograph stations in the Akutan Peak subnetwork, 2013–17.

[NA, not applicable]

Station	2013	2014	2015	2016	2017
AHB.EHZ	83	67	53	73	88
AKBB.BHZ	98	115	97	84	37
AKGG.BHZ	64	125	89	75	114
AKLV.BHZ	55	106	89	69	70
AKMO.BHZ	87	110	85	80	73
AKRB.BHZ	81	109	98	91	124
AKS.EHZ	83	96	71	72	79
AKSA.BHZ	26	67	46	44	36
AKT.BHZ	0	0	0	0	0
AKV.BHZ	NA	NA	NA	0	11
AKV.EHZ	65	100	61	42	NA
HSB.EHZ	37	63	29	32	87
LVA.BHZ	NA	NA	NA	0	36
LVA.EHZ	34	38	45	52	NA
ZRO.EHZ	92	125	105	120	143

Table 4.2. Data-use scores by year for Alaska Volcano Observatory seismograph stations in the Aniakchak Crater subnetwork, 2013–17.

Station	2013	2014	2015	2016	2017
ANNE.EHZ	118	0	15	77	86
ANNW.EHZ	68	0	10	89	63
ANON.EHZ	0	0	0	6	46
ANPB.EHZ	161	0	14	95	96
ANPK.EHZ	45	0	0	0	45
AZAC.EHZ	118	0	8	84	80

Table 4.3. Data-use scores by year for Alaska Volcano Observatory seismograph stations in the Augustine Volcano subnetwork, 2013–17.

[NA, not applicable]

Station	2013	2014	2015	2016	2017
AU22.BHZ	9	18	48	12	5
AUCH.BHZ	NA	27	79	74	106
AUE.EHZ	28	29	33	10	3
AUH.EHZ	70	85	86	109	86
AUI.EHZ	32	0	0	0	0
AUJA.BHZ	0	57	91	156	146
AUJK.EHZ	99	44	0	0	26
AUL.BHZ	85	63	99	168	161
AUL.EHZ	2	4	0	0	0
AUNW.EHZ	0	0	0	0	0
AUP.EHZ	66	77	57	0	0
AUQ.BHZ	12	48	60	150	137
AUSB.BHZ	NA	NA	0	0	56
AUSS.BHZ	NA	NA	7	32	1
AUW.EHZ	103	86	76	22	27
AUWS.BHZ	NA	NA	12	145	126

Table 4.4. Data-use scores by year for Alaska Volcano Observatory seismograph stations in the Mount Cerberus subnetwork, 2013–17.

[NA, not applicable]

Station	2013	2014	2015	2016	2017
CEAP.SHZ	2	121	135	43	28
CEPE.SHZ	0	0	6	59	47
CERA.SHZ	1	114	145	52	25
CERB.SHZ	1	103	113	38	21
CESW.SHZ	1	116	123	54	40
CETU.SHZ	2	84	31	36	28

Table 4.5. Data-use scores by year for Alaska Volcano Observatory seismograph stations in the Mount Cleveland subnetwork, 2013–17.

[NA, not applicable]

Station	2013	2014	2015	2016	2017
CLCO.BHZ	NA	26	76	67	51
CLCO.SHZ	NA	0	5	3	0
CLES.BHZ	NA	26	77	67	50
CLES.SHZ	NA	0	0	4	3

Table 4.6. Data-use scores by year for Alaska Volcano Observatory seismograph stations in the Mount Dutton subnetwork, 2013–17.

[NA, not applicable]

Station	2013	2014	2015	2016	2017
BLDY.EHZ	0	11	18	9	0
DOL.EHZ	68	35	0	0	0
DRR3.EHZ	60	3	0	0	0
DT1.EHZ	47	63	49	40	17
DTN.EHZ	34	0	0	32	12

Table 4.7. Data-use scores by year for Alaska Volcano Observatory seismograph stations in the Fourpeaked Mountain subnetwork, 2013–17.

Station	2013	2014	2015	2016	2017
CDD.EHZ	0	0	0	0	0
FONW.EHZ	77	0	0	0	0
FOPK.EHZ	0	0	0	0	0
FOSS.EHZ	16	3	0	0	0

Table 4.8. Data-use scores by year for Alaska Volcano Observatory seismograph stations in the Mount Gareloi subnetwork, 2013–17.

Station	2013	2014	2015	2016	2017
GAEA.EHZ	63	58	65	105	81
GAKI.EHZ	0	0	6	31	4
GALA.EHZ	30	28	57	103	46
GANE.EHZ	2	0	24	44	43
GANO.EHZ	0	0	36	96	71
GASW.EHZ	0	0	30	86	26

Table 4.9. Data-use scores by year for Alaska Volcano Observatory seismograph stations in the Great Sitkin Volcano subnetwork, 2013–17.

Station	2013	2014	2015	2016	2017
GSCK.EHZ	12	11	48	197	219
GSIG.EHZ	0	0	64	42	0
GSMY.EHZ	159	127	148	145	219
GSSP.EHZ	83	34	75	136	163
GSTD.EHZ	96	88	113	154	87
GSTR.EHZ	111	73	97	175	202

Table 4.10. Data-use scores by year for Alaska Volcano Observatory seismograph stations in the Iliamna Volcano subnetwork, 2013–17.

[NA, not applicable]

Station	2013	2014	2015	2016	2017
ILI.EHZ	33	23	9	5	0
ILNE.SHZ	NA	NA	NA	0	38
ILS.BHZ	NA	NA	0	0	23
ILS.EHZ	216	84	57	0	0
ILSW.BHZ	NA	NA	0	0	44
ILW.BHZ	14	0	0	0	NA
ILW.EHZ	330	51	2	0	0
ILW.SHZ	NA	NA	NA	0	25
INE.EHZ	237	13	9	0	0
IVE.BHZ	10	15	75	9	49
IVE.EHZ	234	61	9	0	0
IVS.EHZ	0	0	0	0	0

Table 4.11. Data-use scores by year for Alaska Volcano Observatory seismograph stations in the Kanaga Volcano subnetwork, 2013–17.

Station	2013	2014	2015	2016	2017
KICM.EHZ	92	90	83	95	53
KIKV.EHZ	118	109	103	136	71
KIMD.EHZ	96	95	105	128	139
KINC.EHZ	88	83	57	96	42
KIRH.EHZ	116	96	79	56	14
KIWB.EHZ	89	13	72	115	66

Table 4.12. Data-use scores by year for Alaska Volcano Observatory seismograph stations in the Katmai volcanic cluster subnetwork, 2013–17.

[NA, not applicable]

Station	2013	2014	2015	2016	2017
ACH.BHZ	NA	NA	NA	NA	35
ACH.EHZ	77	66	99	25	0
ANCK.BHZ	NA	NA	NA	0	27
ANCK.EHZ	60	92	94	29	NA
CAHL.EHZ	99	96	111	35	0
CNTC.EHZ	15	0	0	0	0
KABR.EHZ	64	53	112	48	70
KABU.BHZ	71	106	125	10	63
KAHC.EHZ	127	147	156	71	107
KAHG.BHZ	NA	NA	NA	NA	33
KAHG.EHZ	78	65	70	46	30
KAIC.EHZ	0	0	0	0	0
KAKN.BHZ	54	78	58	77	170
KAPH.EHZ	33	53	60	49	44
KARR.EHZ	77	54	64	45	49
KAWH.EHZ	49	61	49	45	44
KBM.EHZ	71	86	159	64	127
KCE.EHZ	72	75	139	55	127
KCG.EHZ	71	128	100	100	168
KEL.EHZ	86	57	66	46	49
KJL.EHZ	59	50	54	18	0
KVT.EHZ	62	95	197	80	177
MGLS.EHZ	12	20	50	2	0

Table 4.13. Data-use scores by year for Alaska Volcano Observatory seismograph stations in the Korovin Volcano subnetwork, 2013–17.

Station	2013	2014	2015	2016	2017
KOFP.EHZ	104	165	159	130	80
KOKL.EHZ	96	128	114	104	70
KOKV.EHZ	15	4	0	1	8
KONE.EHZ	28	79	64	47	38
KONW.EHZ	51	14	0	0	0
KOSE.EHZ	46	142	114	91	74
KOWE.EHZ	94	141	107	101	65

Table 4.14. Data-use scores by year for Alaska Volcano Observatory seismograph stations in the Little Sitkin Volcano subnetwork, 2013–17.

Station	2013	2014	2015	2016	2017
LSNW.SHZ	13	64	95	72	23
LSPA.SHZ	9	64	96	73	25
LSSA.SHZ	13	49	85	63	23
LSSE.SHZ	9	51	94	76	26

Table 4.15. Data-use scores by year for Alaska Volcano Observatory seismograph stations in the Makushin Volcano subnetwork, 2013–17.

[NA, not applicable]

Station	2013	2014	2015	2016	2017
MAPS.BHZ	119	175	186	192	280
MCIR.BHZ	NA	NA	NA	0	132
MCIR.EHZ	104	98	78	23	NA
MGOD.BHZ	124	107	134	108	290
MGOD.EHZ	29	28	36	68	2
MNAT.BHZ	157	206	225	117	262
MNAT.EHZ	5	0	1	63	1
MREP.EHZ	161	200	173	124	183
MSW.BHZ	150	215	232	182	298
MSW.EHZ	32	9	11	32	NA
MTBL.BHZ	NA	NA	NA	0	16
MTBL.EHZ	141	144	197	127	NA

Table 4.16. Data-use scores by year for Alaska Volcano Observatory seismograph stations in the Okmok Caldera subnetwork, 2013–17.

Station	2013	2014	2015	2016	2017
OKAK.EHZ	97	107	100	59	25
OKCE.BHZ	9	52	16	13	19
OKCF.EHZ	0	1	0	0	0
OKER.EHZ	25	20	41	43	49
OKFG.BHZ	49	67	63	56	111
OKID.EHZ	0	0	0	0	0
OKNC.BHZ	37	32	10	15	80
OKRE.EHZ	29	41	93	38	22
OKSO.BHZ	0	2	75	48	5
OKSP.EHZ	95	96	84	78	31
OKTU.EHZ	86	109	99	51	45
OKWE.EHZ	98	113	67	42	21
OKWR.EHZ	63	76	16	24	39

Table 4.17. Data-use scores by year for Alaska Volcano Observatory seismograph stations in the Pavlof Volcano subnetwork, 2013–17.

[NA, not applicable]

Station	2013	2014	2015	2016	2017
BLHA.EHZ	0	27	23	16	0
HAG.EHZ	43	62	49	49	39
HAG.SHZ	NA	NA	NA	NA	13
PN7A.BHZ	NA	NA	NA	NA	14
PN7A.EHZ	26	44	45	6	NA
PN7A.SHZ	NA	NA	NA	0	25
PS1A.BHZ	NA	NA	NA	NA	19
PS1A.EHZ	29	53	28	33	21
PS4A.BHZ	NA	NA	NA	NA	14
PS4A.EHZ	91	83	59	42	43
PV6.EHZ	26	42	41	0	NA
PV6A.SHZ	NA	NA	NA	0	49
PVV.EHZ	41	64	41	34	36
PVV.SHZ	NA	NA	NA	NA	15

Table 4.18. Data-use scores by year for Alaska Volcano Observatory seismograph stations in the Redoubt Volcano subnetwork, 2013–17.

[NA, not applicable]

Station	2013	2014	2015	2016	2017
DFR.EHZ	170	22	168	213	217
NCT.BHZ	43	43	191	227	215
NCT.EHZ	139	10	12	7	9
RDDF.BHZ	45	126	189	234	191
RDDR.EHZ	0	0	0	0	0
RDJH.BHZ	124	93	48	174	127
RDN.EHZ	76	56	80	13	69
RDSO.BHZ	147	67	131	115	218
RDT.BHZ	NA	NA	NA	NA	33
RDT.EHZ	145	171	163	182	140
RDWB.BHZ	211	132	101	173	94
RED.BHZ	186	123	199	152	226
RED.EHZ	3	6	NA	NA	NA
REF.EHZ	79	31	120	23	0
REF.SHZ	0	0	0	0	13
RSO.EHZ	175	122	193	140	192

Table 4.19. Data-use scores by year for Alaska Volcano Observatory seismograph stations in the Shishaldin Volcano subnetwork, 2013–17.

[NA, not applicable]

Station	2013	2014	2015	2016	2017
BRPK.EHZ	0	44	66	54	42
ISLZ.BHZ	NA	NA	61	64	37
ISLZ.EHZ	25	10	0	0	11
ISNN.EHZ	0	0	45	51	33
ISNN.SHZ	NA	NA	NA	0	10
SSBA.BHZ	34	73	68	44	50
SSLN.BHZ	NA	27	40	41	41
SSLN.EHZ	12	20	17	19	16
SSLS.BHZ	NA	27	56	45	32
SSLS.EHZ	16	5	0	0	0
SSLW.EHZ	28	50	55	50	26

Table 4.20. Data-use scores by year for Alaska Volcano Observatory seismograph stations in the Mount Spurr subnetwork, 2013–17.

[NA, not applicable]

Station	2013	2014	2015	2016	2017
BGL.EHZ	275	107	208	182	202
CGL.EHZ	319	178	242	193	182
CKL.EHZ	259	125	195	270	156
CKN.EHZ	203	139	182	120	161
CKT.EHZ	199	132	161	122	126
CP2.EHZ	64	58	102	13	46
CRP.EHZ	195	113	198	176	169
NCG.EHZ	80	0	0	0	0
SPBG.BHZ	99	102	154	149	117
SPCG.BHZ	168	194	261	369	234
SPCN.BHZ	27	47	187	37	107
SPCP.BHZ	119	95	208	107	209
SPCR.BHZ	87	110	174	136	128
SPNN.BHZ	156	112	60	14	82
SPU.BHZ	NA	NA	NA	NA	0
SPU.EHZ	108	51	186	269	203
SPWE.EHZ	258	111	199	117	0

Table 4.21. Data-use scores by year for Alaska Volcano Observatory seismograph stations in the Tanaga Volcano subnetwork, 2013–17.

Station	2013	2014	2015	2016	2017
TACS.EHZ	0	0	0	0	0
TAFL.EHZ	21	0	29	76	64
TAFP.EHZ	103	100	101	107	91
TANO.EHZ	65	74	66	63	37
TAPA.EHZ	81	85	67	91	67
TASE.EHZ	98	96	105	108	61

Table 4.22. Data-use scores by year for Alaska Volcano Observatory seismograph stations in the Ugahik-Peulik Volcano subnetwork, 2013–17.

Station	2013	2014	2015	2016	2017
PLBL.EHZ	36	39	55	18	21
PLK1.EHZ	78	74	80	23	39
PLK2.EHZ	52	56	57	5	0
PLK3.EHZ	58	63	67	26	38
PLK4.EHZ	29	9	4	1	0
PLK5.EHZ	30	29	45	14	18
PLWL.EHZ	14	5	8	0	3

Table 4.23. Data-use scores by year for Alaska Volcano Observatory seismograph stations in the Mount Veniaminof subnetwork, 2013–17.

Station	2013	2014	2015	2016	2017
BPBC.EHZ	0	0	0	0	0
VNFG.EHZ	57	63	11	40	40
VNHG.EHZ	64	80	16	64	62
VNKR.EHZ	0	0	0	2	43
VNNF.EHZ	21	62	0	2	44
VNSG.EHZ	64	90	0	9	41
VNSS.EHZ	67	97	0	4	61
VNSW.EHZ	0	0	0	0	23
VNWF.EHZ	29	100	0	4	49

Table 4.24. Data-use scores by year for Alaska Volcano Observatory seismograph stations in the Westdahl Peak subnetwork, 2013–17.

[NA, not applicable]

Station	2013	2014	2015	2016	2017
WEBT.BHZ	NA	NA	NA	NA	2
WEBT.EHZ	47	43	45	68	42
WECS.BHZ	NA	NA	0	0	31
WECS.EHZ	9	43	66	78	43
WESE.EHZ	32	39	56	80	74
WESN.EHZ	31	8	53	84	41
WESP.EHZ	51	48	59	63	57
WTUG.EHZ	0	45	54	53	1

Table 4.25. Data-use scores by year for Alaska Volcano Observatory seismograph stations in the Mount Wrangell subnetwork, 2013–17.

[NA, not applicable]

Station	2013	2014	2015	2016	2017
WACK.BHZ	NA	NA	NA	0	138
WACK.EHZ	0	0	0	0	NA
WANC.EHZ	0	0	0	0	0
WASW.EHZ	0	0	0	0	NA
WASW.SHZ	NA	NA	NA	0	106
WAZA.BHZ	NA	NA	NA	NA	67
WAZA.EHZ	0	0	0	0	NA

Table 4.26. Data-use scores by year for Alaska Volcano Observatory regional seismograph stations, 2013–17.

[NA, not applicable]

Station	2013	2014	2015	2016	2017
ADAG.EHZ	75	56	52	39	16
AMKA.BHZ	5	72	79	30	15
BGM.EHZ	0	0	0	0	0
BGR.EHZ	0	0	0	0	0
BKG.EHZ	0	0	0	0	0
ETKA.EHZ	69	18	24	39	3
MMN.EHZ	2	0	0	0	0
OPT.EHZ	0	35	42	15	18
PDB.EHZ	2	0	0	0	0
STLK.BHZ	NA	NA	NA	NA	23
STLK.EHZ	0	214	368	371	244
STLK.SHZ	NA	NA	NA	0	0
SYI.EHZ	0	0	0	0	0

This page left blank intentionally

Appendix 5. Seismic-Velocity Models Used for Locating Earthquakes

One-dimensional velocity models used by the Alaska Volcano Observatory for earthquake location are given in tables 5.1–5.14. Depths are referenced to sea level, with negative values reflecting height above sea level. Cylindrical regions where the models were applied are described in appendix 6.

Table 5.1. Velocity model used by the Alaska Volcano Observatory for Akutan Peak (Power and others, 1996).

[V_P, P-wave or compressional-wave velocity; V_S, S-wave or shear-wave velocity]

Layer	V_p in kilometers per second	Top of layer, in kilometers	V_p/V_s
1	2.30 +0.37 per km depth	−3.0	1.80
2	6.30	7.0	1.80

Table 5.2. Velocity model used by the Alaska Volcano Observatory for the Andreanof Islands region (Toth and Kisslinger, 1984).

[V_P, P-wave or compressional-wave velocity; V_S, S-wave or shear-wave velocity]

Layer	V_p in kilometers per second	Top of layer, in kilometers	V_p/V_s
1	3.50	−3.0	1.73
2	3.88	−2.8	1.73
3	4.25	−2.6	1.73
4	4.62	−2.4	1.73
5	5.00	−2.2	1.73
6	5.50	−2.0	1.73
7	5.62	−1.0	1.73
8	5.74	0.0	1.73
9	5.86	1.0	1.73
10	5.98	2.0	1.73
11	6.10	3.0	1.73
12	6.60	4.0	1.73
13	6.68	5.0	1.73
14	6.80	8.0	1.73
15	6.92	11.0	1.73
16	7.04	14.0	1.73
17	7.16	17.0	1.73
18	7.28	20.0	1.73
19	7.85	23.0	1.73
20	8.05	37.0	1.73

Table 5.3. Velocity model used by the Alaska Volcano Observatory for Augustine Volcano (Power, 1988).

[V_P, P-wave or compressional-wave velocity; V_S, S-wave or shear-wave velocity]

Layer	V_p in kilometers per second	Top of layer, in kilometers	V_p/V_s
1	2.3	−3.0	1.80
2	2.6	−0.7	1.80
3	3.4	0.0	1.80
4	5.1	1.0	1.80
5	6.3	9.0	1.78
6	8.0	44.0	1.78

Table 5.4. Velocity model used by the Alaska Volcano Observatory for Cold Bay region (McNutt and Jacob, 1986).

[V_P, P-wave or compressional-wave velocity; V_S, S-wave or shear-wave velocity]

Layer	V_p in kilometers per second	Top of layer, in kilometers	V_p/V_s
1	3.05	−3.00	1.78
2	3.44	0.00	1.78
3	5.56	1.79	1.78
4	6.06	3.65	1.78
5	6.72	10.18	1.78
6	7.61	22.63	1.78
7	7.90	38.51	1.78

Table 5.5. Velocity model used by the Alaska Volcano Observatory for Iliamna Volcano (Roman and others, 2001).

[V_P, P-wave or compressional-wave velocity; V_S, S-wave or shear-wave velocity]

Layer	V_p in kilometers per second	Top of layer, in kilometers	V_p/V_s
1	4.8	−3.0	1.78
2	6.1	−1.6	1.78
3	6.2	1.7	1.78
4	6.3	2.9	1.78
5	6.4	3.1	1.78
6	7.1	16.5	1.78

Table 5.6. Velocity model used by the Alaska Volcano Observatory for the Katmai volcanic cluster (Searcy, 2003).

[V_P, P-wave or compressional-wave velocity; V_S, S-wave or shear-wave velocity]

Layer	V_p in kilometers per second	Top of layer, in kilometers	V_p/V_s
1	5.05	−3.0	1.78
2	5.10	1.0	1.78
3	5.41	2.0	1.78
4	5.49	3.0	1.78
5	5.65	4.0	1.78
6	5.67	5.0	1.78
7	5.69	6.0	1.78
8	5.76	7.0	1.78
9	5.80	8.0	1.78
10	6.00	9.0	1.78
11	6.04	10.0	1.78
12	6.08	12.0	1.78
13	6.30	15.0	1.78
14	6.73	20.0	1.78
15	7.54	25.0	1.78
16	7.78	33.0	1.78

Table 5.7. Velocity model used by the Alaska Volcano Observatory for Makushin Volcano (Cheryl Searcy, written communications, 2010).

[V_P, P-wave or compressional-wave velocity; V_S, S-wave or shear-wave velocity]

Layer	V_p in kilometers per second	Top of layer, in kilometers	V_p/V_s
1	3.88	−3.0	1.86
2	3.92	0.0	1.88
3	3.99	1.0	1.61
4	4.11	2.0	1.66
5	4.81	3.0	1.70
6	5.40	4.0	1.91
7	5.82	4.5	1.77
8	6.40	5.0	1.70
9	6.53	9.0	1.68
10	6.92	10.0	1.71
11	7.37	11.0	1.82
12	7.68	23.0	1.78
13	8.08	28.0	1.78

Table 5.8. Velocity model used by the Alaska Volcano Observatory for Okmok Caldera (Masterlark and others, 2010).

[V_P, P-wave or compressional-wave velocity; V_S, S-wave or shear-wave velocity]

Layer	V_p in kilometers per second	Top of layer, in kilometers	V_p/V_s
1	3.830	−3.0	1.73
2	3.891	0.0	1.73
3	5.084	1.0	1.73
4	5.187	2.0	1.73
5	5.470	3.0	1.73
6	6.185	4.0	1.73
7	6.191	10.0	1.73
8	6.454	12.0	1.73
9	6.896	16.0	1.73
10	7.414	20.0	1.73

Table 5.9. Velocity model used by the Alaska Volcano Observatory for Redoubt Volcano (Lahr and others, 1994).

[V_P, P-wave or compressional-wave velocity; V_S, S-wave or shear-wave velocity]

Layer	V_p in kilometers per second	Top of layer, in kilometers	V_p/V_s
1	2.90	−3.0	1.80
2	5.10	−1.7	1.80
3	6.40	1.5	1.72
4	7.00	17.0	1.78

Table 5.10. Velocity model used by the Alaska Volcano Observatory for Mount Spurr (Jolly and others, 1994).

[V_P, P-wave or compressional-wave velocity; V_S, S-wave or shear-wave velocity]

Layer	V_p in kilometers per second	Top of layer, in kilometers	V_p/V_s
1	5.1	−3.00	1.81
2	5.5	−2.00	1.81
3	6.3	5.25	1.74
4	7.2	27.25	1.78

Table 5.11. Velocity model used by the Alaska Volcano Observatory for Tanaga Volcano (Power, written commun., 2005).

[V_P, P-wave or compressional-wave velocity; V_S, S-wave or shear-wave velocity]

Layer	V_p in kilometers per second	Top of layer, in kilometers	V_p/V_s
1	4.0	−3.0	1.78
2	4.5	−1.2	1.78
3	5.0	0.0	1.78
4	5.6	4.0	1.78
5	6.9	10.0	1.78
6	7.2	15.0	1.78
7	7.8	20.0	1.78
8	8.1	33.0	1.78

Table 5.12. Velocity model used by the Alaska Volcano Observatory for Mount Veniaminof (Sánchez, 2005).

[V_P, P-wave or compressional-wave velocity; V_S, S-wave or shear-wave velocity]

Layer	V_p in kilometers per second	Top of layer, in kilometers	V_p/V_s
1	4.82	−3.0	1.73
2	5.23	4.0	1.88
3	5.23	10.0	1.38
4	6.49	15.0	1.65
5	6.52	20.0	1.51
6	8.18	25.0	1.89
7	8.21	33.0	1.90
8	8.21	47.0	1.80
9	8.30	65.0	1.78

Table 5.13. Velocity model used by the Alaska Volcano Observatory for Westdahl Peak (Dixon and others, 2005).

[V_P, P-wave or compressional-wave velocity; V_S, S-wave or shear-wave velocity]

Layer	V_p in kilometers per second	Top of layer, in kilometers	V_p/V_s
1	3.03	−3.0	1.71
2	3.18	0.0	1.71
3	5.03	2.0	1.71
4	5.70	8.0	1.71
5	6.30	10.0	1.71
6	6.82	16.0	1.71
7	7.17	26.0	1.71
8	8.16	38.0	1.71

Table 5.14. Regional velocity model used by the Alaska Volcano Observatory (Fogleman and others, 1993).

[V_P, P-wave or compressional-wave velocity; V_S, S-wave or shear-wave velocity]

Layer	V_p in kilometers per second	Top of layer, in kilometers	V_p/V_s
1	5.3	−3.0	1.78
2	5.6	4.0	1.78
3	6.2	10.0	1.78
4	6.9	15.0	1.78
5	7.4	20.0	1.78
6	7.7	25.0	1.78
7	7.9	33.0	1.78
8	8.1	47.0	1.78
9	8.3	65.0	1.78

Appendix 6. Cylindrical Model Regions Used for Locating Earthquakes

This appendix shows the cylindrical model regions used by the Alaska Volcano Observatory for locating earthquakes. Table 6.1 gives cylindrical extent parameters for local velocity models used at each volcano, and figures 6.1–6.4 show the cylindrical model regions defined by multiple cylinders.

Table 6.1. Cylindrical extent parameters for local velocity models used by the Alaska Volcano Observatory at monitored volcanoes.

[Latitude and longitude are the center of each model. Depths of the top and bottom of each model are referenced to sea level with negative depths reflecting height above sea level. The one-dimensional models applied in each cylindrical area are given in tables in appendix 5]

Volcano/region	Velocity model	Latitude	Longitude	Radius, in kilometers	Top depth, in kilometers	Bottom depth, in kilometers)
Mount Spurr	Table 5.10	61.60	−152.40	20	−3.3	50
Mount Spurr	Table 5.10	61.47	−152.33	20	−3.3	50
Mount Spurr	Table 5.10	61.33	−152.25	20	−3.3	50
Mount Spurr	Table 5.10	61.17	−152.35	20	−3.3	50
Mount Spurr	Table 5.10	61.00	−152.45	20	−3.3	50
Redoubt Volcano	Table 5.10	60.83	−152.55	20	−2.0	50
Redoubt Volcano	Table 5.9	60.66	−152.66	20	−2.0	50
Redoubt Volcano	Table 5.9	60.49	−152.75	20	−2.0	50
Redoubt Volcano	Table 5.9	60.34	−152.86	20	−2.0	50
Iliamna Volcano	Table 5.5	60.03	−153.09	20	−3.0	50
Augustine Volcano	Table 5.3	59.36	−153.42	20	−1.3	50
Katmai volcanic cluster	Table 5.6	58.17	−155.35	20	−2.3	50
Katmai volcanic cluster	Table 5.6	58.29	−154.86	20	−2.3	50
Katmai volcanic cluster	Table 5.6	58.35	−155.09	20	−2.3	50
Katmai volcanic cluster	Table 5.6	58.43	−154.38	20	−2.3	50
Mount Veniaminof	Table 5.12	56.18	−159.38	30	−2.5	50
Cold Bay	Table 5.4	55.42	−161.89	20	−2.8	50
Cold Bay	Table 5.4	55.18	−162.27	20	−2.8	50
Cold Bay	Table 5.4	54.76	−163.97	30	−2.8	50
Westdahl Peak	Table 5.13	54.52	−164.65	20	−1.5	50
Akutan Peak	Table 5.1	54.15	−165.97	20	−1.3	50
Makushin Volcano	Table 5.7	53.89	−166.92	20	−1.8	50
Okmok Caldera	Table 5.8	53.40	−168.16	20	−1.1	50
Andreanof Islands	Table 5.2	52.08	−176.13	20	−1.7	50
Andreanof Islands	Table 5.2	51.93	−176.75	20	−1.7	50
Andreanof Islands	Table 5.2	51.92	−177.17	20	−1.7	50
Tanaga Volcano	Table 5.11	51.89	−178.15	20	−1.8	50

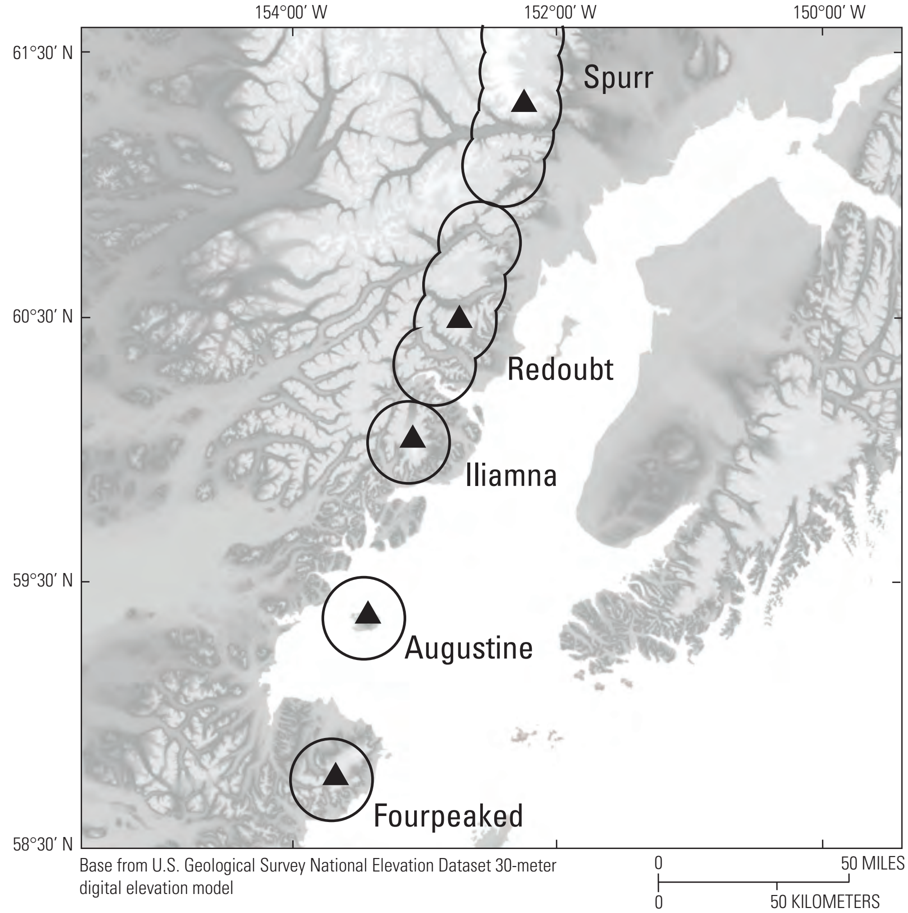

Figure 6.1. Map showing volcanic zones for the Cook Inlet volcanoes, Alaska. Five overlapping cylinders model the Mount Spurr volcanic zone. Four overlapping cylinders model the Redoubt volcanic zone. Single cylinders model the Iliamna Volcano, Augustine Volcano, and Fourpeaked Mountain volcanic zones. See figure 1 for map location.

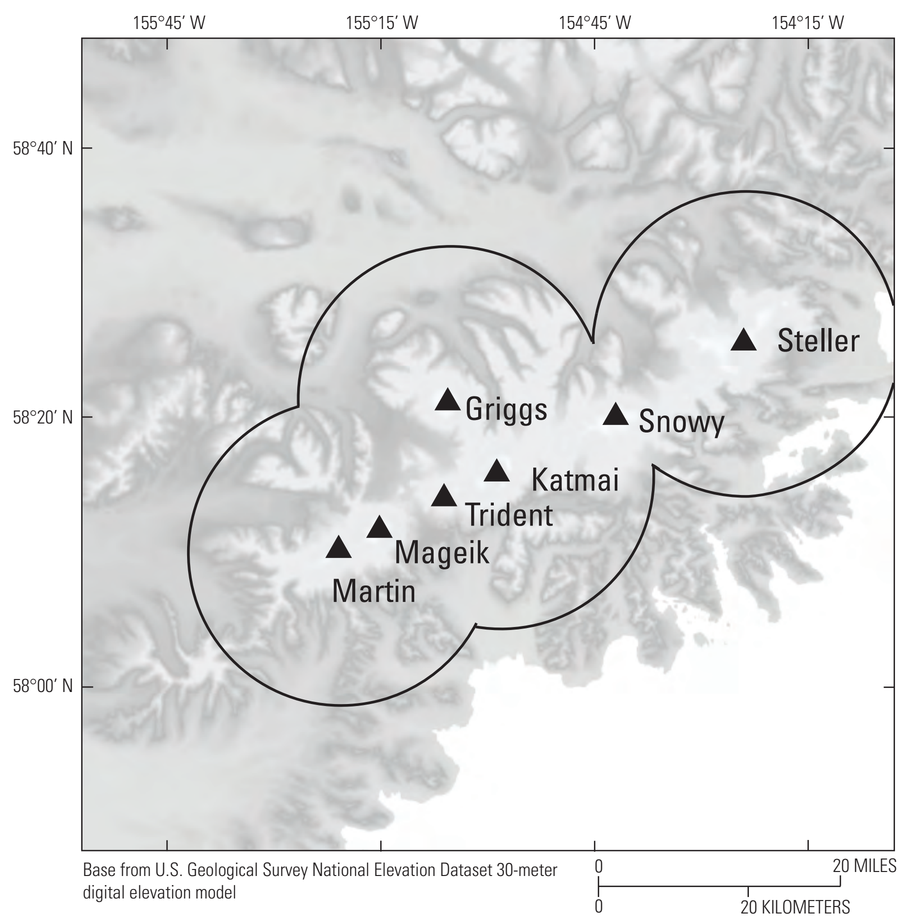

Figure 6.2. Map showing the volcanic zone for the Katmai volcanic cluster, Alaska. The volcanic zone is modeled using four overlapping cylinders centered on Mount Martin, Mount Katmai, Mount Griggs, and Mount Steller. See figure 1 for map location.

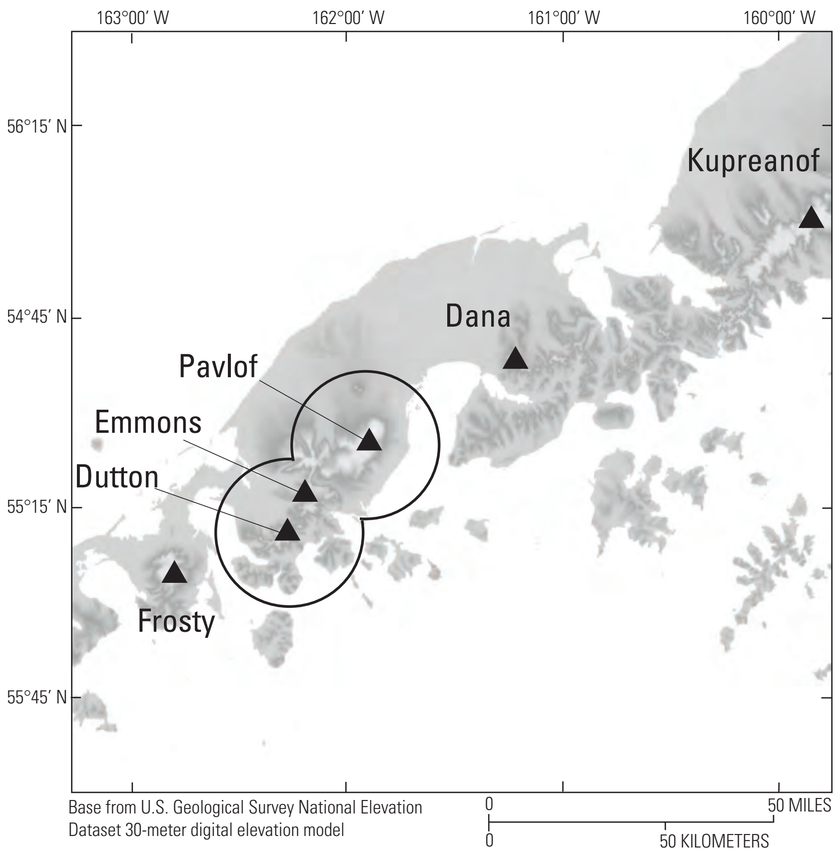

Figure 6.3. Map showing the volcanic zones for Pavlof Volcano and Mount Dutton, Alaska. The volcanic zone is modeled using two overlapping cylinders centered on Mount Dutton and Pavlof VolcanoSee figure 1 for map location (Mount Dana, Mount Emmons, Mount Kupreanof, and Frosty Peak are not shown).

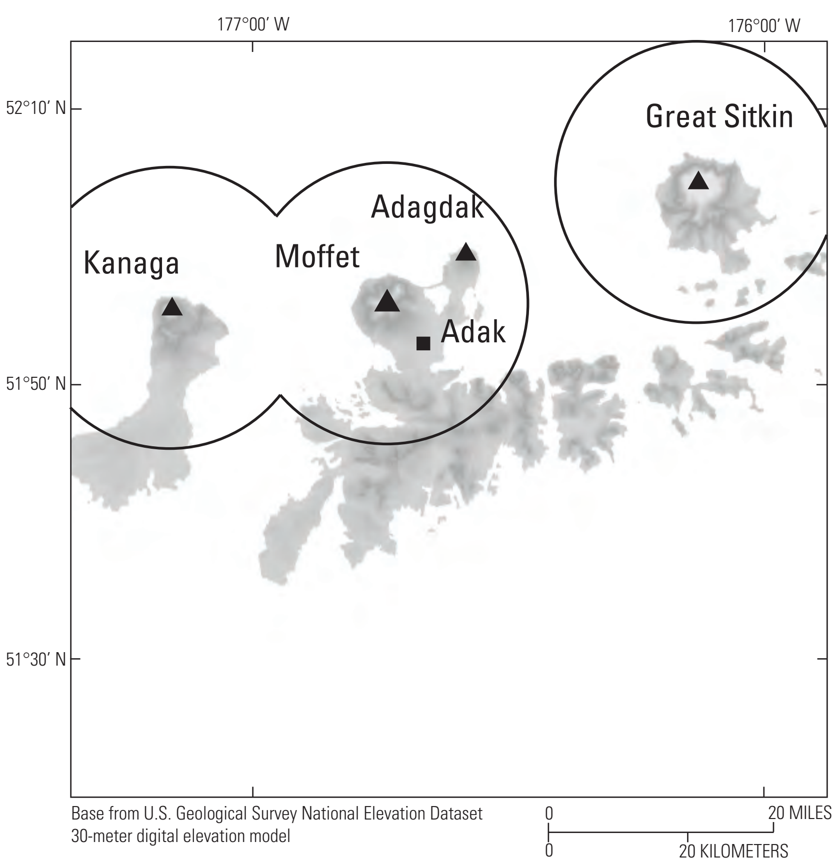

Figure 6.4. Map showing the volcanic zones in the Adak region, Alaska. The volcanic zones are modeled using cylinders centered on Kanaga Volcano, Mount Moffett, and Great Sitkin Volcano See figure 1 for map location (Mount Moffett and Mount Adagdak are not shown).

Appendix 7. Description of Earthquake List Parameters

The data supplement that accompanies this report (ds1115_datasupplement.zip; available only online at https://doi.org/10.3133/ds1115) includes an Excel (.xlsx) spreadsheet (also available as a comma separated value, .csv, file)—ds1115_2013to2017earthquakesummary.xlsx—that has a listing of all volcano-related seismic events included in the Alaska Volcano Observatory catalog of seismic events recorded by the Advanced National Seismic System *(ANSS) Quake Monitoring System. The* following parameters are used in the catalog (shown as formatted in the data supplement):

- Date and time in Coordinated Universal Time (year, month, day, hour, minute, and second)
- Hypocenter in latitude and longitude in decimal degrees in the World Geodetic System 1984 (WGS 84) datum. Depth is specified in kilometers below mean sea level.
- Magnitude—magnitude (mag) and magnitude type (mag type)—with local magnitude (M_L) being the preferred magnitude over duration magnitude (M_d). If a magnitude could not be determined by other means the magnitude was set (M_h)
- Hypocentral errors are shown as the weighted root-mean-square travel-time residual error (RMS); the depth error (ERZ) defined as the largest projection of the three principal errors on a vertical line; and the horizontal error (ERH) defined as the length of the largest projection of the three principal errors on a horizontal plane.
- Event gap (gap) is the largest azimuthal gap between azimuthally adjacent stations.
- Distance to the closest seismograph station (dist).
- Number of phases (n), P-phase and S-phase combined, number of P-phases (np), and number of S-phases (ns), used in the hypocentral solution.
- Quality (quality) of the solution is a one-letter quality code based on errors and goodness-of-fit; quality criteria are:

    A. RMS≤0.15 second (s) and ERZ≤2.0 km and ERH≤1.0 kilometer (km);

    B. RMS≤0.30 s and ≤5.0km and ERH≤2.5 km;

    C. RMS≤0.50 s and ERZ erz≤5.0 km and ERH≤5.0 km;

    D. Worse than above.

- Type of event (event type) as listed in table 7.1.
- Region of the event (event region) is the full name of the geographical region as listed in table 7.2.
- Volcanic Center which the earthquake is closest to.
- Database ID (event id) is a unique number assigned to each event origin in the AVO AQMS database.

Table 7.1. Event codes used in the Alaska Volcano Observatory (AVO) catalog of seismic events.

[Each event was identified by a description code and stored as a comment in the event-location pick file, which is a database parameter]

Event code	Description
le	An earthquake included in the AVO catalog of which is thought to be a volcano-tectonic earthquake.
lp	An earthquake included in the AVO catalog of which is thought to be a low-frequency or hybrid earthquake .
re	An earthquake included in the AVO catalog that is thought to be tectonic in origin.
other	Located events with any other cause.

Table 7.2. Event regions and the volcanic center in each geographical region used in the Alaska Volcano Observatory (AVO) catalog of seismic events.

Event region	Volcano center
Central Alaska	Mount Wrangell
Cook Inlet	Augustine Volcano, Iliamna Volcano, Redoubt Volcano, Mount Spurr
Alaska Peninsula	Aniakchak Crater, Mount Dutton, Fourpeaked Mountain, Katmai volcanic cluster, Pavlof Volcano, Ugashik-Peulik Volcano, Mount Veniaminof
Unimak Island	Isanotski Volcano, Shishaldin Volcano, Westdahl Peak
Fox Islands	Akutan Peak, Makushin Volcano, Okmok Caldera, Mount Resheshnoi
Islands of the Four Mountains	Mount Cleveland
Andreanof Islands	Mount Gareloi, Great Sitkin Volcano, Kanaga Volcano, Korovin Volcano, Tanaga Volcano
Rat Islands	Mount Cerberus, Little Sitkin Volcano

Appendix 8. Previous Alaska Volcano Observatory Earthquake Catalogs

1989–90: Power, J.A., March, G.D., Lahr, J.C., Jolly, A.D., and Cruse, G.R., 1993, Catalog of earthquake hypocenters at Redoubt Volcano and Mount Spurr, Alaska—October 12, 1989–December 31, 1990: U.S. Geological Survey Open-File Report 93–685–A, 57 p., https://doi.org/10.3133/ofr93685A.

1991–93: Jolly, A.D., Power, J.A., Stihler, S.D., Rao, L.N., Davidson, G., Paskievitch, J., Estes, S., and Lahr, J.C., 1996, Catalog of earthquake hypocenters for Augustine, Redoubt, Iliamna, and Mount Spurr Volcanoes, Alaska—January 1, 1991–December 31, 1993: U.S. Geological Survey Open-File Report 96–70, 90 p., https://doi.org/10.3133/ofr9670.

1994–99: Jolly, A.D., Stihler, S.D., Power, J.A., Lahr, J.C., Paskievitch, J., Tytgat, G., Estes, S., Lockhart, A.B., Moran, S.C., McNutt, S.R., and Hammond, W.R., 2001, Catalog of earthquake hypocenters at Alaskan volcanoes—January 1, 1994–December 31, 1999: U.S. Geological Survey Open-File Report 01–189, 202 p., https://doi.org/10.3133/ofr01189.

2000–01: Dixon, J.P, Stihler, S.D., Power, J.A., Tytgat, G., Estes, S., Moran, S.C., Paskievitch, J., and McNutt, S.R., 2002, Catalog of earthquake hypocenters at Alaska volcanoes—January 1, 2000–December 31, 2001: U.S. Geological Survey Open-File Report 02–342, 56 p., https://doi.org/10.3133/ofr02342.

2002: Dixon, J.P., Stihler, S.D., Power, J.A., Tytgat, G., Moran, S.C., Sánchez, J.J., Estes, S., McNutt, S.R., and Paskievitch, J., 2003, Catalog of earthquake hypocenters at Alaska volcanoes—January 1–December 31, 2002: U.S. Geological Survey Open-File Report 03–267, 58 p., https://doi.org/10.3133/ofr03267.

2003: Dixon, J.P., Stihler, S.D., Power, J.A., Tytgat, G., Moran, S.C., Sánchez, J.J., Estes, S., McNutt, S.R., and Paskievitch, J., 2004, Catalog of earthquake hypocenters at Alaska volcanoes—January 1–December 31, 2003: U.S. Geological Survey Open-File Report 2004–1234, 59 p., https://doi.org/10.3133/ofr20041234.

2004: Dixon, J.P., Stihler, S.D., Power, J.A., Tytgat, G., Estes, S., Prejean, S.G., Sánchez, J.J., Sanches, R., McNutt, S.R., and Paskievitch, J., 2005, Catalog of earthquake hypocenters at Alaskan volcanoes—January 1 through December 31, 2004: U.S. Geological Survey Open-File Report 2005–1312, 74 p., https://doi.org/10.3133/ofr20051312.

2005: Dixon, J.P., Stihler, S.D., Power, J.A., Tytgat, G., Estes, S., and McNutt, S.R., 2007, Catalog of earthquake hypocenters at Alaskan volcanoes—January 1 through December 31, 2005: U.S. Geological Survey Open-File Report 2007–1264, 78 p., https://doi.org/10.3133/ofr20061264.

2006: Dixon, J.P., Stihler, S.D., Power, J.A., and Searcy, C.K., 2008, Catalog of earthquake hypocenters at Alaskan Volcanoes—January 1 through December 31, 2006: U.S. Geological Survey Data Series 326, 78 p., https://doi.org/10.3133/ds326.

2007: Dixon, J.P., Stihler, S.D., Power, J.A., and Searcy, C.K., 2008, Catalog of earthquake hypocenters at Alaskan volcanoes—January 1 through December 31, 2007: U.S. Geological Survey Data Series 367, 82 p., https://doi.org/10.3133/ds367.

2008: Dixon, J.P., and Stihler, S.D, 2009, Catalog of earthquake hypocenters at Alaskan volcanoes—January 1 through December 31, 2008: U.S. Geological Survey Data Series 467, 88 p., https://doi.org/10.3133/ds467.

2009: Dixon, J.P., Stihler, S.D, Power, J.A., and Searcy, C.K., 2010, Catalog of earthquake hypocenters at Alaskan volcanoes—January 1 through December 31, 2009: U.S. Geological Survey Data Series 531, 84 p., https://doi.org/10.3133/ds531.

2010: Dixon, J.P., Stihler, S.D, Power, J.A., and Searcy, C.K., 2011, Catalog of earthquake hypocenters at Alaskan volcanoes—January 1 through December 31, 2010: U.S. Geological Survey Data Series 645, 82 p., https://doi.org/10.3133/ds645.

2011: Dixon, J.P., Stihler, S.D, Power, J.A., and Searcy, C.K., 2012, Catalog of earthquake hypocenters at Alaskan volcanoes—January 1 through December 31, 2011: U.S. Geological Survey Data Series 730, 90 p., https://doi.org/10.3133/ds730.

2012: Dixon, J.P., Stihler, S.D., Power, J.A., Haney, M.M., Parker, T., Searcy, C.K., and Prejean, S.G., 2013, Catalog of earthquake hypocenters at Alaskan volcanoes—January 1 through December 31, 2012: U.S. Geological Survey Data Series 789, 84 p., https://doi.org/10.3133/ds789.

This page left blank intentionally

Appendix 9. Selected Publications Using Alaska Volcano Observatory Data

Bennington, N.L., Haney, M.M., De Angelis, S., Thurber, C.H., and Freymueller, J., 2015, Monitoring changes in seismic velocity related to an ongoing rapid inflation event at Okmok volcano, Alaska: Journal of Geophysical Research Solid Earth, v. 120, no. 8, p. 5664–5676, https://doi.org/10.1002/2015JB011939.

Brown, J.R., Prejean, S.G., Beroza, G.C., Gomberg, J.S., and Haeussler, P.J., 2013, Deep low-frequency earthquakes in tectonic tremor along the Alaska-Aleutian subduction zone: Journal of Geophysical Research B—Solid Earth, v. 118, no. 3, p. 1079–1090, https://doi.org/10.1029/2012JB009459.

Bull, K.F., and Buurman, H., 2013, An overview of the 2009 eruption of Redoubt Volcano, Alaska: Journal of Volcanology and Geothermal Research, v. 259, p. 2–15, https://doi.org/10.1016/j.jvolgeores.2012.06.024.

Buurman, H., West, M.E., and Thompson, G., 2013, The seismicity of the 2009 Redoubt eruption: Journal of Volcanology and Geothermal Research, v. 259, p. 16–30, https://doi.org/10.1016/j.jvolgeores.2012.04.024.

Buurman, H., West, M.E., and Roman, D.C., 2013, Using repeating volcano-tectonic earthquakes to track post-eruptive activity in the conduit system at Redoubt Volcano, Alaska: Geology, v. 41, no. 4, p. 511–514, https://doi.org/10.1130/G34089.1.

Buurman, H., and West, M.E., 2013, Magma fracture and hybrid earthquakes in the conduit of Augustine Volcano: Geophysical Research Letters, v. 40, no. 23, p. 6038–6042, https://doi.org/10.1002/2013GL057864.

Buurman, H., Nye, C.J., West, M.E., and Cameron, C.E., 2014, Regional controls on volcano seismicity along the Aleutian Arc: Geochemistry, Geophysics, Geosystems, v. 15, no. 4, p. 1147–63, https://doi.org/10.1002/2013GC005101.

Cusano, P., Palo, M., and West, M.E., 2015, Long-period seismicity at Shishaldin volcano (Alaska) in 2003–2004: Indications of an upward migration of the source before a minor eruption: Journal of Volcanology and Geothermal Research, v. 291, p. 14–24, https://doi.org/10.1016/j.jvolgeores.2014.12.008.

DeRoin, N., McNutt, S.R., and Thompson, G., 2015, Duration-amplitude relationships of volcanic tremor and earthquake swarms preceding and during the 2009 eruption of Redoubt Volcano, Alaska: Journal of Volcanology and Geothermal Research, v. 292, p. 56–69, https://doi.org/10.1016/j.jvolgeores.2015.01.003.

Dmitrieva, K., Hotovec-Ellis, A.J., Prejean, S.G., and Dunham, E.M., 2013, Frictional-faulting model for harmonic tremor before Redoubt Volcano eruptions: Nature Geoscience, v., 6, no. 8, p. 652–656, https://doi.org/10.1038/ngeo1879.

Fee, D., McNutt, S.R., Lopez, T.M., Arnoult, K.M., Szuberla, C.A.L., and Olson, J.V., 2013, Combining local and remote infrasound recordings from the 2009 Redoubt Volcano eruption: Journal of Volcanology and Geothermal Research, v. 259, p. 100–114, https://doi.org/10.1016/j.jvolgeores.2011.09.012.

Fee, D., Haney, M.M., Matoza, R., Szuberla, C., Lyons, J., and Waythomas, C., 2016, Seismic Envelope-Based Detection and Location of Ground-Coupled Airwaves from Volcanoes in Alaska, Bulletin of the Seismological Society of America, v. 106. no. 3, p. 1024–1035, https://doi.org/10.1785/0120150244.

Fee, D., Haney, M.M., Matoza, R.S., Van Eaton, A.R., Cervelli, P., Schneider, D.J., and Iezzi, A.M., 2017, Volcanic tremor and plume height hysteresis from Pavlof Volcano, Alaska: Science, v. 355, no. 6320, p. 45–48, https://doi.org/10.1126/science.aah6108.

Gomberg, J., and Prejean, S.G., 2013, Triggered tremor sweet spots in Alaska: Journal of Geophysical Research, v. 118, no. 12, p. 6203–6218, https://doi.org/10.1002/2013JB010273.

Haney, M.M., Chouet, B.A., Dawson, P.B., and Power, J.A., 2013, Source characterization for an explosion during the 2009 eruption of Redoubt Volcano from very-long-period seismic waves: Journal of Volcanology and Geothermal Research, v. 259, p. 77–88, https://doi.org/10.1016/j.jvolgeores.2012.04.018.

Haney, M.M., 2014, Backprojection of volcanic tremor: Geophysical Research Letters, v. 41, p. 1923–1928, https://doi.org/10.1002/2013GL058836.

Haney, M.M, Hotovec-Ellis, A.J., Bennington, N.L., De Angelis, S, and Thurber, C., 2015, Tracking changes in volcanic systems with seismic interferometry, *in* Beer, M., Kougioumtzoglou I., Patelli, E., and Au, I.S-K., eds., Encyclopedia of earthquake engineering: Springer, Berlin, Heidelberg, p. 3767–3786, https://doi.org/10.1007/978-3-642-36197-5_50-1.

Haney, M.M., Matoza, R.S., Fee, D., and Aldridge, D.F., 2017, Seismic equivalents of volcanic jet scaling laws and multipoles in acoustics: Geophysical Journal International, v. 213, no. 1, p. 623–636, https://doi.org/10.1093/gji/ggx554.

Hotovec, A.J., Prejean, S.G., Vidale, J.E., and Gomberg, J., 2013, Strongly gliding harmonic tremor during the 2009 eruption of Redoubt Volcano: Journal of Volcanology and Geothermal Research, v. 259, p. 88–99, https://doi.org/10.1016/j.jvolgeores.2012.01.001.

Kasatkina, E., Koulakov, I., West, M.E., and Izbekhov, P., 2014, Seismic structure changes beneath Redoubt Volcano during the 2009 eruption inferred from local earthquake tomography: Journal of Geophysical Research: Solid Earth, v. 119, no. 6, p. 4938–4954, https://doi.org/10.1002/2013JB010935.

Ketner, D.M., and Power, J.A., 2013, Characterization of seismic events during the 2009 eruption of Redoubt Volcano, Alaska: Journal of Volcanology and Geothermal Research, v. 259, p. 45–62, https://doi.org/10.1016/j.jvolgeores.2012.10.007.

McNutt, S.R., Thompson, G., West, M.E., Fee, D., Stihler, S., and Clark, E., 2013, Local seismic and infrasound observations of the 2009 explosive eruptions of Redoubt Volcano, Alaska: Journal of Volcanology and Geothermal Research, v. 259, p. 63–76, https://doi.org/10.1016/j.jvolgeores.2013.03.016.

Murphy, R., Thurber, C.H., Prejean, S.G., and Bennington, N., 2014, Three-dimensional seismic velocity structure and earthquake relocations at Katmai, Alaska: Journal of Volcanology and Geothermal Research, v. 276, p. 121–131, https://doi.org/10.1016/j.jvolgeores.2014.02.22.

Ohlendorf, S.J., Thurber, C.H., Pesicek, J.D., and Prejean, S.G., 2014, Seismicity and seismic structure at Okmok Volcano, Alaska: Journal of Volcanology and Geothermal Research, v. 278–279, p. 103–119, https://doi.org/10.1016/j.jvolgeores.2014.04.002.

Pollitz, F.F., Wech, A., Kao, H., and Burgmann, R., 2013, Annual modulation of non-volcanic tremor in northern Cascadia: Journal of Geophysical Research: Solid Earth, v. 118, no. 5, p. 2445–2549, https://doi.org/10.1002/jgrb.50181.

Power, J.A., Stihler, S.D., Chouet, B.A., Haney, M.M., and Ketner, D.M., 2013, Seismic observations of Redoubt Volcano, Alaska—1989–2010 and a conceptual model of the Redoubt magmatic system: Journal of Volcanology and Geothermal Research, v. 259, p. 31–44, https://doi.org/10.1016/j.jvolgeores.2012.09.014.

Roman, D.C,. and Gardine, M.D., 2013, Seismological evidence for long-term and rapidly accelerating magma pressurization preceding the 2009 eruption of Redoubt Volcano, Alaska: Earth and Planetary Science Letters, v. 371–372, p. 226–234, https://doi.org/10.1016/j.epsl.2013.03.040.

Smith, C.M., McNutt, S.R., and Thompson, G., 2016, Ground-coupled airwaves at Pavlof Volcano, Alaska, and their potential for eruption monitoring: Bulletin of Volcanology, v. 78, no. 7, p. 52–64, https://doi.org/10.1007/s00445-016-1045-0.

Syracuse, E.M., Maceira, M., Zhang, H., and Thurber, C.H., 2015, Seismicity and structure of Akutan and Makushin Volcanoes, Alaska, using joint body and surface wave tomography: Journal of Geophysical Research Solid Earth, v. 120, no. 2, p. 1036–1052, https://doi.org/10.1002/2014JB011616.

Werner, C., Kern, C., Coppola, D., Lyons, J.J., Kelly, P.J., Wallace, K.L., Schneider, D.J., and Wessels, R.L., 2017, Magmatic degassing, lava dome extrusion, and explosions from Mount Cleveland volcano, Alaska, 2011–2015—Insights into the continuous nature of volcanic activity over multi-year timescales: Journal of Volcanology and Geothermal Research, v. 337, p. 98–110, https://doi.org/10.1016/j.jvolgeores.2017.03.001.

Menlo Park Publishing Service Center, California
Manuscript approved for publication July 16, 2019
Edited by James W. Hendley II
Layout and design by Kimber Petersen

USGS

Dixon and others—**Catalog of Seismograph and Infrasound Stations at Alaskan Volcanoes—January 1, 2013, through December 31, 2017**—Data Series 1115, August 2019

ISSN 2327-638X (online)
https://doi.org/10.3133/ds1115